COMPRESSIVE CREEP OF A LIGHTWEIGHT,

HIGH STRENGTH CONCRETE MIXTURE

by

Edward C. Vincent

Thesis presented to the faculty of the

Virginia Polytechnic Institute and State University

In partial fulfillment of the requirements for the degree of

Master of Science

in

Civil Engineering

Committee:

Richard E. Weyers, Chair

Thomas E. Cousins

Carin L. Roberts-Wollmann

January 10, 2003

Blacksburg, VA

Keywords: compressive creep, prediction models, shrinkage, lightweight aggregate

COMPRESSIVE CREEP OF A LIGHTWEIGHT, HIGH STRENGTH CONCRETE MIXTURE

by

Edward C. Vincent

ABSTRACT

Concrete undergoes volumetric changes throughout its service life. These changes are a result of applied loads and shrinkage. Applied loads result in an instantaneous recoverable elastic deformation and a slow, time dependent, inelastic deformation called creep. Creep without moisture loss is referred to as basic creep and with moisture loss is referred to as drying creep. Shrinkage is the combination of autogeneous, drying, and carbonation shrinkage. The combination of creep, shrinkage, and elastic deformation is referred to as total strain.

The prestressed concrete beams in the Chickahominy River Bridge have been fabricated with a lightweight, high strength concrete mixture (LTHSC). Laboratory test specimens have been cast using the concrete materials and mixture proportions used in the fabrication of the bridge beams. Two standard cure and two match cure batches have been loaded for 329 and 251 days, respectively.

Prestress losses are generally calculated with the total strain predicted by the American Concrete Institute Committee 209 recommendations, ACI 209, or the European design code, CEB Model Code 90. Two additional models that have been proposed are the B3 model by Bazant and Baweja, and the GL2000 model proposed by Gardner and Lockman. The four models are analyzed to determine the most precise model for the LTHSC mixture. Only ACI 209 considered lightweight aggregates during model development. GL2000 considers aggregate stiffness in the model.

ACI 209 was the best predictor of total strain and individual time dependent deformations for the accelerated cure specimens. CEB Mode Code 90 was the best predictor of total strain for the standard cure specimens. The best overall predictor of time dependent deformations was the GL2000 model for the standard cure specimens.

ACKNOWLEDGEMENTS

First, I would like to express my gratitude to Dr. Richard E. Weyers for his guidance and assistance throughout this project. I also greatly appreciate the guidance of Dr. Thomas Cousins and Dr. Carin Roberts-Wollmann as members of my research committee.

I would like to thank the Virginia Transportation Research Council for providing the funding for this project.

I am grateful for the many people that contributed to this project. I owe a great deal of gratitude to David Mokarem for his help in getting this project underway. I am also grateful to Richard Meyerson for his work involving a previous creep study. In addition, I would like to thank technicians, Brett Farmer and Denis Huffman for their insight and technical expertise.

My appreciation goes out to the faculty of the Structural Engineering and Materials Program for the valuable learning experiences and leading me realize that a glass of water is not really half full or half empty, but has a safety factor of two. I also would like to thank Dr. Anderson-Cook in the Statistics Department for the valuable learning experiences.

Most importantly, I would like to thank my mother, Catherine Ritchey. I cannot give enough credit for her love and support. I also would like to thank my grandparents, Frank and Opal, my sister, Valerie, and my stepfather, Tom, for their love and support.

I would like to thank my friends Michael Brown, Patricia Buchanan, James Fazio Jr., Allison Haden, Brian McCormick, David Mokarem, Matthew Rowe, Kevin Siegel, and Megan Wheeler for their support and friendship throughout the years.

TABLE OF CONTENTS

LIST OF FIGURES

LIST OF TABLES

CHAPTER 1: INTRODUCTION

Concrete undergoes volumetric changes throughout its service life. These changes are a result of applied loads and shrinkage. Applied loads result in an instantaneous recoverable elastic deformation and a slow, time dependent, inelastic deformation called creep. Creep without moisture loss is referred to as basic creep and with moisture loss is referred to as drying creep.

Shrinkage is a combination of autogeneous, drying, and carbonation shrinkage of the hardened concrete. Plastic shrinkage is not included since it occurs due to moisture loss before the concrete has set. Autogeneous shrinkage is a result of the hydration process. The hydrated cement paste has a smaller volume than the cement and water reactants. Drying shrinkage occurs as surface water evaporates and internal water moves outward in an attempt for hygral equilibrium. The opposite reaction is called swelling. Carbonation shrinkage occurs with the carbonation of the hydrated cement products with carbon dioxide in the atmosphere.

Creep testing is conducted on sealed or unsealed specimens. Sealed specimens with an applied stress have volumetric changes due to elastic deformation, basic creep, and autogeneous shrinkage. Sealed specimens without an applied stress deform due to autogeneous shrinkage. Basic creep is the total deformation of a loaded, sealed specimen minus the elastic deformation and autogeneous shrinkage.

Unsealed specimens are the most commonly used test method. Unsealed specimens without an applied stress have volumetric changes due to autogeneous and drying shrinkage. The total deformation of unsealed specimens is the result of an applied stress producing an elastic deformation, creep, and shrinkage. Creep includes both basic and drying creep. Shrinkage includes autogeneous and drying shrinkage. Drying creep of a loaded specimen is the total deformation minus the elastic deformation, basic creep, and autogeneous shrinkage and requires the testing of both sealed and unsealed specimens. Therefore, creep is typically examined as the total of basic and drying creep.

CHAPTER 2: PURPOSE AND SCOPE

The objective of this study is to determine the magnitude of creep in a lightweight, high strength concrete mixture used in the prestressed beams of the Chickahominy River Bridge. Each set of specimens were tested under laboratory exposure conditions after undergoing the standard cure or an accelerated cure with the match cure system. The creep results were compared with the four most current prediction models and the best was identified and examined. The results of this study may be used to determine the best model to predict prestress losses of this lightweight, high strength concrete mixture. The results may also be compared with the results of field assessment task of the project.

The lightweight, high strength concrete mixture ingredients and proportions from Bayshore Concrete Products Corporation and used in the fabrication of the bridge beams were used in this study. At loading, the maturity of the accelerated cured specimens were consistent with that of the bridge beams at the centroid of the prestressing strand. The curing methods, accelerated and standard cures, are a variable. The ambient laboratory exposure conditions were held constant.

CHAPTER 3: METHODS AND MATERIALS

3.1 Introduction

The objective of this study is to determine the magnitude of creep in a lightweight, high strength concrete mixture used in the prestressed concrete beams of the Virginia Route 106 bridge over the Chickahominy River. The mixture proportions and materials are the same as in the fabricated field beams and presented in Table 1. Batch weights are presented in Appendix B.

The study variables included two curing methods, ASTM C 512 standard method and an accelerated match cure and two specimen sizes. The two specimen sizes are discussed with the creep testing procedure. The standard cure method consists of a seven day moist cure at 73.4 ± 3.0°F (23.0 ± 1.7°C). The accelerated cure consists of elevating the specimen temperature to increase the rate of hydration. The standard cure method followed ASTM C 512 as standard test method. The purpose of an accelerated cure is to decrease the curing time needed to get the required strength. The accelerated cure method is being used to replicate the curing method the prestressed concrete industry uses on prestressed concrete beams. The temperature profile for the accelerated cure batches in the laboratory was measured with thermocouples placed at the centroid of the prestressing strand in the two Bayshore beams. The temperature data was collected with a data acquisition system. The Sure Cure System was used as a match curing method. The accelerated cure temperature profiles for the Bayshore beams and laboratory specimens are presented in Appendix B.

Table 2 presents the fresh concrete properties for the two standard cure batches. Table 3 presents the fresh concrete properties for the two accelerated cure batches and two of the Bayshore beams.

Table 1 LTHSC Test Matrix

Curing Method	Mix	Age at Loading	Shrinkage Prisms
Standard Cure	2 batches	7 and 28 days	Yes
Match Cured	2 batches	1, 7, and 28 days	No

Table 2 Duration of weekly testing

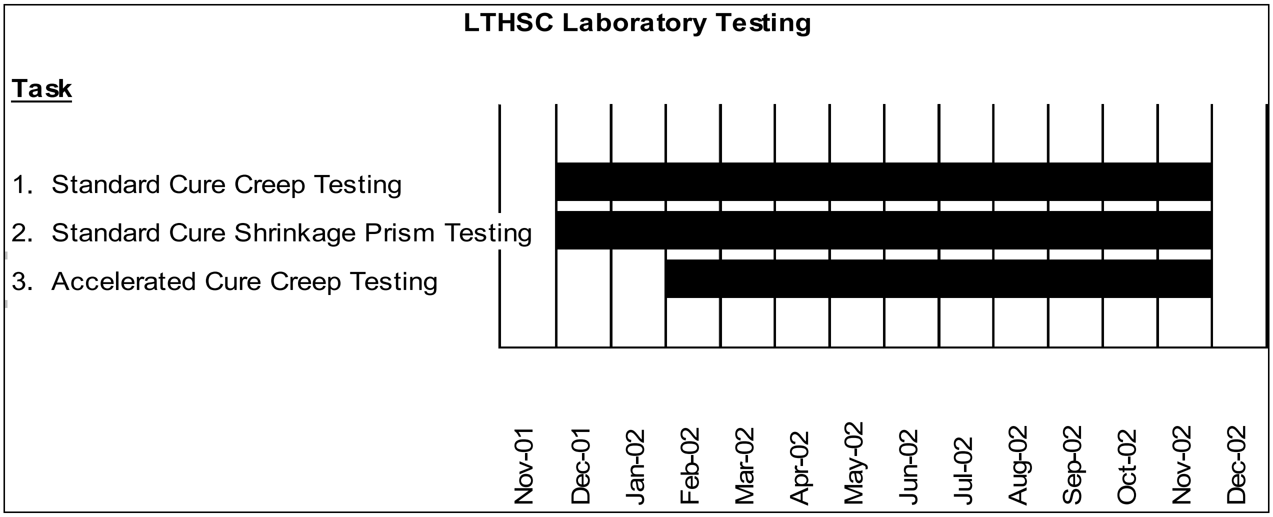

Table 3 Bayshore Mixture Proportions

Materials	SSD weights per cubic yard	SSD weights per cubic meter
Portland Cement (Type II)	451 lb.	268 kg.
Slag Cement (Grade 120)	301 lb.	179 kg.
Coarse Aggregate (lightweight)	696 lb.	413 kg.
Coarse Aggregate (normal weight)	605 lb.	359 kg.
Fine Aggregate (lightweight)	390 lb.	231 kg.
Fine Aggregate (normal weight)	541 lb.	321 kg.
Water	255 lb.	151 kg.
AEA (Daravair)	12 oz.	355 ml.
WR (Hycol)	22 oz.	651 ml.
HRWR (Adva)	56 oz.	1656 ml.
CI or Accel (DCI)	3 gal.	11.4 L

Table 4 Fresh Concrete Properties for the Standard Cure Batches

Fresh Concrete Properties	LTHSC 2B	LTHSC 3B
Slump, mm (in.)	165 (6.5)	140 (5.5)
Air Content (%)	6.5	5.5
Temperature, ^{o}C (^{o}F)	26 (78)	26 (78)
Unit Weight, kg/m^3 (pcf)	1880 (117.3)	1910 (119.1)
Yield	1.02	1.01
w/cm ratio	0.369	0.369
Curing Method	Standard	Standard

Table 5 Fresh Concrete Properties for the Accelerated Cure Batches

Fresh Concrete Properties	LTHSC 4B	LTHSC 5B	Bayshore BB1	Bayshore BB2	VDOT specs.
Slump, mm (in.)	100 (4.0)	150 (6.0)	180 (7)	215 (8.5)	0-100 (0-4)
Air Content (%)	6.0	7.1	5.5	6.0	3 – 6
Temperature, ^oC (^oF)	24 (75)	24 (76)	21(70)	20 (68)	----
Unit Weight, kg/m^3 (pcf)	1930 (120.3)	1875 (117.1)	1950 (122.0)	1900 (118.8)	----
Yield	1.00	1.02	0.98	1.01	----
w/cm ratio	0.369	0.369	0.369	0.369	< 0.4
Curing Method	Sure Cure	Sure Cure	Steam	Steam	N/A

3.2 Aggregate Properties

The concrete mixture has two fine and two coarse aggregates, a normal and lightweight aggregate. The lightweight aggregate is both a fine and #67 expanded slate from the Carolina Stalite Company. The normal weight aggregates are a natural sand and # 67 crushed diabase. The specific gravity and absorption values for the aggregates were measured according to ASTM C 127 and 128. The measured specific gravity and absorption values can be found in Appendix B.

Carolina Stalite's website includes reports from the laboratories of Law Engineering and Environmental Services and Froechling & Robertson, Inc. that document the lightweight aggregate meeting the requirements of ASTM C 330.

3.3 Cement Properties

The mixture includes a Type I/II Portland Cement and a ground granulated blast furnace slag (GGBFS). The GGBFS is a Grade 120. Grade specifies the fineness of the mineral admixture, which is related to the magnitude of hydraulic activity and potential strength. With a finer slag, the increased surface area increases the rate of hydration. The Grade of GGBFS in this study is constant.

3.4 Chemical Admixtures

The mixture uses four chemical admixtures manufactured by Grace Construction Products. They include a high range water reducer (Adva), mid-range water reducer (Hycol), corrosion inhibitor (DCI), and air entrainment (Daravair). Additional information can be found on Grace's website. The air entrainment and high range water reducer will be adjusted in order to get similar slumps and air contents to the recorded values from the actual bridge beams. The actual values for the beams and the laboratory mixes were presented in Tables 2 and 3.

3.5 Creep Testing

Creep testing was conducted on four batches of unsealed specimens. The first two batches used the standard cure method and the second two used the accelerated cure method. Each batch consisted of three loaded and unloaded specimens along with strength and modulus cylinders. Shrinkage prisms were also cast with the standard cure batches.

Creep specimen preparation followed two procedures that were dictated by the standard and accelerated curing methods. The ASTM C 512 standard cure method allowed the specimens to be cast in standard 150 mm x 300 mm (6 in. x 12 in.) steel cylinder molds. The standard moist cure was for seven days before loading. The contact points screwed into brass inserts that were cast in place on diametrically opposite sides with a 200mm (8 in.) gage length.

The second method included a 15 hour accelerated cure. The Sure Cure System would result in the specimen size being reduced to 100 mm x 200 mm (4 in. x 8 in.) which requires adjustment to ASTM C 512. The Sure Cure System allows the temperature profile of the actual bridge beams to be followed during curing. The maturity data can be found in Appendix B. Additional information about the Sure Cure System can be found in Appendix E. The brass inserts could not be used with this method due to heating pads surrounding the perimeter of the molds. Therefore, after curing, holes were drilled on diametrically opposite sides of the specimens with a 150mm (6 in.) gage lengths. The contact points were attached in the holes with a five-minute epoxy.

The loaded specimens have a vertically applied stress. The vertical deformation is needed across the circular cross section so measurements are taken on each of the diametrically opposed sides of a cylinder. The average of the measurements from both sides is one deformation measurement. The sides are identified as "A" and "B".

The Whittemore gage was used to measure the change in distance between contact points over time. Four measurements were taken on each side to reduce operator error. The precision of the Whittemore gage is a function of operator consistency. The gage needs to be held and pressed against the contact points in the same manor for measurements at all times. Four measurements were taken per side in order for the operator to determine the consistency of multiple measurements. If the operator sees a large variation, then the measurement technique needs to be examined. For this study, all within batch measurements met the ASTM C 512 precision requirements for a single operator. The between batch requirements were not achieved for the accelerated cure batches, but the batches seemed to be significantly different in compressive strength.

The Whittemore gage measures deformations to 0.0025 mm (0.0001 in.). It is able to measure ± 6 mm (0.25 in.) from the initial gage length. The gage length is adjustable from 100 mm to 300 mm (4 in. to 12 in.) at 50 mm (2 in.) intervals. The accelerated cure specimens are 100 mm x 200 mm (4 in. x 8 in.) cylinders with a 150 mm (6 in.) gage length. The standard cure specimens are 150 mm by 300 mm (6 in. by 12 in.) cylinders with a 200 mm (8 in.) gage length.

All creep and shrinkage specimens were sulfur capped according to ASTM 617 immediately after curing. The three total strain specimens per batch were stacked vertically and loaded to 40 percent of their compressive strength. After attaching the contact points and sulfur capping, loading took place approximately three hours after the end of the curing cycles. The load was increased at 7 and 28 days to maintain a load of 40 percent of the measured compressive strength.

The load frames have been calibrated using a load cell, pressure gages, and strain gages. Additional information is available in Appendix D.

Deformation measurements were taken immediately before and after loading or increasing the load to record the elastic deformation. After loading, measurements were taken at 2 hours, 6 hours, and then daily for a week. Measurements were continued weekly thereafter. For presentation, measurements are reported weekly up to 28 days and then once every four weeks. Creep measurements were taken on two standard cure batches and two accelerated cure batches for 329 and 251 days, respectively.

The strains were taken as the change in length at a given time divided by the initial length. Since ASTM C512 does not specify the order to subtract the shrinkage strain from the total strain, the three loaded and unloaded cylinders were paired based on corresponding strain magnitudes. Therefore, the high, medium, and low total strains were subtracted from the high, medium, and low shrinkage strains, respectively.

3.6 Shrinkage Testing

Shrinkage Prisms were cast and tested according ASTM C 157. The 75 mm x 75 mm x 280 mm (3 in. x 3 in. x 11.25 in.) prisms were stored adjacent to the creep frames in the creep room at 73.4 ± 3 ^{o}F (23.0 ± 1.7^{o}C) and 45 ± 4 % relative humidity. The relative humidity was slightly lower than the specified 50 ± 4 % due to the room's environmental control unit. A comparator was used to take measurements according to ASTM 490-98. Measurements were taken on the same time schedule as the creep testing.

3.7 Strength and Modulus Testing

Compressive and tensile strength cylinders and an elastic modulus cylinder were cast according to ASTM C 192 for each batch. After curing, all strength and modulus specimens were sulfur capped per ASTM 617 and stored with the creep and shrinkage specimens in the creep room.

The creep room temperature was 73.4 ± 3 ^{o}F (23.0 ± 1.7^{o}C) and the relative humidity was 45 ± 4 %. The target relative humidity was 50 % ± 4 %.

Compressive strengths tests were conducted on 100 mm x 200 mm (4 in. x 8 in.) cylindrical specimens according to ASTM C39. Each measurement is the mean of two tests. Compressive strength measurements were taken at 7, 28, 56, and 90 days for the standard cure batches and at 1, 7, and 28 days for the accelerated cure batches. The Sure Cure System limited the number of accelerated cure specimens that could be tested.

Splitting tensile strength tests were conducted according to ASTM C 496. Each strength measurement is the mean of two tests. Tensile measurements were taken at 7 and 28 days for the standard cure batches and at 17 hours and 28 days for the accelerated cure batches.

The modulus of elasticity was measured according to ASTM C 469. Measurements were repeated at various times on one specimen per batch. The modulus of elasticity was measured on 150 mm x 300 mm (6 in. x 12 in.) and 100 mm x 200 mm (4 in. x 8 in.) cylinders for the standard and accelerated cure batches, respectively. Measurements were taken at seven, 28, 56, and 90 days for the standard cure batches and at one, seven, 28, 56, and 90 days for the accelerated cure batches.

3.8 Thermal Coefficient

The thermal coefficient for this mix was measured with the batch 2 shrinkage specimens after the end of data collection. The strain measurements were taken at ambient conditions before and after thermal measurements to insure that the strains were due to thermal conditions and not moisture loss. Three 150 mm x 300 mm (6 in. x 12 in.) cylinders were subjected to temperatures of 33^{o}F to 120^{o}F (0^{o}C to 49^{o}C) for three days at each temperature.

CHAPTER 4: RESULTS

4.1 Introduction

The compressive strength, tensile strength, modulus of elasticity, and thermal coefficient data for both the lightweight high strength concrete (LTHSC) standard and accelerated cure batches are summarized in the following sections. The standard and accelerated experimental total strain, creep strain, and shrinkage strains per batch are presented. Whereas the measured strain values are tabulated in Appendix F. Predicted values for the four models are also included. The precision of the experimental values are examined as are the residuals of four prediction models. The chapter concludes with the presentation of the standard cure, shrinkage prism results.

Each strength measurement is the average of two tested cylinders. Strength and modulus specimens were stored in the same environmental conditions as the creep and shrinkage specimens after the standard or accelerated cure regimens. The standard cure method was applied to batches 2 (2B) and 3 (3B). The accelerated cure method was applied to batches 4 (4B) and 5 (5B). Batch 1 (1B) was discarded due to an excessive air content.

Strength and modulus measurements for the LTHSC bridge beams (BB1 and BB2) are also presented. The compressive strength measurements are reported by Bayshore Concrete Products. Splitting tensile strength and modulus of elasticity were measured by VTRC.

The mixture proportions and fresh concrete properties are provided in Appendix B.

4.2 Compressive Strength

4.2.1 Standard Cure

Figure 1 presents the LTHSC standard cure compressive strengths at 7 and 28 days. The figure also presents f'_{ci}, the specified release strength, and f'_c, the 28 day design strength for the Chickahominy River bridge. The specified compressive strength at release and at 28 days is 31MPa (4500 psi) and 55 MPa (8000 psi), respectively. The seven day compressive strengths were 36 MPa and 35 MPa (5450 and 5100 psi) for batch 2 and 3, respectively. The 28 day compressive strengths were 43 MPa and 43 MPa (6210 psi and 6290 psi) for batch 2 and 3, respectively.

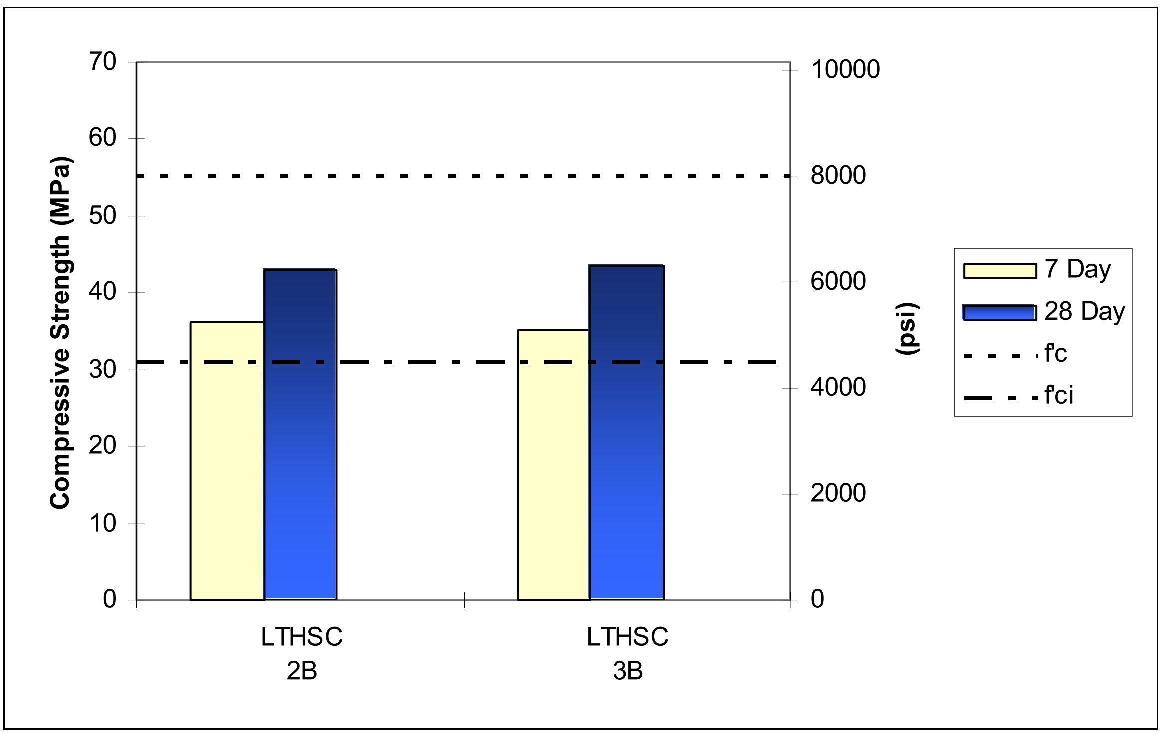

Figure 1 Standard Cure Compressive Strengths

4.2.2 Accelerated Cure

Figure 2 presents the LTHSC accelerated cure compressive strengths at 17 hours, one day, seven days, and 28 days. The figure also presents f'_{ci}, the specified release strength, and f'_c, the 28 day design strength for the Chickahominy River bridge. The specified compressive strength at release and at 28 days is 31MPa (4500 psi) and 55 MPa (8000 psi), respectively. The 17 hour compressive strengths were 44 MPa and 32 MPa (6300 psi and 4620 psi) for batch 4 and 5, respectively. The 17 hour compressive strengths were 30 MPa (4350 psi) for Bayshore beam 1. The one day compressive strengths were 33 MPa and 32 MPa (4800 psi and 4620 psi) for Bayshore beams 1 and 2, respectively. The seven day compressive strengths were 43 MPa and 38 MPa (6250 psi and 5570 psi) for batch 4 and 5, respectively. The seven day compressive strengths were 49 MPa and 48 MPa (7110 psi and 6900 psi) for Bayshore beams 1 and 2, respectively. The 28 day compressive strengths were 50 MPa and 38 MPa (7320 psi and 5470 psi) for batch 4 and 5, respectively. The 28-day compressive strengths were 57 MPa and 55 MPa (8310 psi and 7900 psi) for Bayshore beams 1 and 2, respectively.

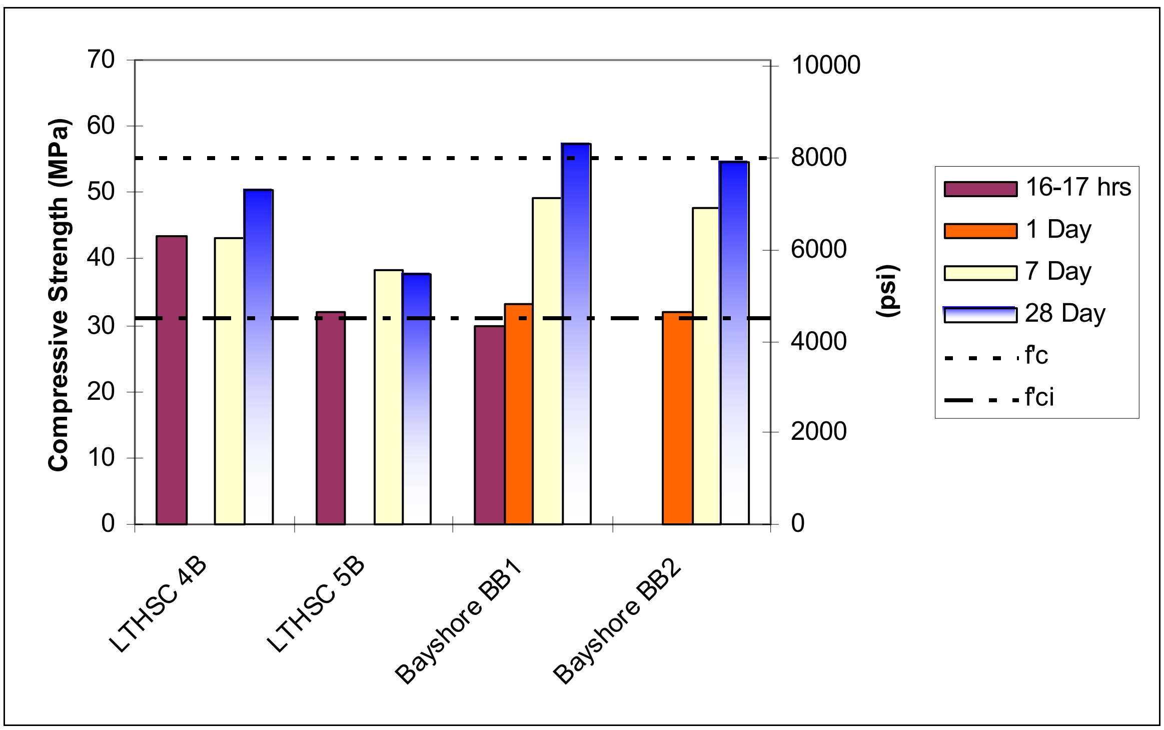

Figure 2 Accelerated Cure Compressive Strengths

4.3 Tensile Strength

Figure 3 presents the LTHSC tensile strengths at 17 hours, seven days, and 28 days. The figure also presents the AASHTO allowable release stress of 200 psi and the 28 day design cracking stress of 492 psi for lightweight aggregate concretes. The design cracking stress is calculated using the 28 day design compressive strength. The 17 hour tensile strengths were 4.1 MPa and 3.2 MPa (590 psi and 470 psi) for batch 4 and 5, respectively. The seven day tensile strengths were 4.0 MPa and 3.4 MPa (580 psi and 500 psi) for batches 2 and 3, respectively. The 28 day tensile strengths were 4.7 MPa, 4.5 MPa, 4.5 MPa, and 4.0 MPa (690 psi, 650 psi, 650 psi, and 580 psi) for batches 2 through 5, respectively. The 28 day tensile strengths were 4.8 MPa and 4.0 MPa (690 psi and 580 psi) for Bayshore beams 1 and 2, respectively.

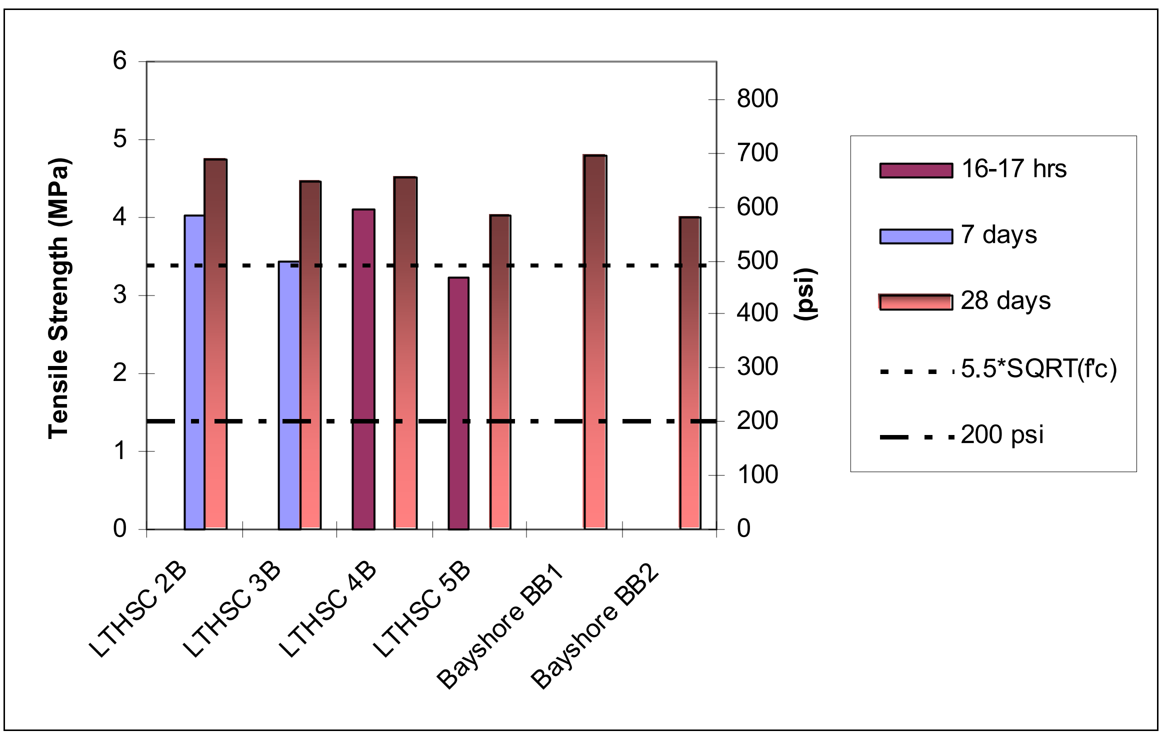

Figure 3 Tensile Strength

4.4 Modulus of Elasticity

4.4.1 Standard Cure

Figure 4 presents the lightweight high strength concrete standard cure modulus of elasticity at 7, 28, 56, and 90 days. The figure also presents the computed AASHTO design modulus of elasticity for lightweight aggregate concretes. The design modulus of elasticity is calculated using the 28 day design compressive strength and unit weight. The seven day modulus of elasticity was 20 GPa and 19 GPa (2.90 x10^6 psi and 2.74 x10^6 psi) for batch 2 and 3, respectively. The 28 day modulus of elasticity was 20 GPa and 19 GPa (2.96 x10^6 psi and 2.74 x10^6 psi) for batch 2 and 3, respectively. The 56 day modulus of elasticity was 21 GPa and 18 GPa (3.04 x10^6 psi and 2.64 x10^6 psi) for batch 2 and 3, respectively. The 90 day modulus of elasticity was 20 GPa and 20 GPa (2.94 x10^6 psi and 2.84 x10^6 psi) for batch 2 and 3, respectively.

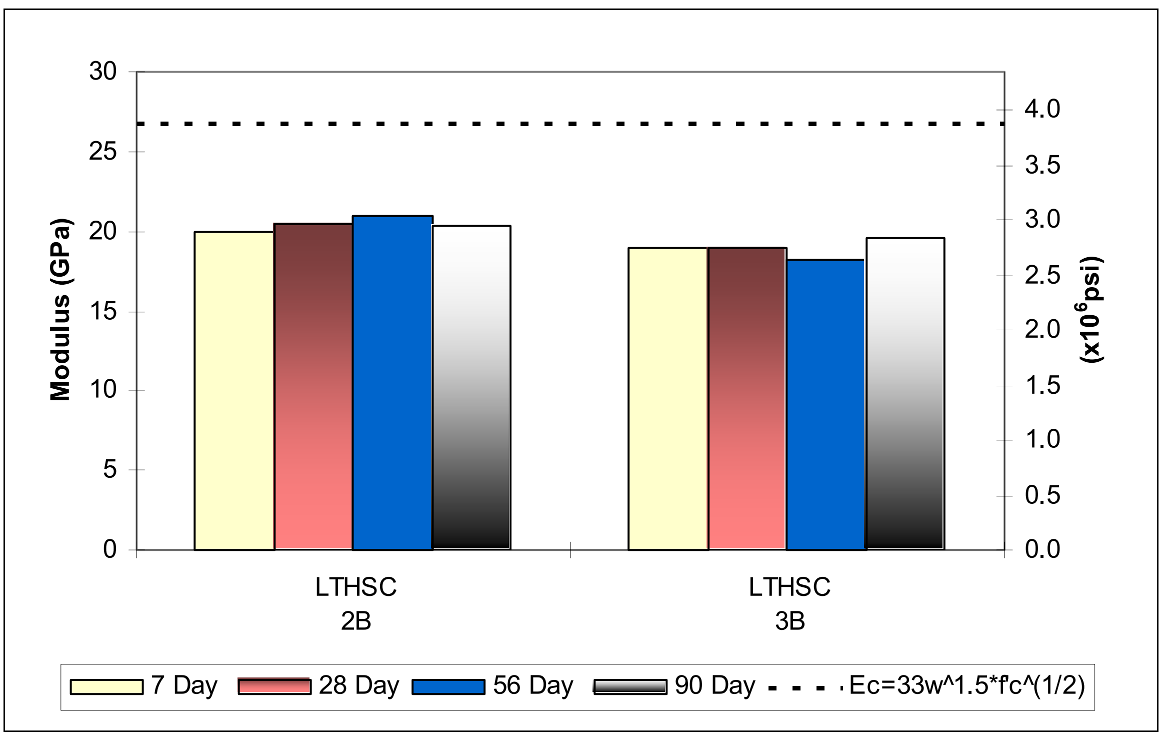

Figure 4 Standard Cure Modulus of Elasticity

4.4.2 Accelerated Cure

Figure 5 presents the LTHSC accelerated cure modulus of elasticity at 17 hours, seven days, 28 days, 56 days, and 90 days. The figure also presents the computed AASHTO design modulus of elasticity for lightweight aggregate concretes. The design modulus of elasticity is calculated using the 28 day design compressive strength and unit weight. The 17 hour modulus of elasticity was 22 GPa and 19 GPa (3.23 $x10^6$ psi and 2.70 $x10^6$ psi) for batch 4 and 5, respectively. The seven day modulus of elasticity was 18 GPa and 19 GPa (2.67 $x10^6$ psi and 2.82 $x10^6$ psi) for batch 4 and 5, respectively. The 28 day modulus of elasticity was 18 GPa and 20 GPa (2.64 $x10^6$ psi and 2.94 $x10^6$ psi) for batch 4 and 5, respectively. The 28 day modulus of elasticity was 20 GPa and 21 GPa (2.91 $x10^6$ psi and 3.04 $x10^6$ psi) for the Bayshore beams 1 and 2, respectively. The 56 day modulus of elasticity was 21 GPa and 18 GPa (3.07 $x10^6$ psi and 2.62 $x10^6$ psi) for batch 4 and 5, respectively. The 90 day modulus of elasticity was 20 GPa and 16 GPa (2.85 $x10^6$ psi and 2.32 $x10^6$ psi) for batch 4 and 5, respectively.

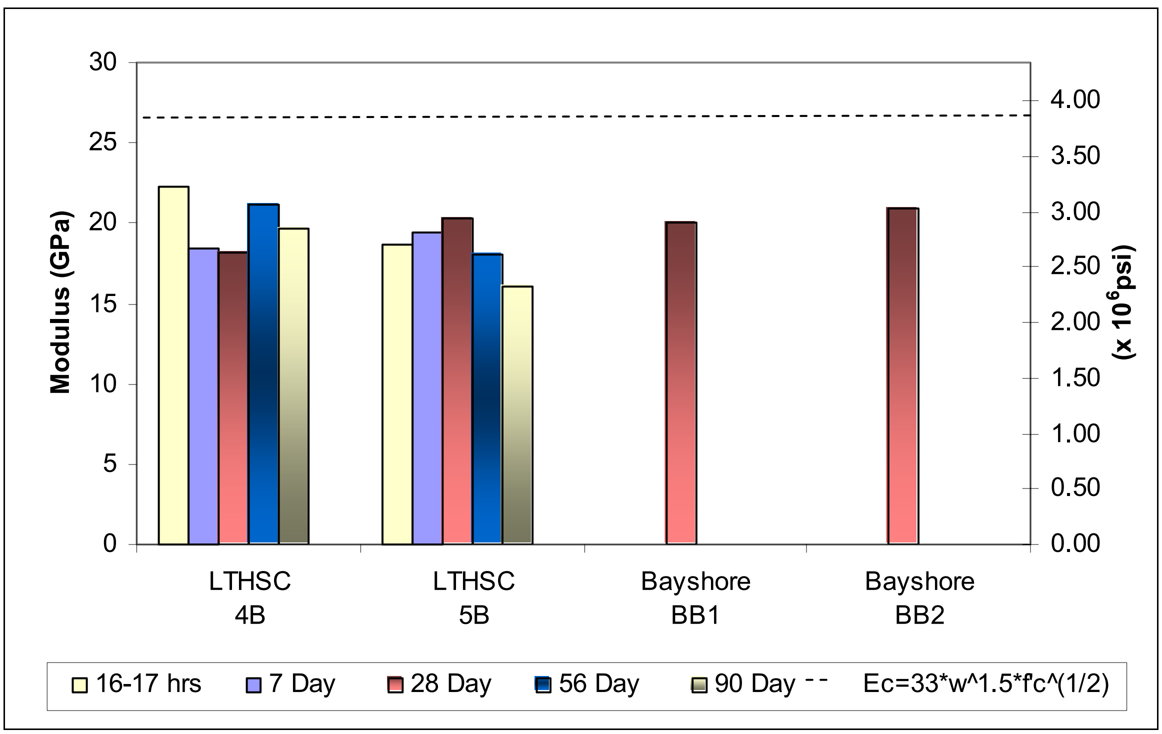

Figure 5 Accelerated Cure Modulus of Elasticity

4.5 Thermal Coefficient

The coefficient of thermal expansion for the LTHSC mixture was found to be 5.3 microstrain per ^{o}F (9.5 microstrain per ^{o}C) with a confidence interval of ± 0.13 microstrain microstrain per ^{o}F (±0.24 microstrain per ^{o}C).

4.6 Experimental and Predicted Strains

This section presents the experimental and predicted total, shrinkage, and creep strains. The deformations were measured at least weekly, but for time frames greater than 28 days, a value is presented only every four weeks.

Figures 6 through 9 present the experimental strains from two standard cure and two accelerated cure batches. At a given time, each strain value is the average value from three specimens with the error bars representing the 95 percent confidence limits. The 95 percent confidence limits represent the probability of 95 out of 100 population measurements falling within the specified range. The error bars can also be described as being at a five percent significant level.

Total strain specimens for each batch are in the same load frame so there is no deviation in the applied stress within a batch. The accelerated and standard cure batches were initially loaded to 40 percent of the one day and seven day compressive strengths, respectively. The applied stress of 40 percent of the compressive strength was maintained by increasing the load at seven and 28 days for the accelerated cure batches and at 28 days for the standard cure batches.

The total, shrinkage, and creep strains are predicted with the four most current creep and shrinkage prediction models. The following models are included:

- ACI 209R-92 (ACI 209)
- Comite Euro-International Du Beton Model Code 1990 (CEB 90)
- Bazant’s B3 Model (B3)
- Gardner and Lockman’s GL2000 Model (GL2000)

The SAK model by Sakata was also considered, but was not included because of the limitations in the scope of mixtures used during model development and the age of loading for accelerated curing.

ACI 209 model was applied when predicting prestressed concrete losses for the Virginia Route 106 bridge over the Chickahominy River.

Figures 10 through 17 present the predicted total, shrinkage, and creep strains. The values are predicted using the experimentally measured compressive strengths and modulus of elasticity for each batch. If the LTHSC design strength was used, the elastic strain would have been under predicted based on the measured values and current prediction equations. Time dependent deformation would also be under predicted based on the strength. A strong cement paste matrix is more resistant to time dependent losses than a weaker matrix.

Model details are presented in Appendix A.

4.6.1 Standard Cure Experimental Strains

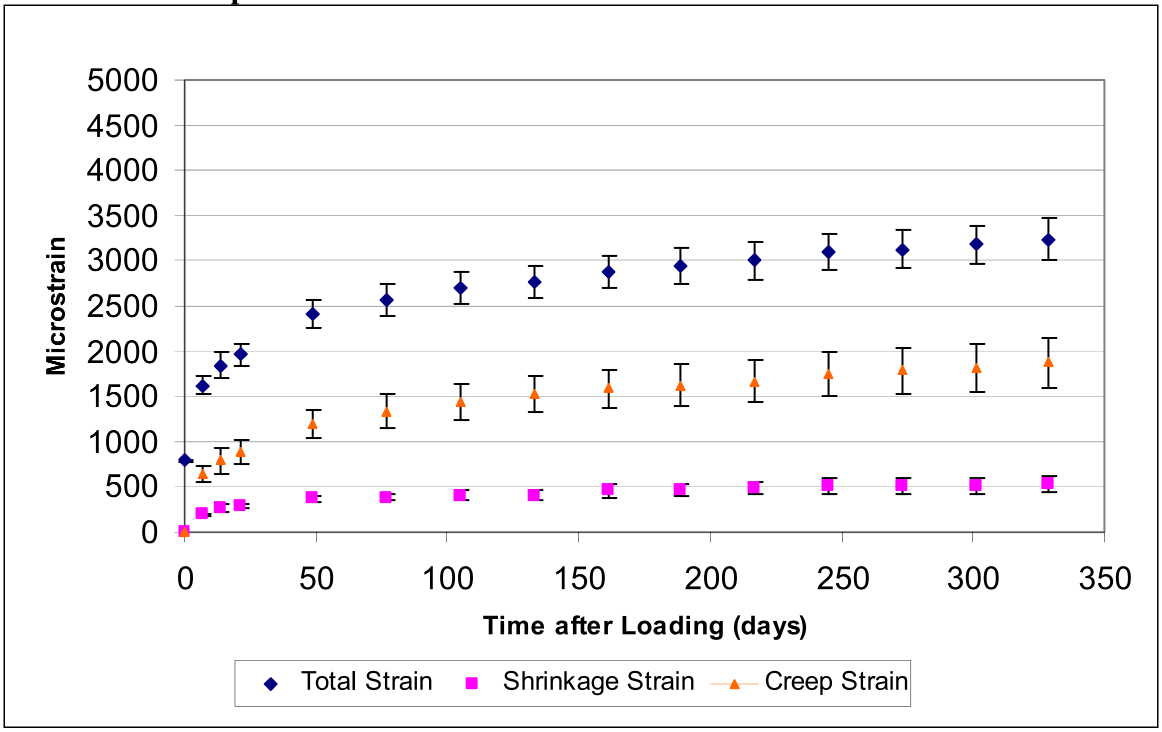

Figure 6 Standard Cure Batch 2: Total, Creep, and Shrinkage Strain (6 by 12 in. cylinders)

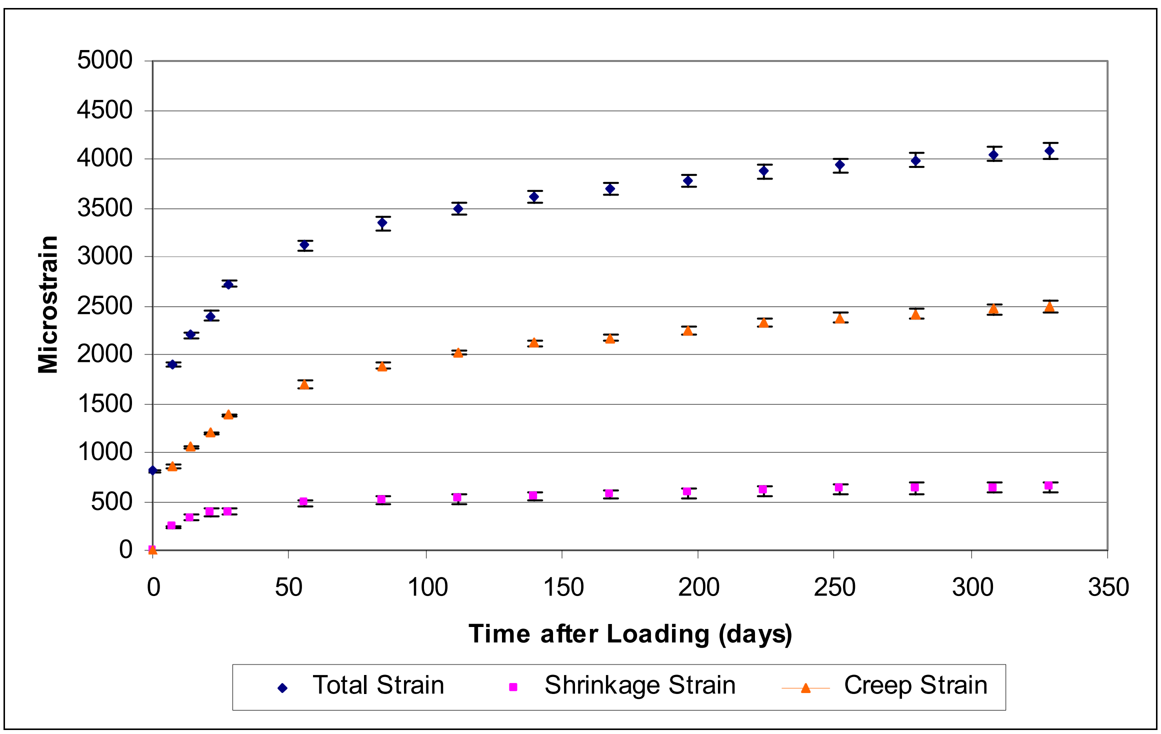

Figure 7 Standard Cure Batch 3: Total, Creep, and Shrinkage Strain (6 by 12 in. cylinders)

4.6.2 Accelerated Cure Experimental Strains

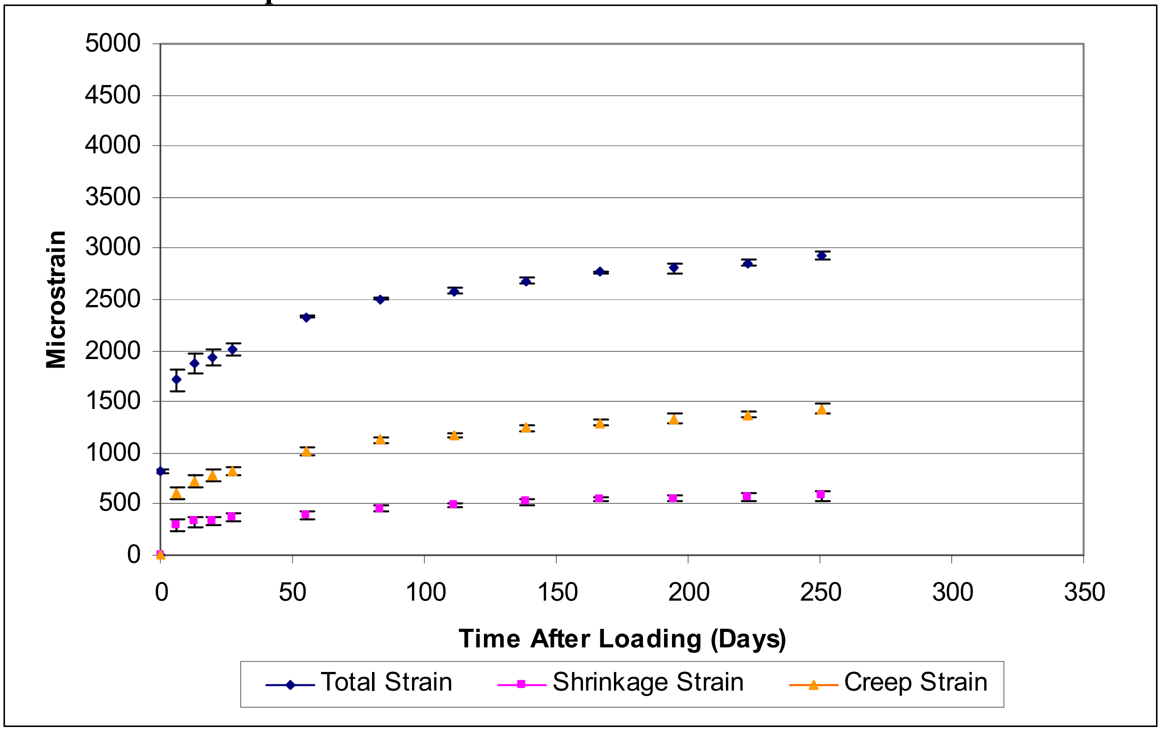

Figure 8 Accelerated Cure Batch 4: Total, Creep, and Shrinkage Strain (4 by 8 in. cylinders)

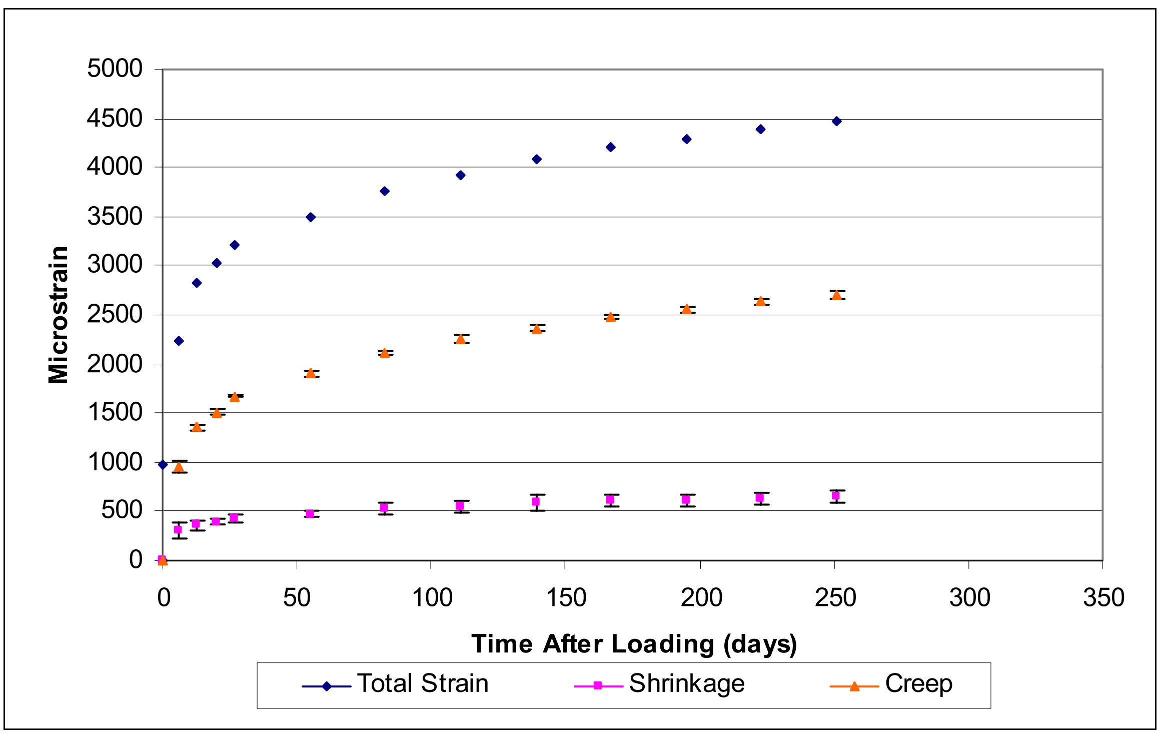

Figure 9 Accelerated Cure Batch 5: Total, Creep, and Shrinkage Strain (4 by 8 in. cylinders)

4.6.3 Standard Cure Predicted Strains

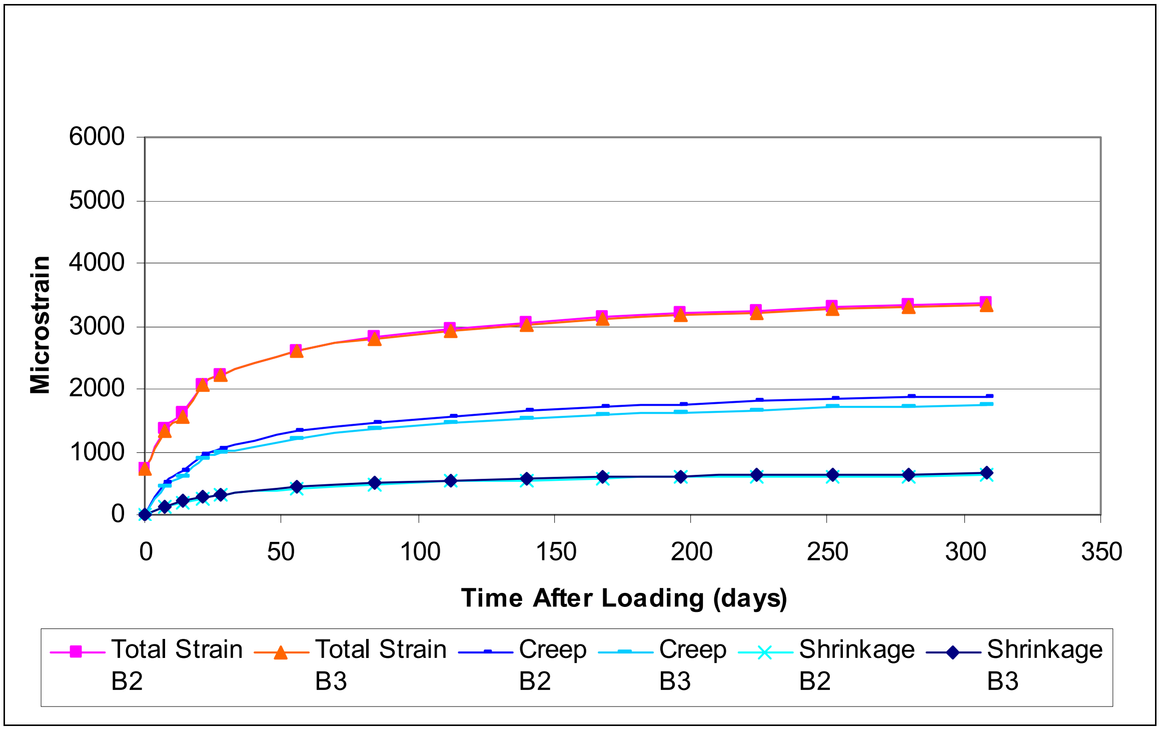

Figure 10 ACI 209 Standard Cure

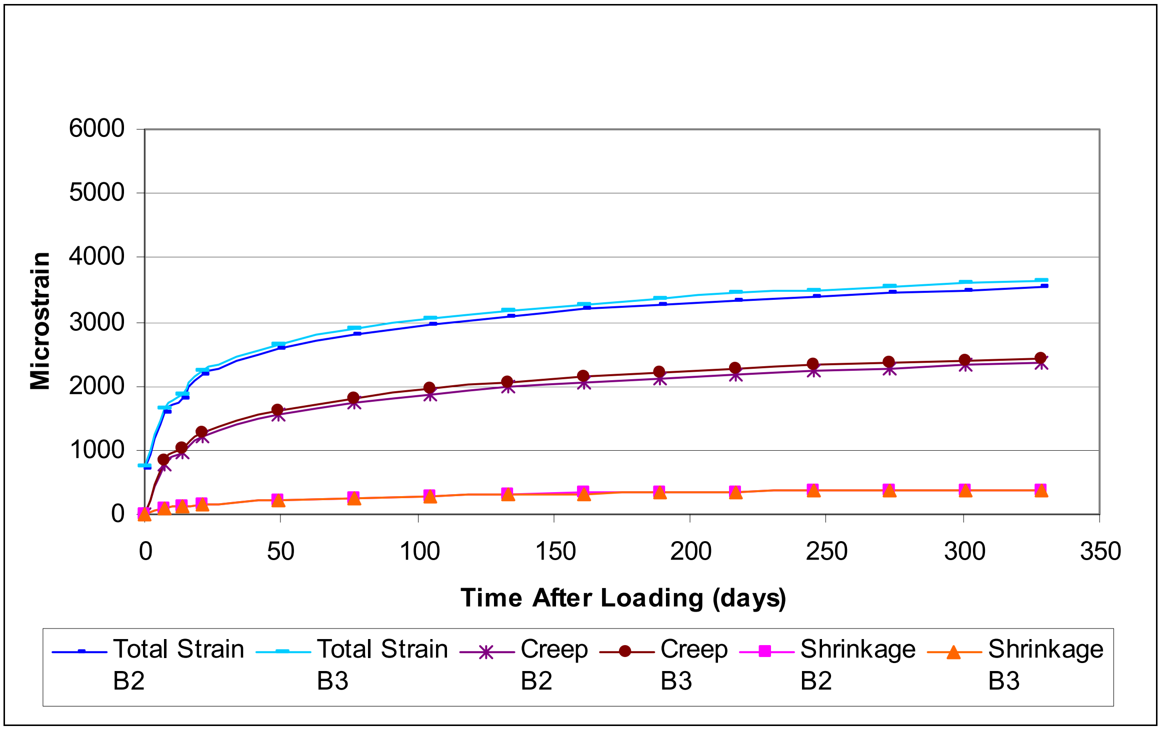

Figure 11 CEB 90 Standard Cure

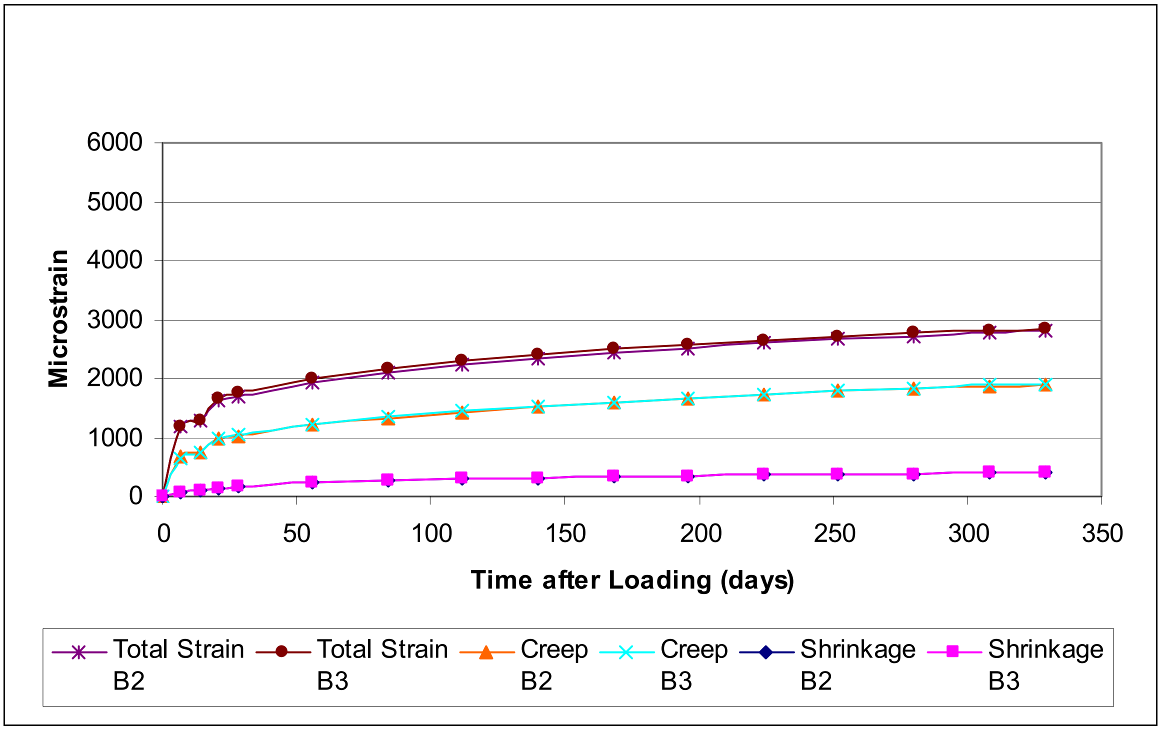

Figure 12 B3 Standard Cure

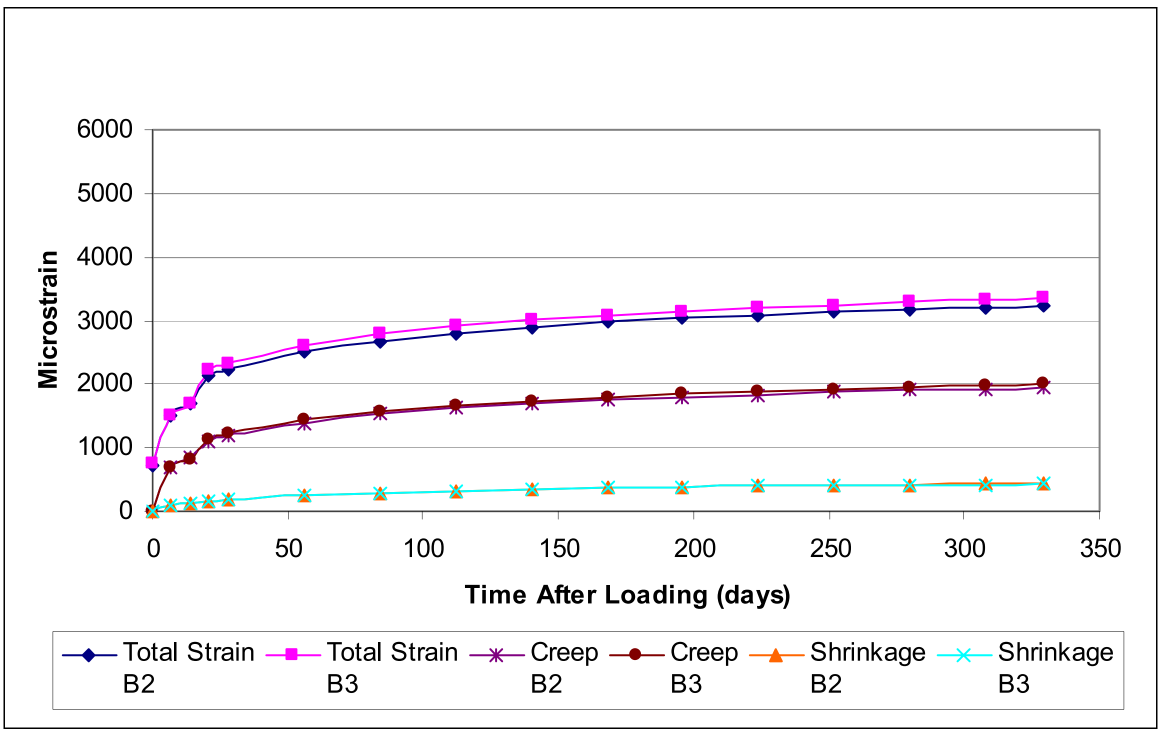

Figure 13 GL2000 Standard Cure

4.6.4 Predicted Accelerated Cure Strains

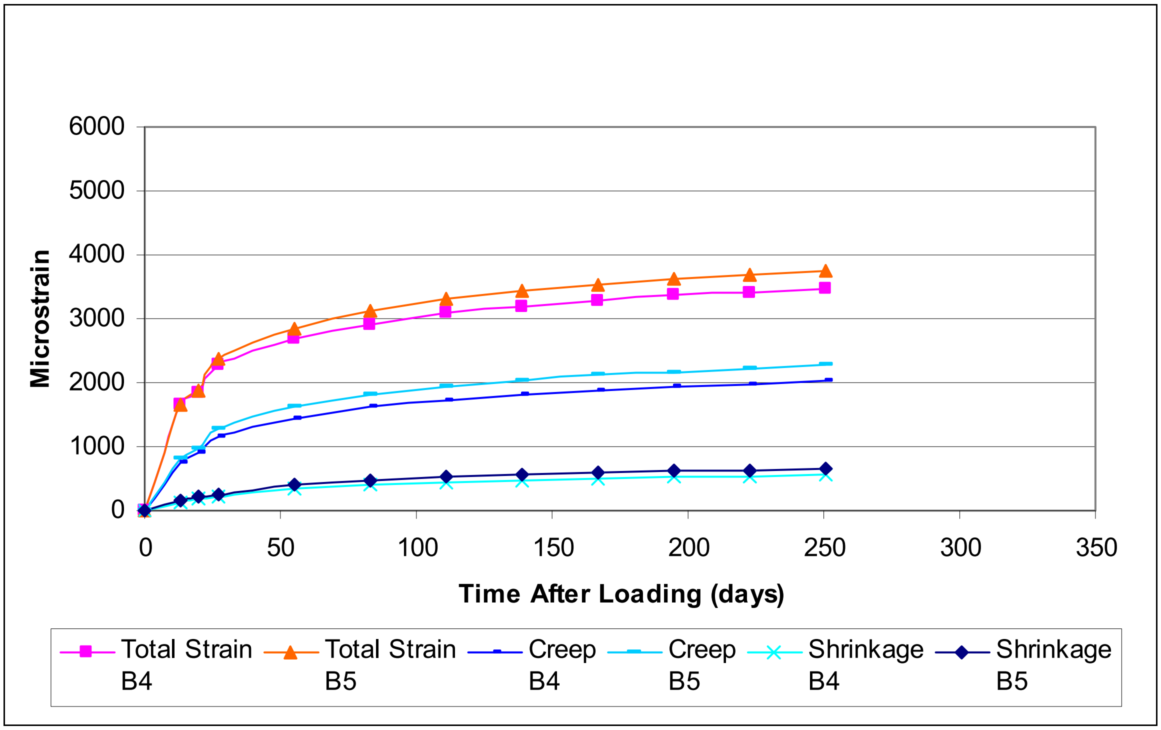

Figure 14 ACI 209 Accelerated Cure

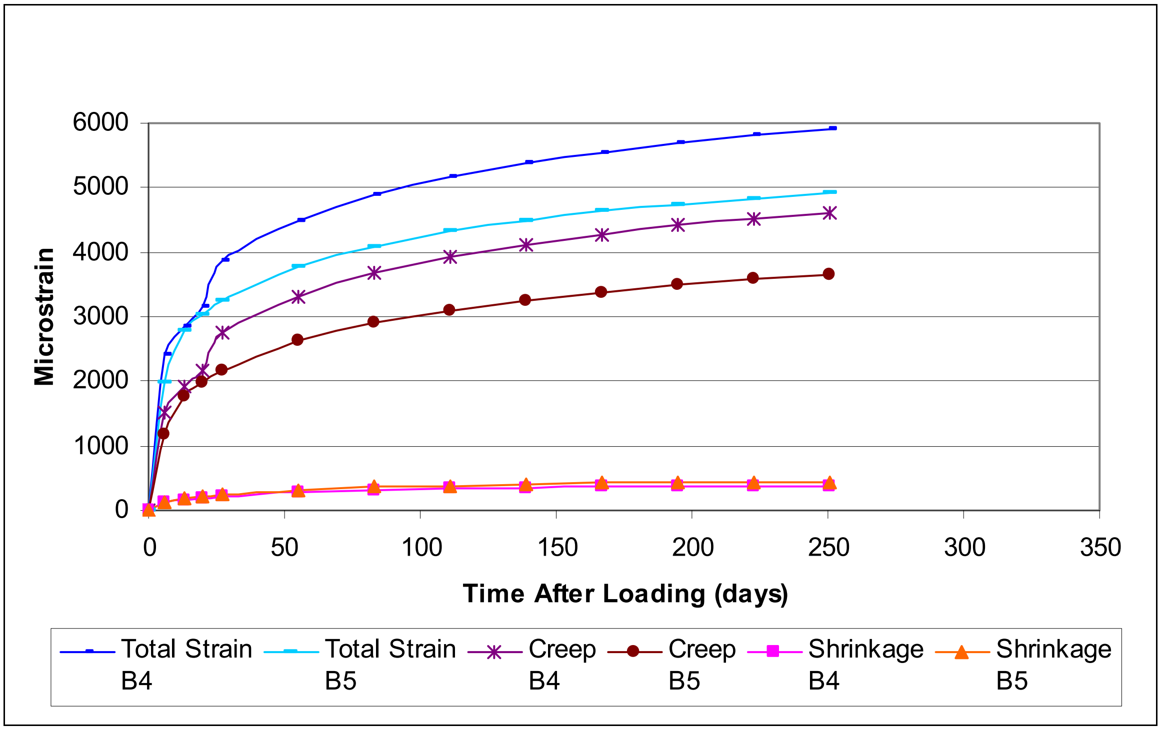

Figure 15 CEB 90 Accelerated Cure

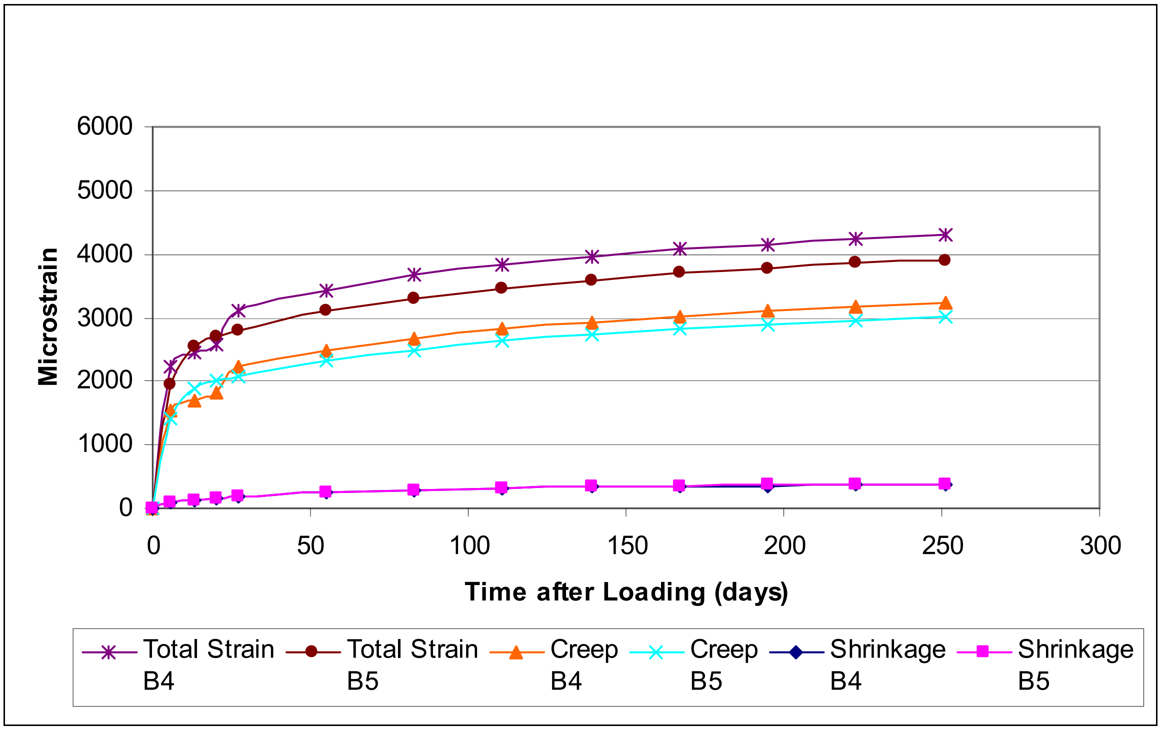

Figure 16 B3 Accelerated Cure

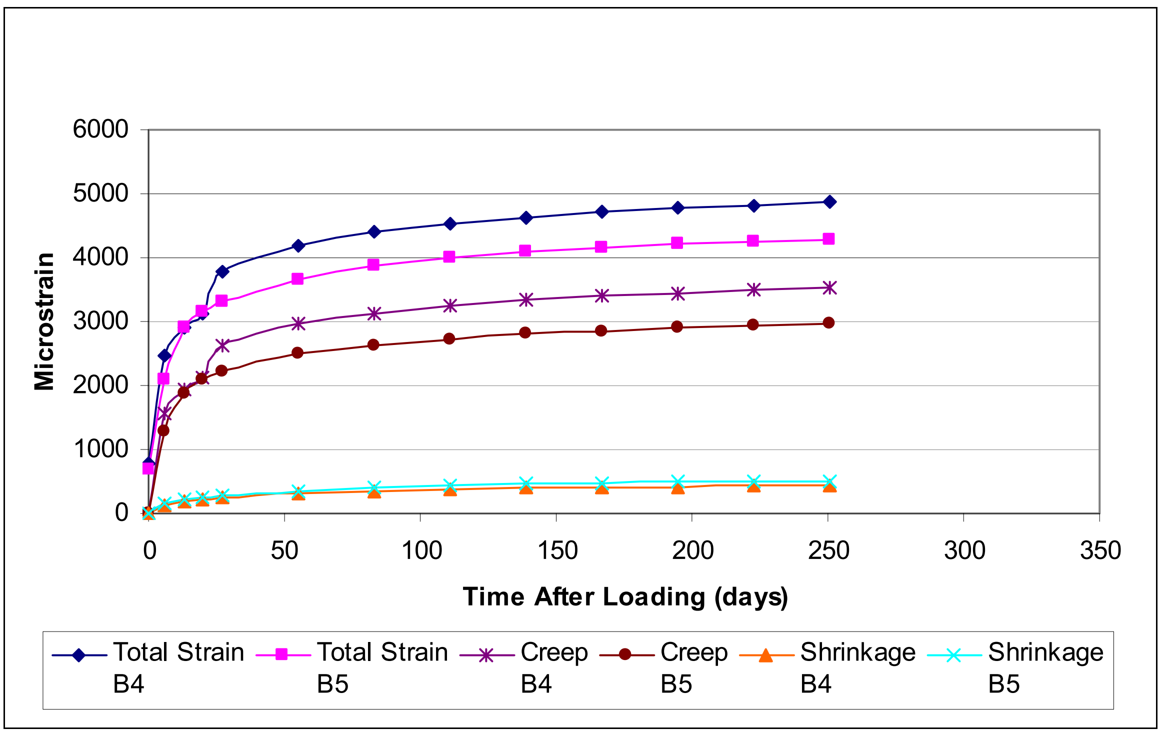

Figure 17 GL2000 Accelerated Cure

4.7 Prediction Model Residuals

A residual is the difference between a model and the experimental value at a given time. Residuals identify a model as either over predicting, a positive value, or under predicting, a negative value. The residuals are calculated as the predicted model mean for a batch minus the experimental value for a test specimen at a given time.

Figures 18 through 39 present the residuals plotted over time. The residuals are plotted as the mean and the 95 percent confidence limits at the given test time. The standard cure residuals are for batches 2 and 3 combined for a total of six test values. Whereas the accelerated cure residuals are for batches 4 and 5 separately.

4.7.1 Standard Cure Total Strain Residuals

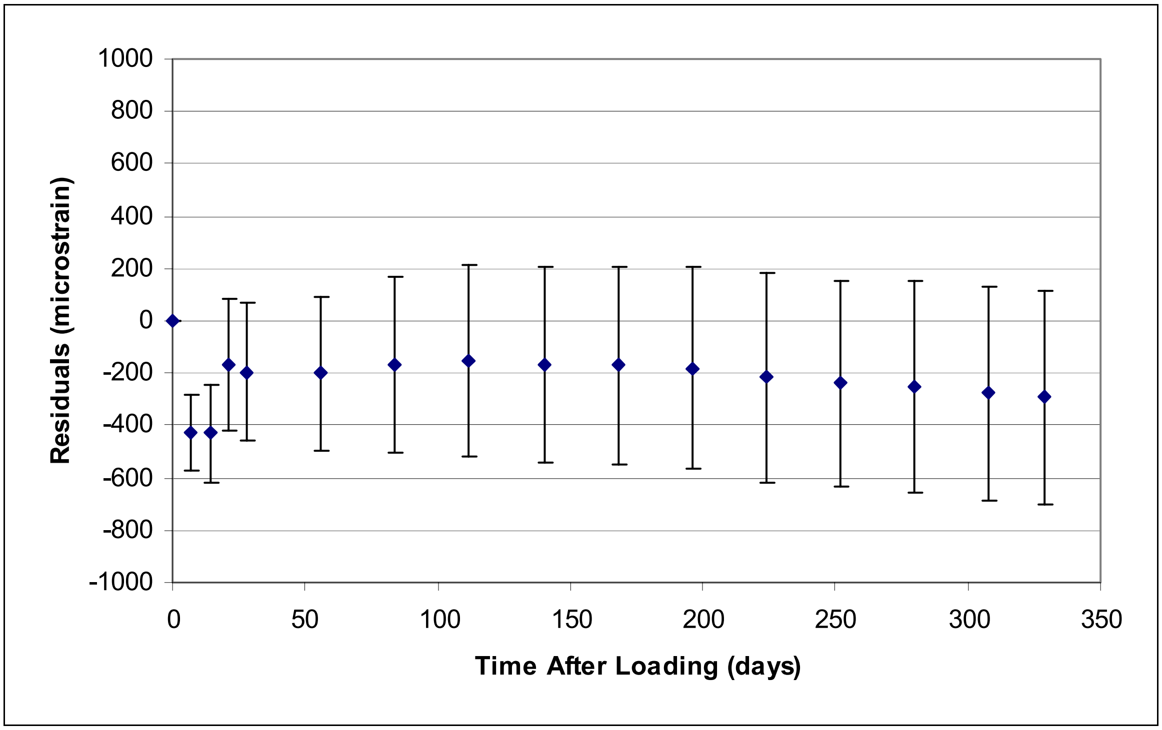

Figure 18 ACI 209 and Standard Cure Total Strain Residuals

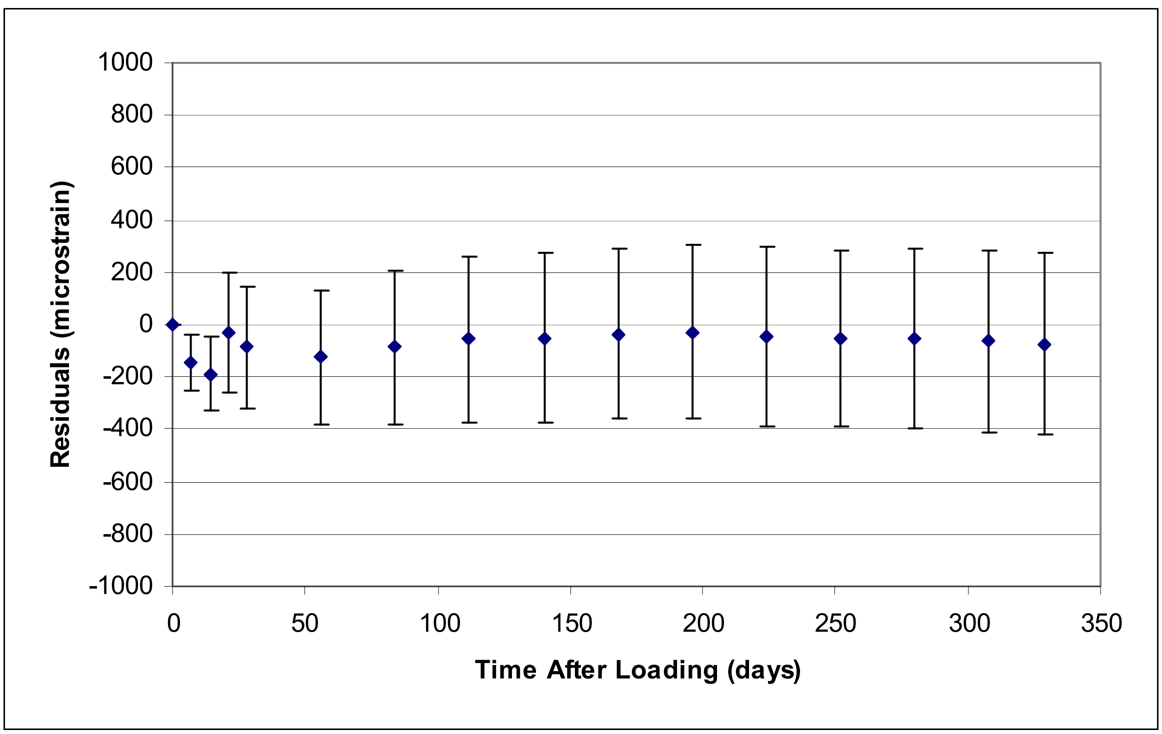

Figure 19 CEB 90 and Standard Cure Total Strain Residuals

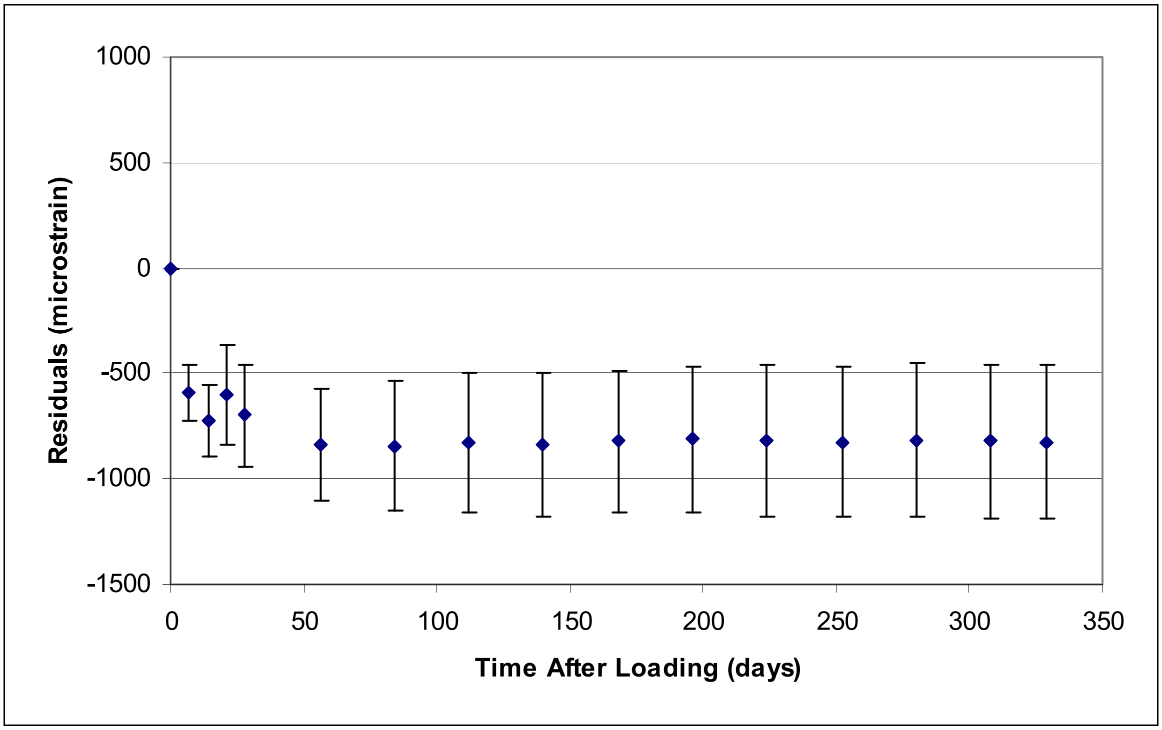

Figure 20 B3 and Standard Cure Total Strain Residuals

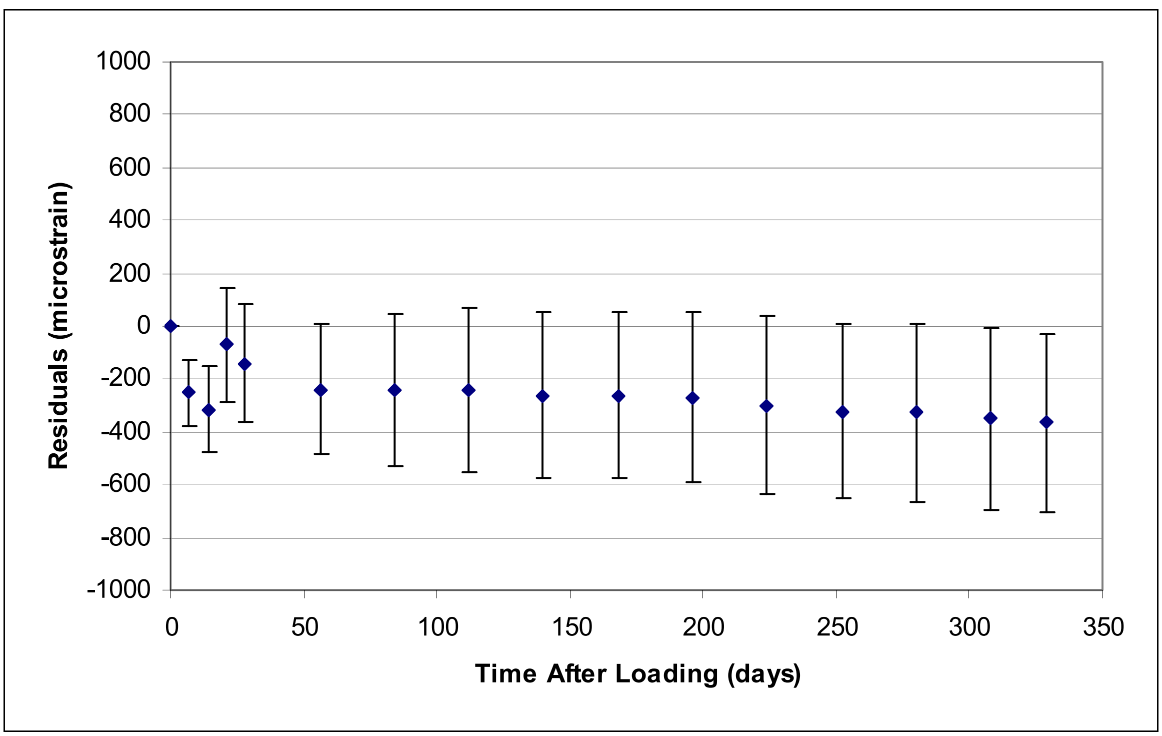

Figure 21 GL2000 and Standard Cure Total Strain Residuals

4.7.2 Standard Cure Shrinkage Strain Residuals

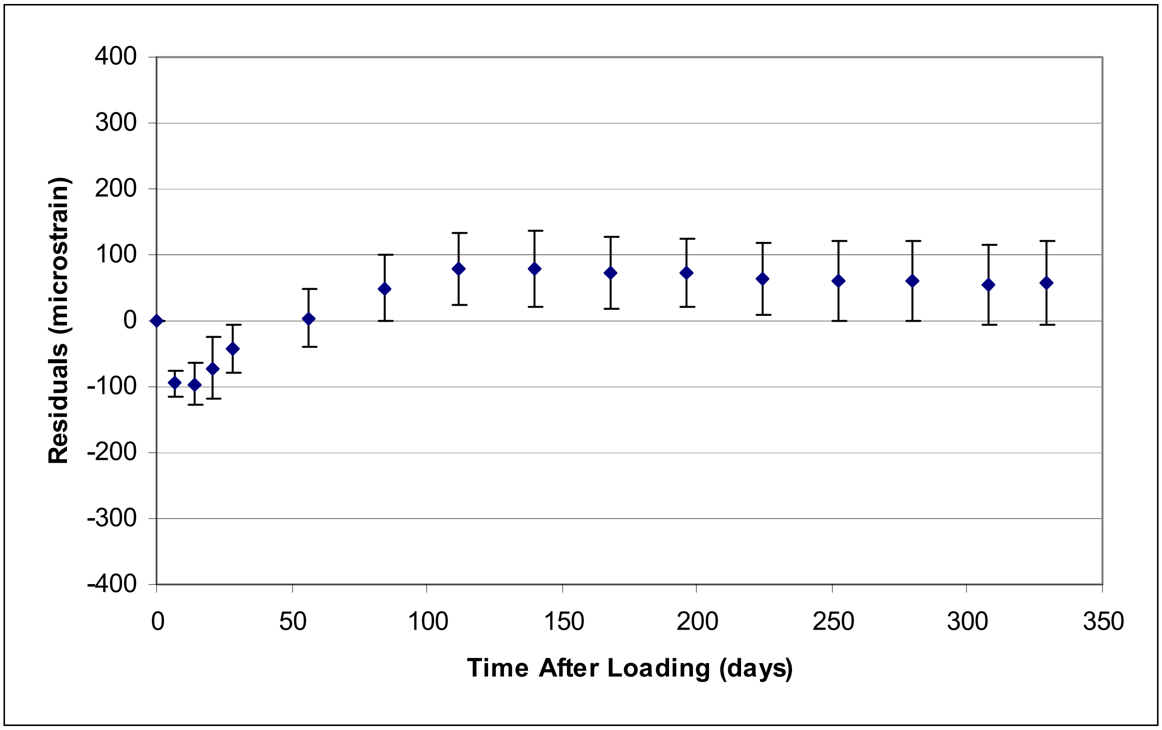

Figure 22 ACI 209 and Standard Cure Shrinkage Residuals

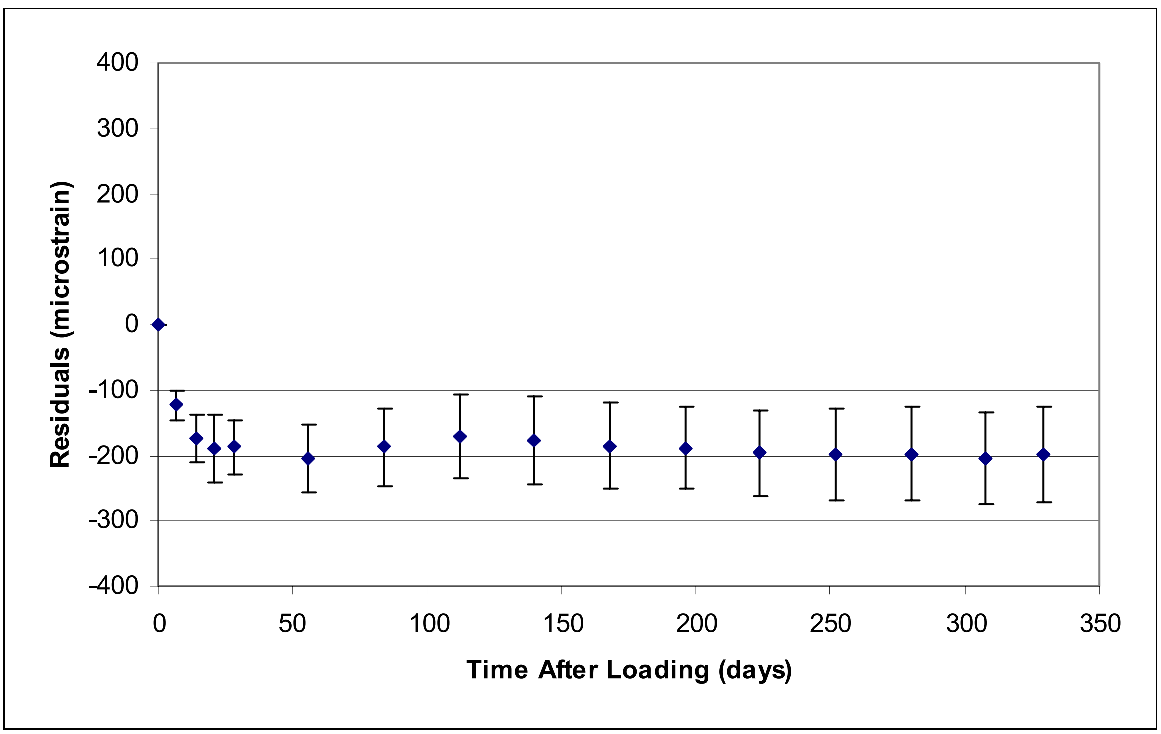

Figure 23 CEB 90 and Standard Cure Shrinkage Residuals

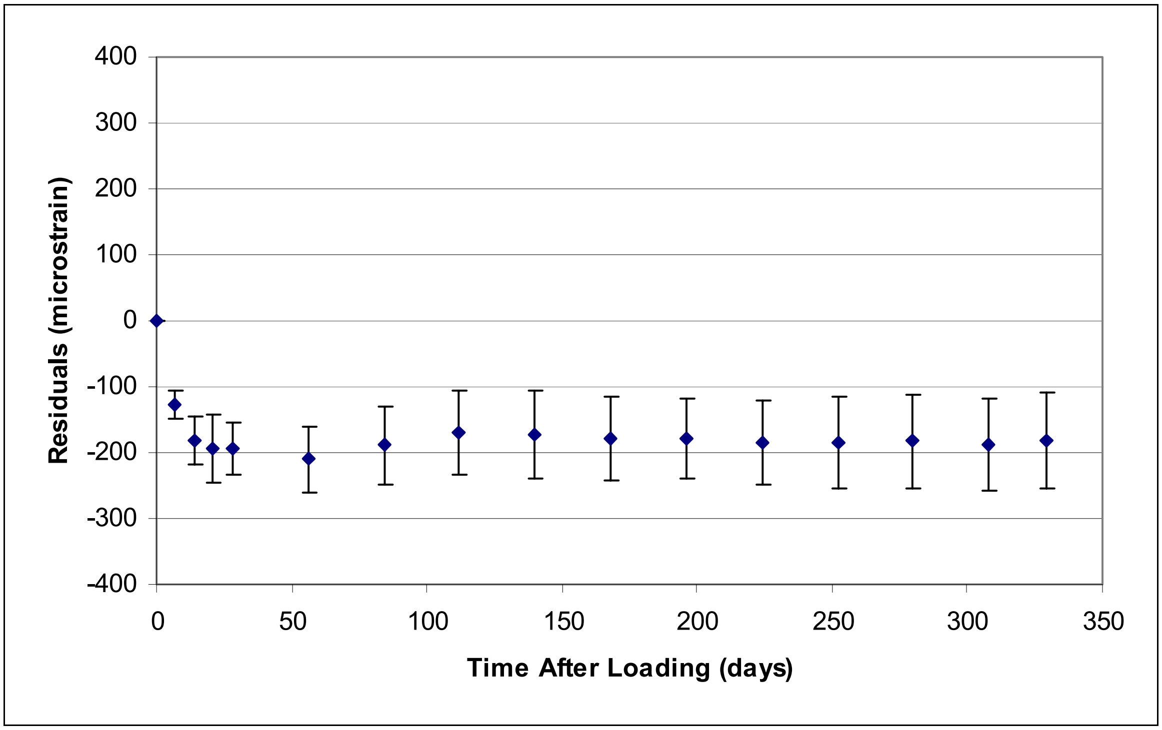

Figure 24 B3 and Standard Cure Shrinkage Residuals

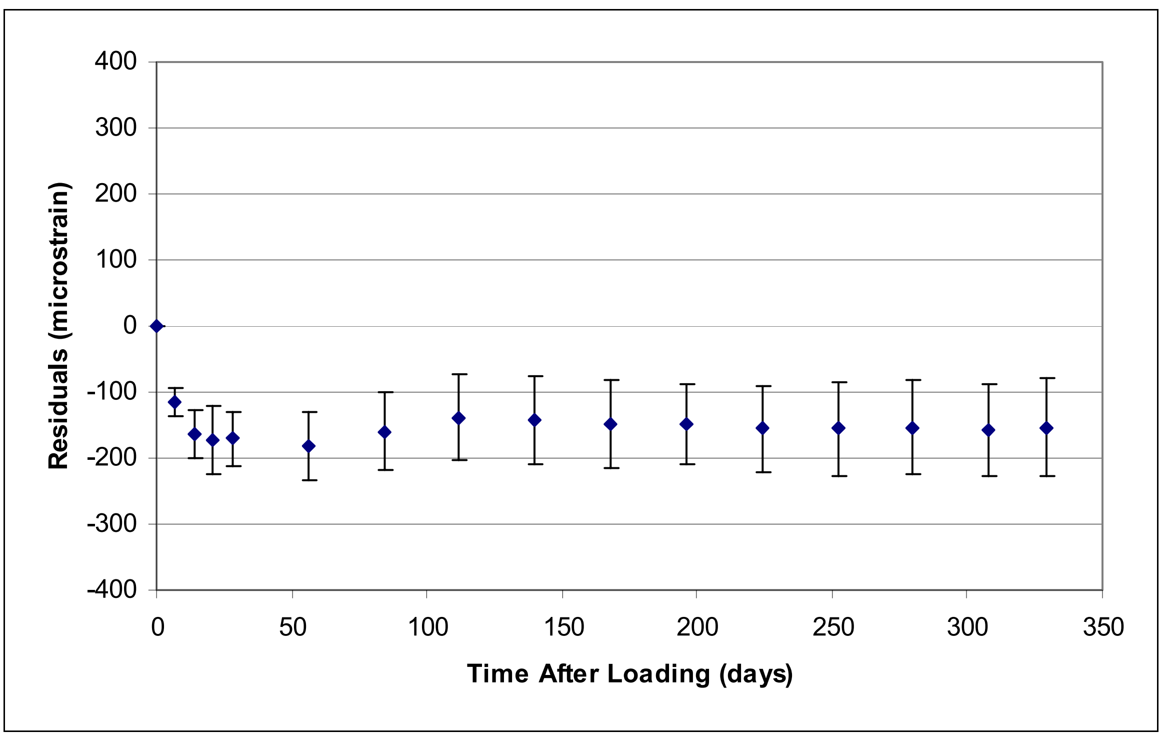

Figure 25 GL2000 and Standard Cure Shrinkage Residuals

4.7.3 Standard Cure Creep Strain Residuals

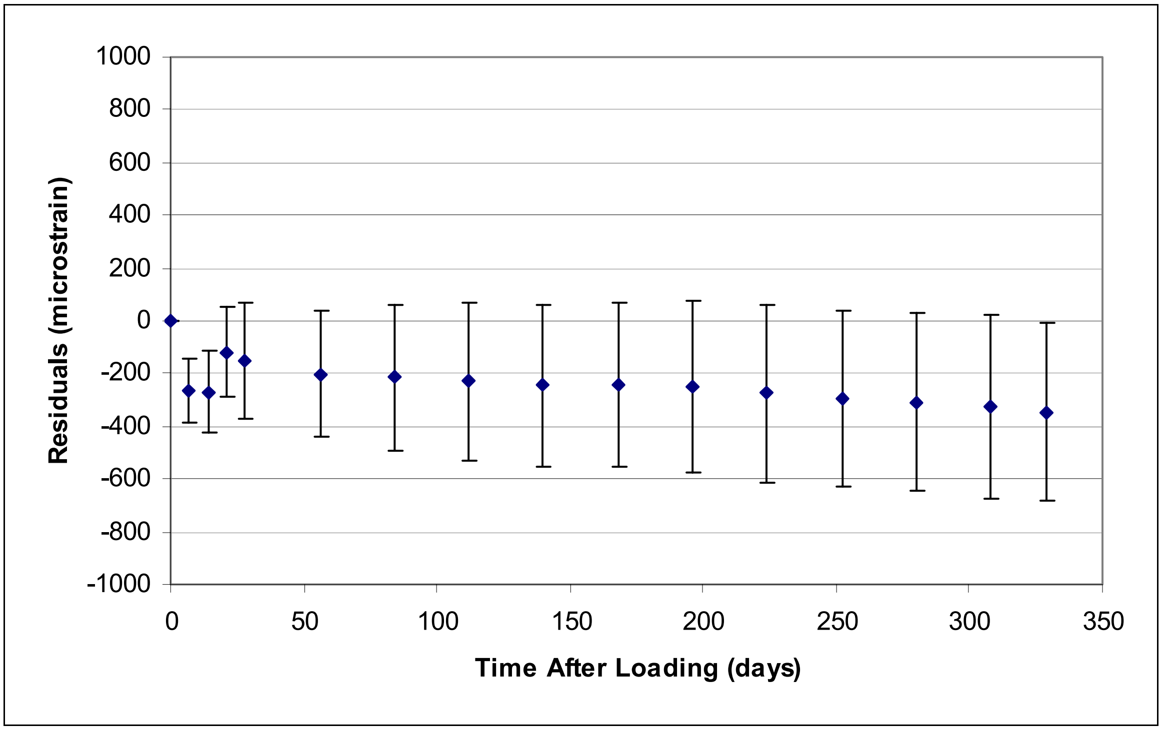

Figure 26 ACI 209 and Standard Cure Creep Residuals

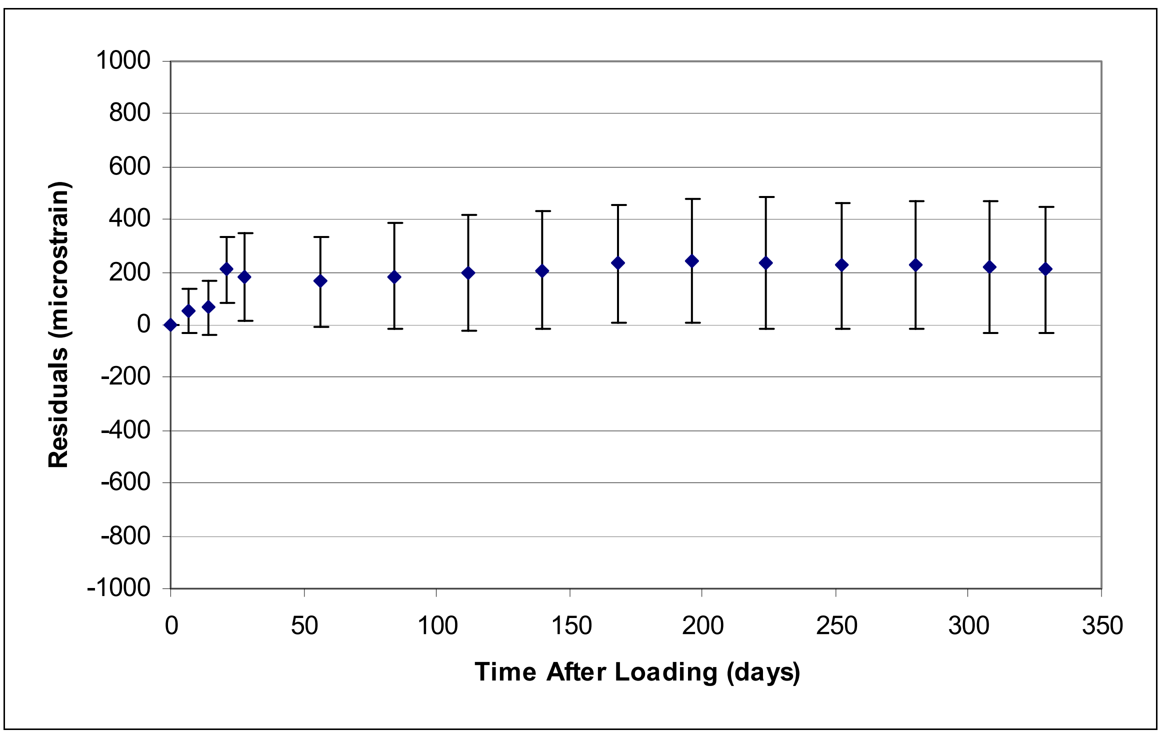

Figure 27 CEB 90 and Standard Cure Creep Residuals

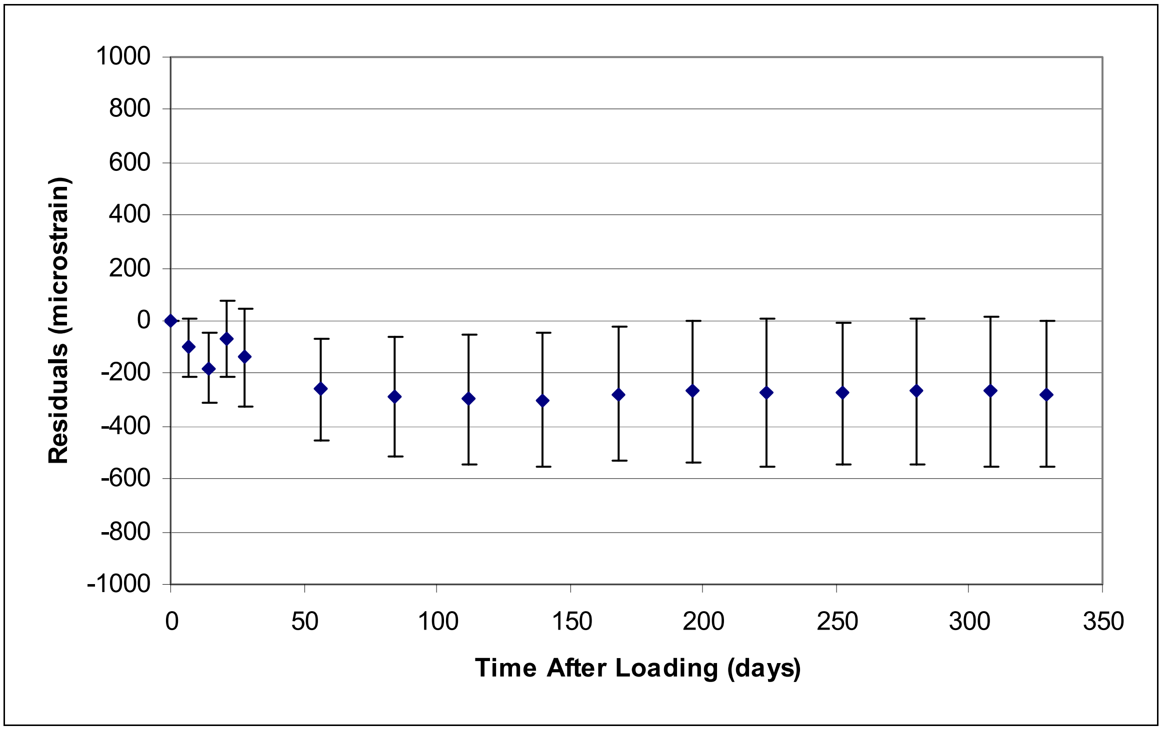

Figure 28 B3 and Standard Cure Creep Residuals

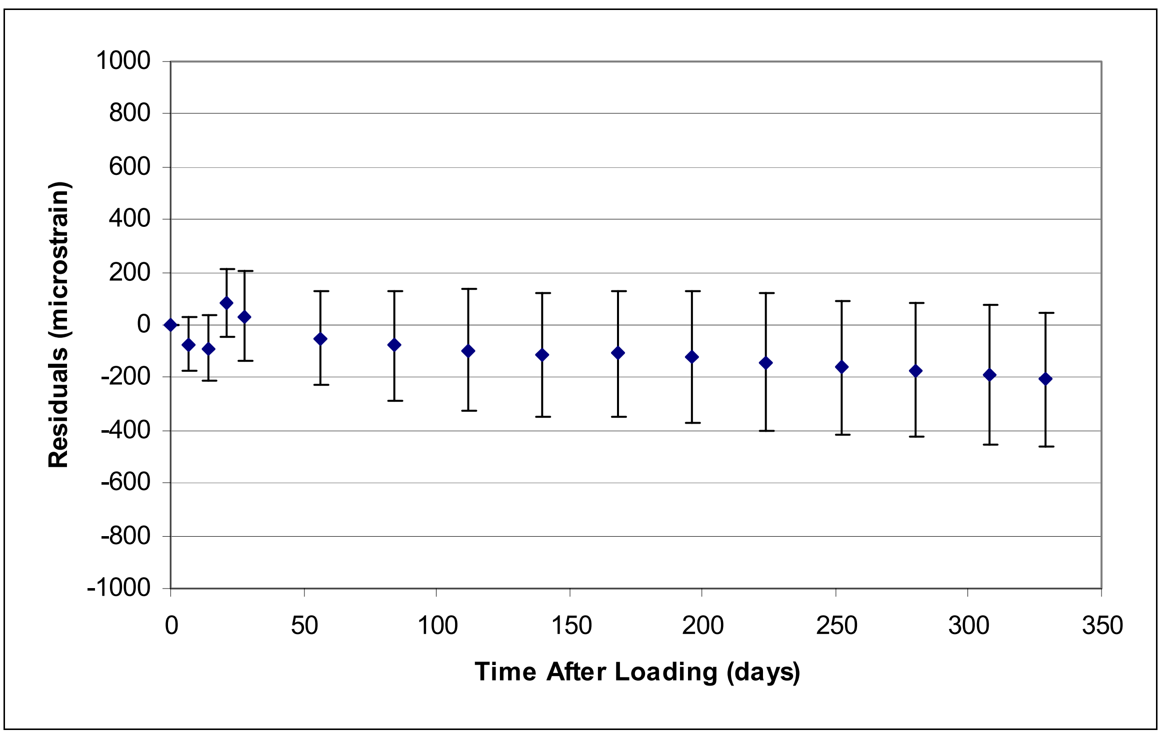

Figure 29 GL2000 and Standard Cure Creep Residuals

4.7.4 Accelerated Cure Total Strain Residuals

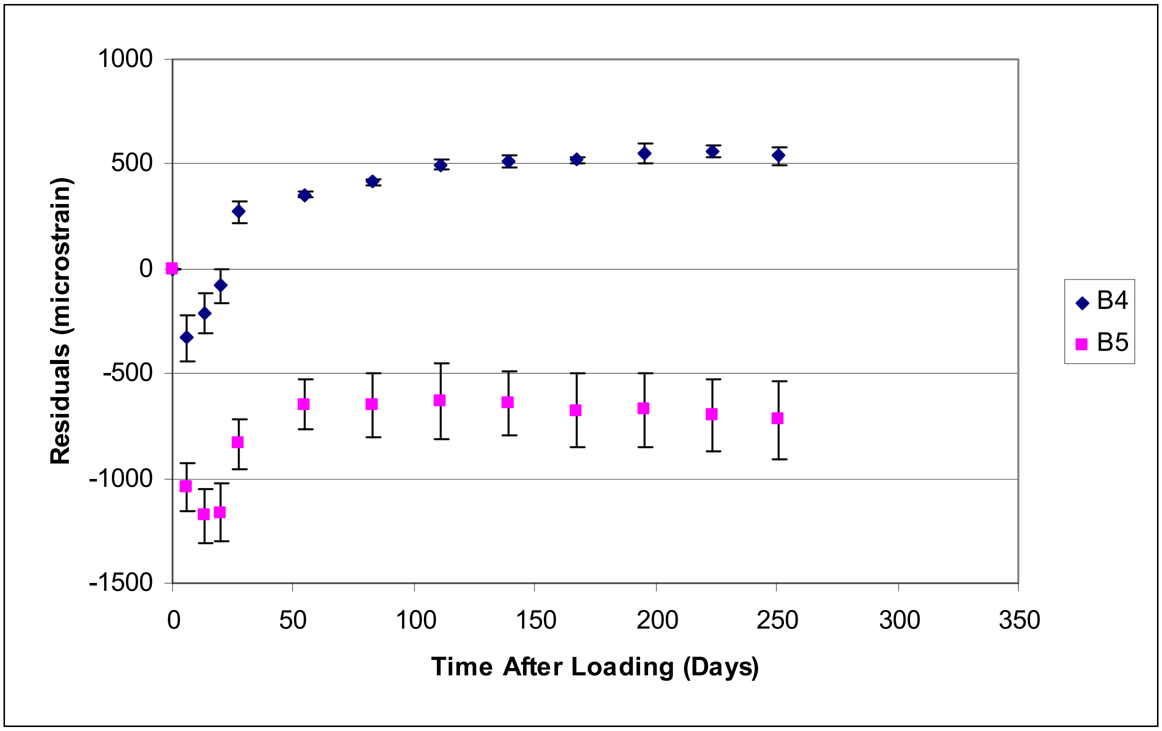

Figure 30 ACI 209 and Accelerated Cure Total Strain Residuals per Batch

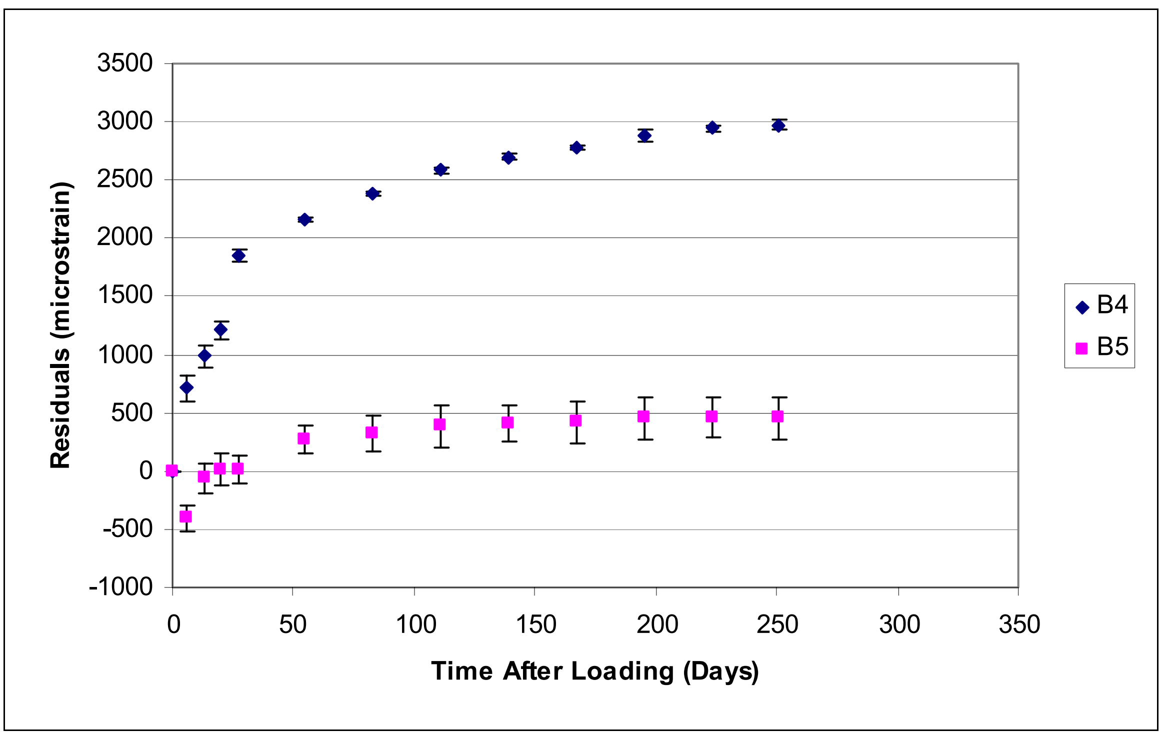

Figure 31 CEB 90 and Accelerated Cure Total Strain Residuals per Batch

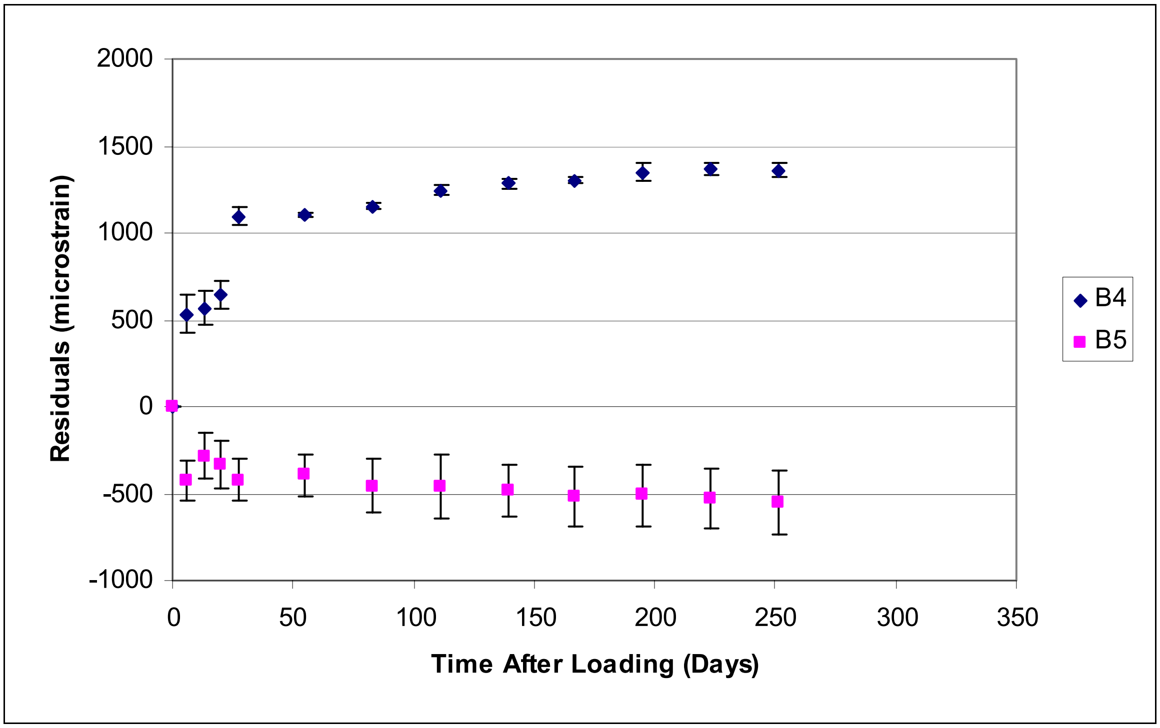

Figure 32 B3 and Accelerated Cure Total Strain Residuals per Batch

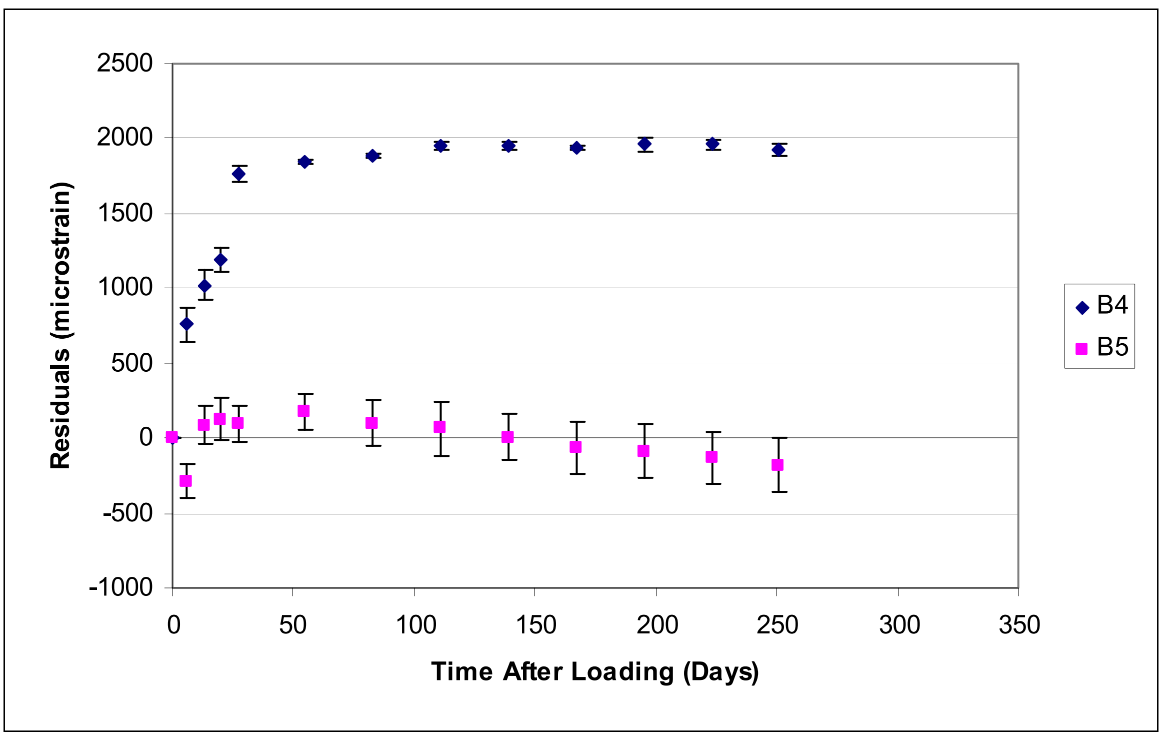

Figure 33 GL2000 and Accelerated Cure Total Strain Residuals per Batch

4.7.5 Accelerated Cure Shrinkage Strain Residuals

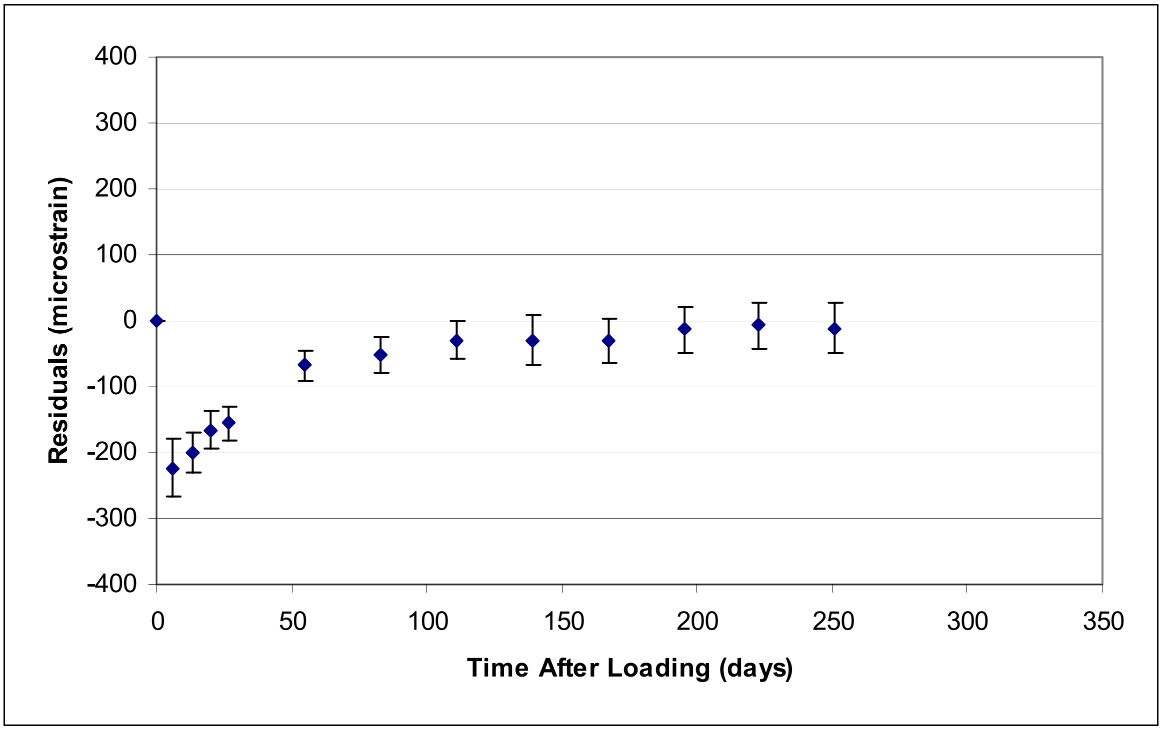

Figure 34 ACI 209 and Accelerated Cure Shrinkage Residuals

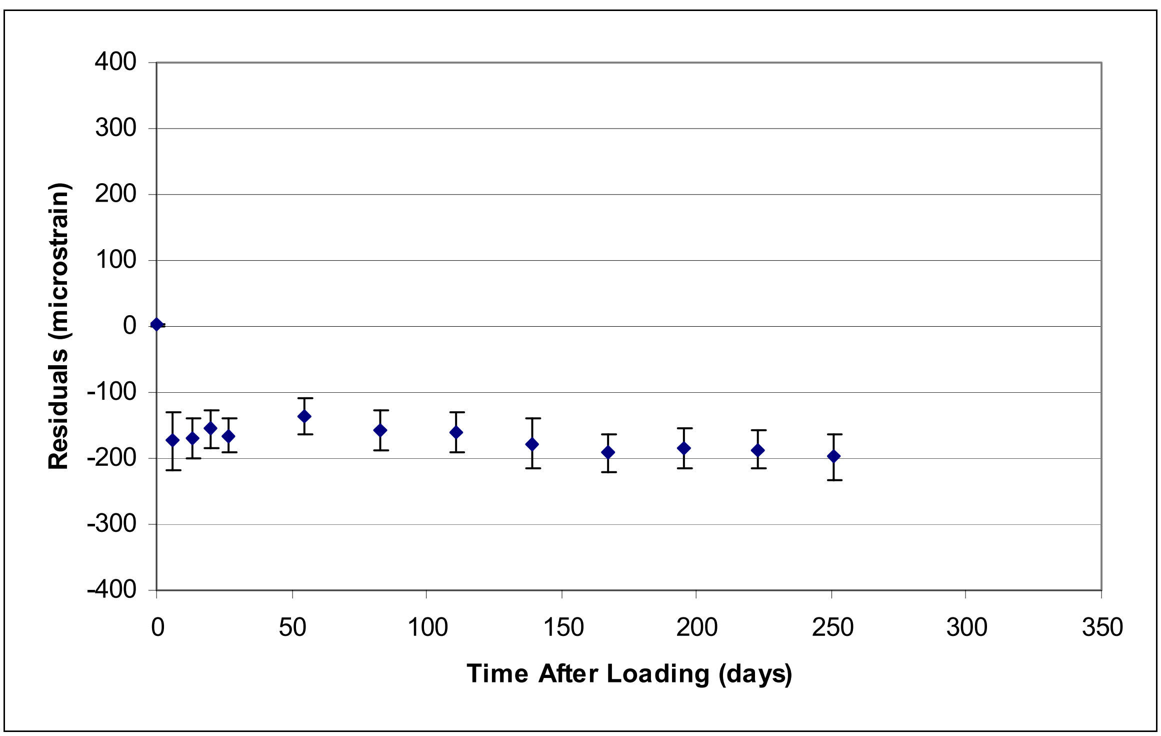

Figure 35 CEB 90 and Accelerated Cure Shrinkage Residuals

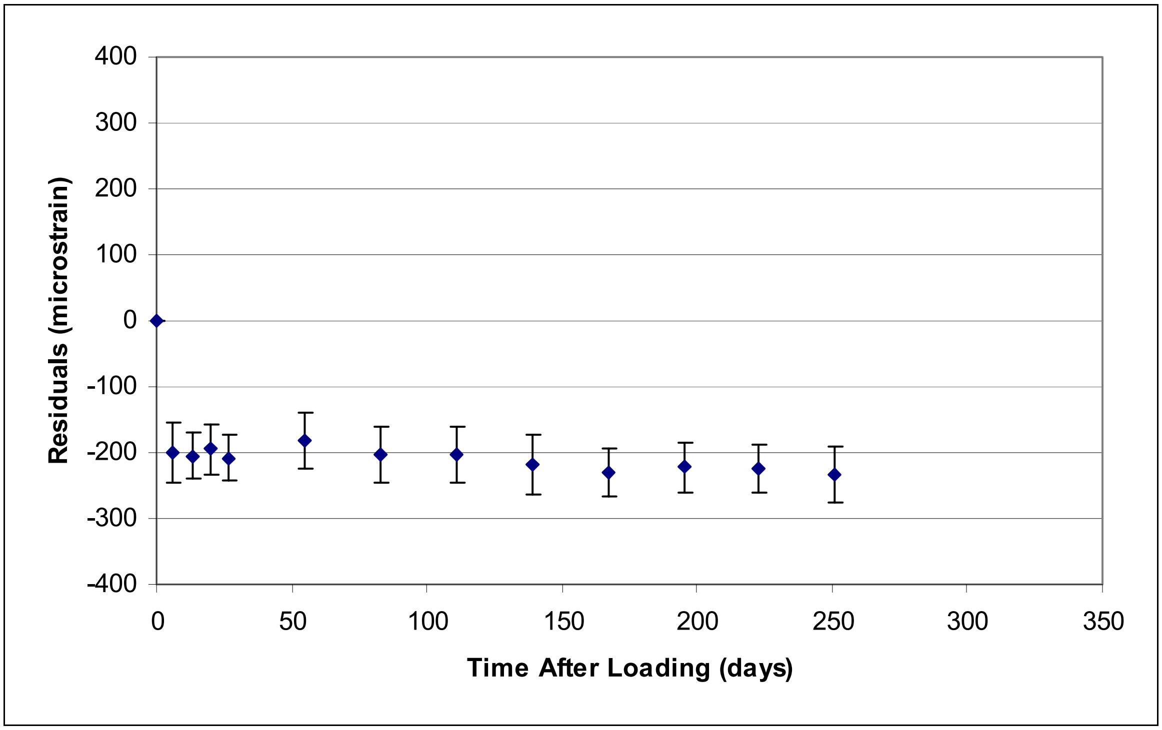

Figure 36 B3 and Accelerated Cure Shrinkage Residuals

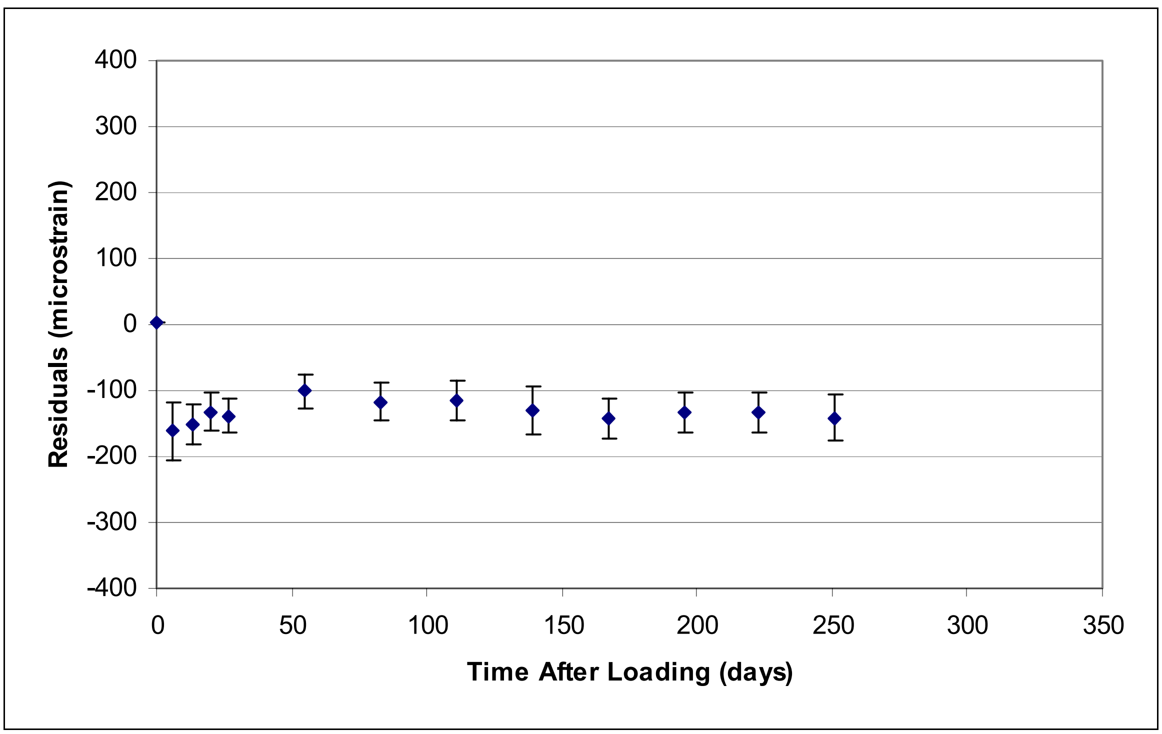

Figure 37 GL2000 and Accelerated Cure Shrinkage Residuals

4.7.6 Accelerated Cure Creep Strain Residuals

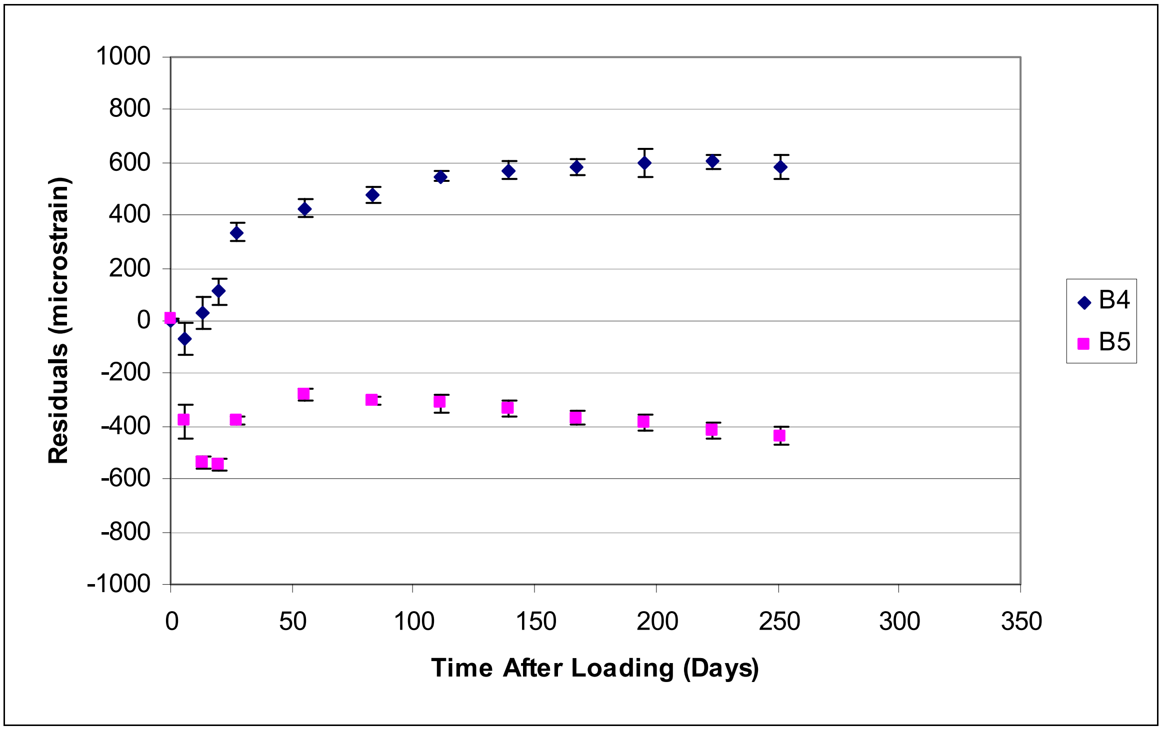

Figure 38 ACI 209 and Accelerated Cure Creep Strain Residuals per Batch

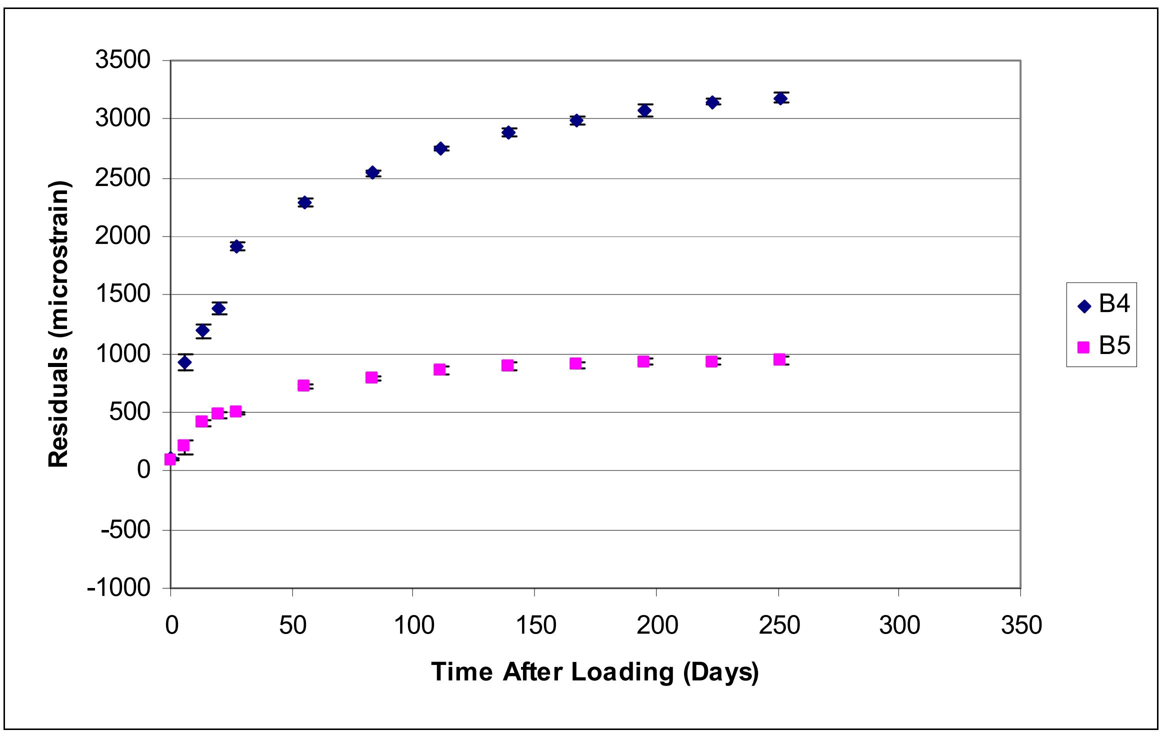

Figure 39 CEB 90 and Accelerated Cure Creep Strain Residuals per Batch

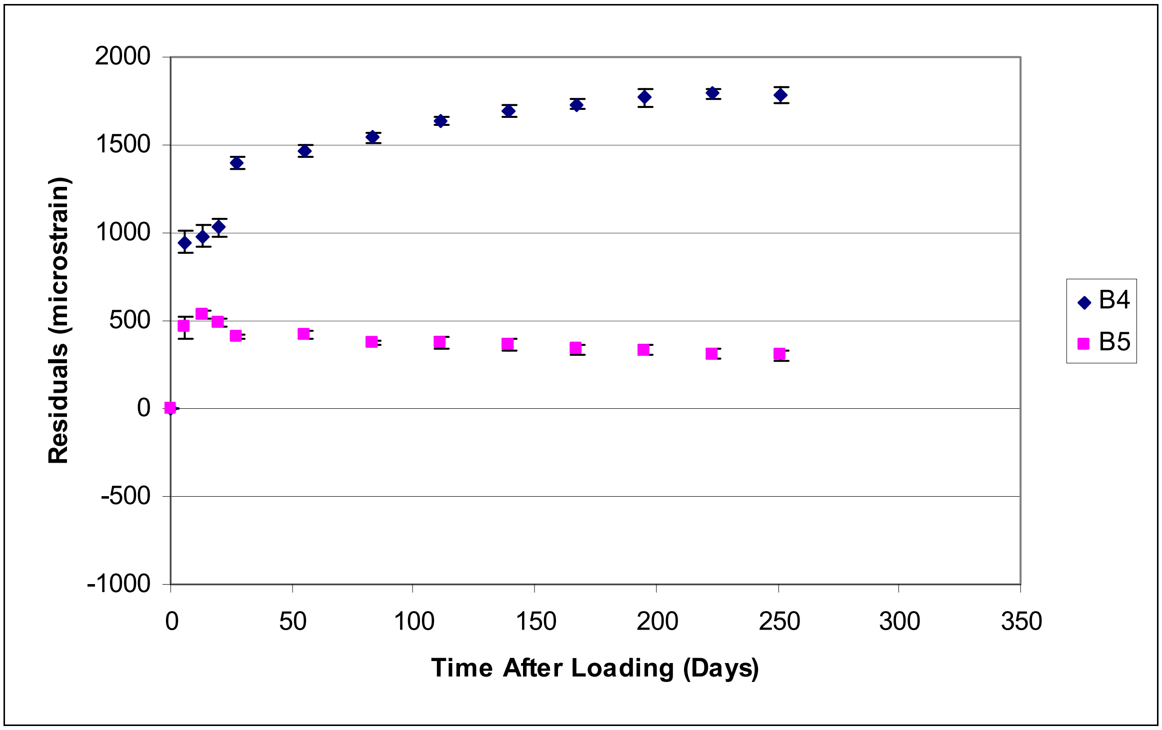

Figure 40 B3 and Accelerated Cure Creep Strain Residuals per Batch

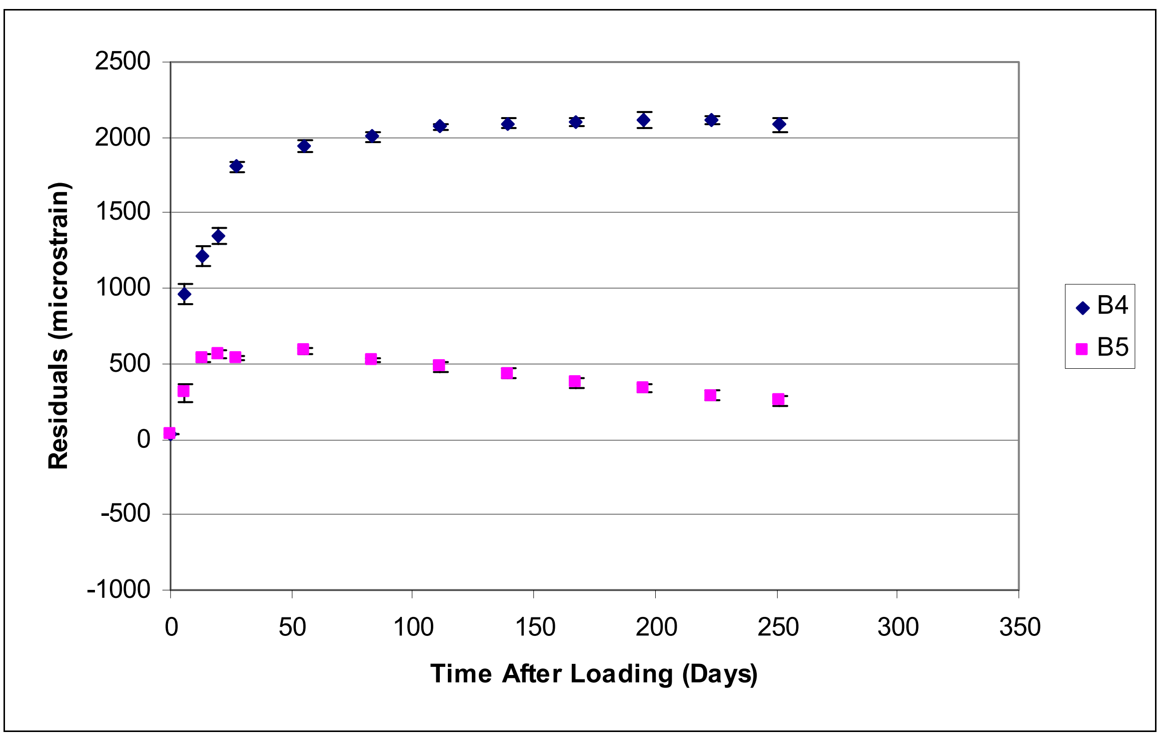

Figure 41 GL2000 and Accelerated Cure Creep Strain Residuals per Batch

4.8 Shrinkage Prisms

Three 75 mm x 75 mm x 285 mm (3 in. x 3 in. x 11.25 in.) shrinkage prisms were made for each standard cure batch per ASTM C157. Shrinkage prisms cannot be cast with the Sure Cure system currently. The shrinkage was calculated as percent shrinkage. Percent shrinkage is equivalent to microstrain x 10^{-4}.

Figure 42 presents the mean percent length change with 95 percent confidence limits and the ACI 209 and the CEB 90 predictions. The ACI 209 model initially under predicts shrinkage and over predicts after 50 days. The CEB 90 model is the best early age predictor, but under predicts shrinkage after 28 days.

Figure 43 presents the percent length change for the shrinkage prisms with 95 percent confidence limits and the B3 and GL2000 predictions. The B3 model initially under predicts shrinkage up to 80 days and then falls within the prisms 95 percent confidence limits. The GL2000 model under predicts shrinkage throughout drying. The GL2000 model is examined in a K factor sensitivity analysis for the cement type.

4.8.1 Standard Cure Shrinkage Prisms

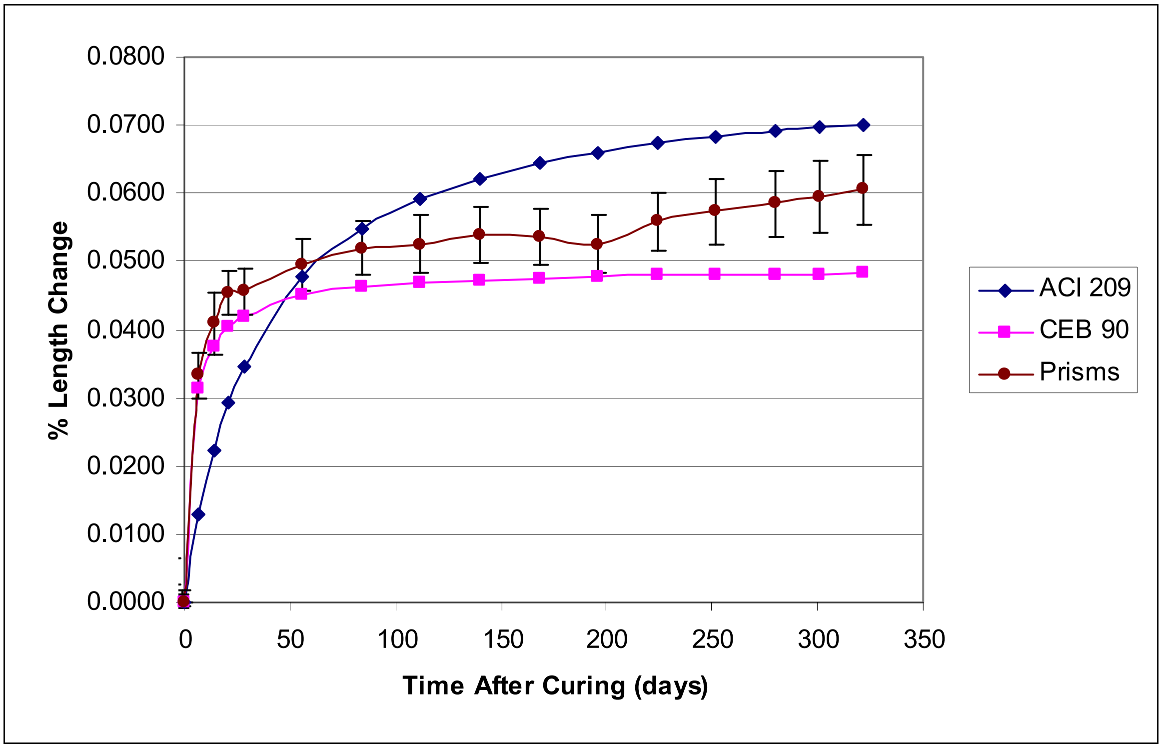

Figure 42 Prism Data with ACI 209 and CEB 90 Models

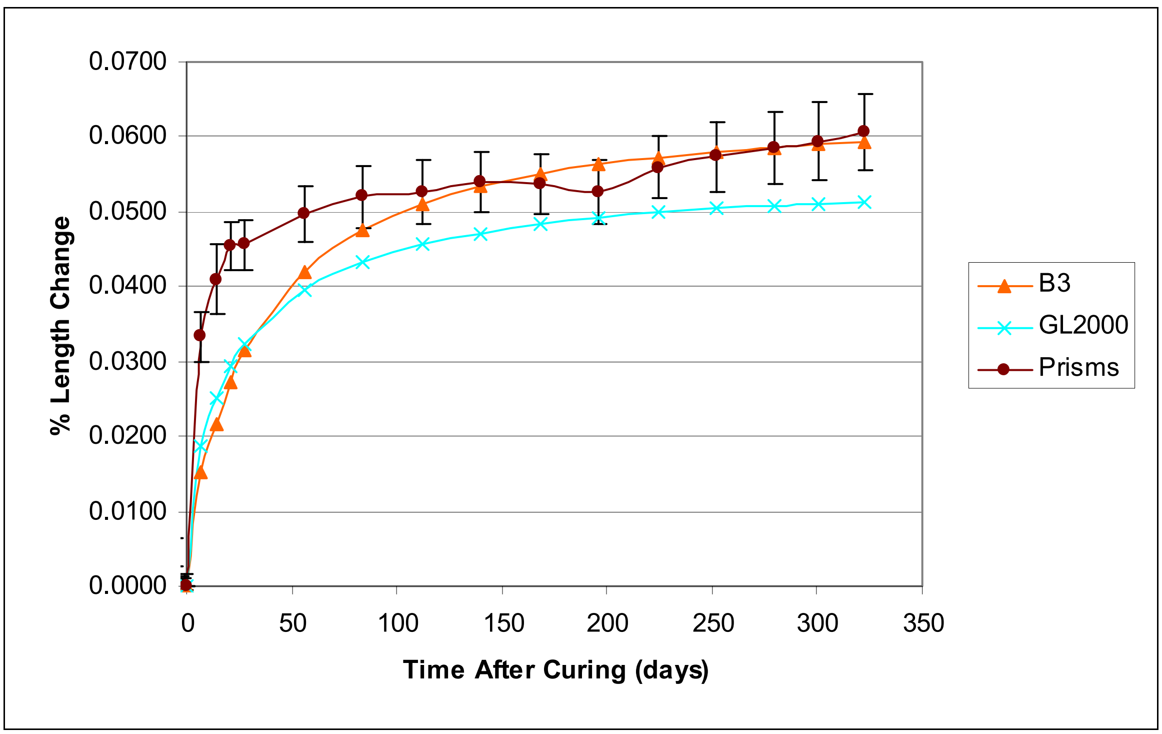

Figure 43 Prism Data with B3 and GL2000 Models

CHAPTER 5: DISCUSSION AND ANALYSIS

5.1 Introduction

This chapter discusses physical properties of the LTHSC mixture and an analysis of the four prediction models. The physical properties include the compressive strength, tensile strength, and modulus of elasticity. The model analysis includes the residual squared method, a sensitivity analysis, and the best prediction model is identified.

5.2 Compressive Strength

Figure 1 presents the LTHSC standard cure compressive strengths. The strengths of the two standard cure batches at seven and 28 days is not significantly different.

Figure 2 presents the accelerated cure compressive strengths for the two LTHSC batches and the Bayshore bridge beams. The LTHSC compressive strengths immediately after curing are approximately the same or greater than the Bayshore results. The Bayshore specimens had a larger strength increase with time. The Bayshore specimens were stored outside with the beams. The environmental conditions in this area are relatively humid considering the plant is surrounded by water on three sides. These conditions appear to have allowed hydration to continue. After curing, the LTHSC specimens were exposed to a drying environment of 45% relative humidity, as were the loaded and unloaded specimens.

The strength gain after curing is similar between the two standard cure batches. Batch 4 is approximately 35 percent stronger than batch 5 after curing. The accelerated curing process has increased the variability of the batches. Maturity is calculated as the area under the temperature-time curve from 14^{o}F or -10^{o}C (Mehta). The maturity difference between the Bayshore Beams is 20 percent, 1000 and 830^{o}C-hr. The maturity of batch 4 (1040 ^{o}C-hr) is 10 percent higher than batch 5 (940 ^{o}C-hr) since it had two hours less of a preset before the temperature increase began. This was due to an experimental error with the match cure system. The maturity of batch 4 is close to that of beam 1. The target maturity was to be the average of the two beams Maturity data is presented in Appendix B.

An additional difference between batches 4 and 5 is the unit weight of 1930 kg/m^3 and 1875 kg/m^3 (120.3 pcf and 117.1 pcf), respectively. The Bayshore beams had unit weights of 1955 kg/m^3 and 1905 kg/m^3 (122.0pcf and 118.8 pcf) for BB1 and BB2, respectively. There is a variability between batches or beams, but this is similar in the laboratory and in the field. The variability in unit weight corresponds with the variation in compressive strengths. A higher unit weight results in a higher compressive strength between the accelerated cure batches and between the beam beams.

The accelerated cure between batch strength differences are directly related to the creep strains not meeting the ASTM precision requirements. If the maturity and/or unit weight is significantly different then creep behavior is likely to be significantly different between batches.

Neither the accelerated or the standard cure batches reached the 55 Mpa (8000 psi) design strength. This can be attributed to the specimens being placed in a drying environment, which slowed hydration and strength gain. The Bayshore specimens reached the required strength and were stored outside with the beams in a relatively humid environment. Figure 1 and 2 shows the measured compressive strengths at loading or release. The standard cure, accelerated cure, and bridge beam specimens reached the required release strength of 31 MPa (4500 psi) at loading or release.

5.3 Tensile Strength

Figure 3 presents the tensile strength data for the four batches and the bridge beams. The LTHSC 28 day tensile strength measurements are within the range of the Bayshore measurements. There is a strong correlation between the tensile strength being equivalent to one tenth of the compressive strength for the LTHSC specimens. The Bayshore specimens had higher compressive strengths, but the tensile strengths were not significantly different from the LTHSC specimens. Both the laboratory and beam tensile tests were greater than the AASHTO 28 day design cracking stress for lightweight aggregate concretes.

5.4 Modulus of Elasticity

Figure 4 presents the LTHSC modulus of elasticity for the standard cure batches. The measurements at various times were conducted on the same specimen for each batch. The differences in the measurements were not significantly different.

Figure 5 presents the modulus of elasticity for the accelerated batches and the bridge beams. The Bayshore 28 day modulus measurements are slightly higher than the respective LTHSC measurements, which supports the observation that the specimens appear to have continued hydration in a moist environment after the accelerated cure. The variability of the LTHSC measurements is a function of the testing procedure and the specimen size. Cyclic loading could be affecting the variability also.

Figures 4 and 5 present the AASHTO equation for lightweight aggregate concrete as significantly over predicting the modulus of elasticity.

The modulus of elasticity was measured on 150 mm x 300 mm (6 in. x 12 in.) and 100 mm x 200 mm (4 in. x 8 in.) cylinders for the standard cure and the accelerated cure methods, respectively. The variability between measurements appears to be less for the larger specimen size. The smaller volume to surface area for the 100 mm x 200 mm (4 in. x 8 in.) specimen could contribute to the increased variability.

5.5 Thermal Coefficient

The linear coefficient of thermal expansion for the LTHSC mixture was found to be 5.3 microstrain per ^{o}F (9.5 microstrain per ^{o}C) with a confidence interval of ± 0.13 microstrain microstrain per ^{o}F (±0.24 microstrain per ^{o}C). This agrees with the ACI 213 Guide for Structural Light weight Aggregate Concrete which states the thermal coefficient for lightweight concrete is 4 to 6 microstrain per ^{o}F (7 to 11 microstrain per ^{o}C) depending on the amount of natural sand used.

5.6 Experimental and Predicted Strains

Figures 6 through 9 present the total strain, creep strain, and shrinkage strain for the individual batches. Each data point is the mean of three measurements and the error bars represent the 95 percent confidence limits. The small confidence limits indicate a small variability within batch. Batch 2 had the largest within batch variability.

Figures 10 through 17 present the predicted total strain, creep and shrinkage for each batch from the ACI 209, CEB 90, B3, and GL2000 models. The increased load at 28 days can be seen in the plot of predicted total strain values. The increase in load causes an instantaneous increase of the elastic strain. This can also be seen in the experimental values when additional data points are plotted.

The model limitations must be considered when applying the models to lightweight concrete. Only one of the four models, ACI 209, included lightweight aggregate concretes in development of the model. Although, the GL 2000 model does consider aggregate stiffness. The LTHSC proportions meet the cement type requirements for the four examined models, but the models were not developed on test data that included additional mineral admixtures. GL2000 considers this by allowing the model to be calibrated for additional binders with a K factor. Additional prediction model information is in Appendix A.

5.7 Experimental Strain Relationships

Figure 44 through 46 present the relationship between the average strains of the accelerated cure data verse the standard cure data. The standard cure and accelerated cure specimens have a 38 mm (1.5 in.) and 25 mm (1.0 in.) volume to surface area ratios, respectively. The specimens had different curing regimens, but the size factor seems most significant. The equivalency line represents paired data of equal magnitude. The average strain data sets have been paired based on time after loading. If a plotted point is above the equivalency line, the y-axis data has a larger magnitude than the x-axis. Explanations are attached to the relevant figures.

Figure 44 presents the average total strain of the two data sets. The accelerated cure deformation is slightly greater than the standard cure. The smaller specimen has higher total strain as the moisture loss across its cross section is more significant.

Figure 45 presents the creep strain data sets. The creep strain for the smaller, accelerated cure specimen is higher at lower strains or early ages. The smaller specimen experienced drying creep at a higher initial rate. Over time, the data sets meet at the equivalency line.

Figure 46 presents the shrinkage strain data sets. The accelerated cure specimens have a higher magnitude of shrinkage strain due to drying shrinkage over a smaller cross section.

Figure 47 presents the standard cure volume to surface relationship between the prisms and the shrinkage cylinders. The prisms have a volume to surface area ratio of 19 mm (0.75 in.) compared to 38mm (1.5 in.) for the shrinkage cylinders. The smaller specimens initially have a greater magnitude of shrinkage, but the meet at the equivalency line at later ages.

Figures 44 through 47 show the relationship between specimen sizes. Smaller shrinkage specimens initially lose moisture at a quicker rate. They also show that the average creep is not significantly different between the standard and accelerated cure methods. The average total strain is lower for the accelerated cure specimens, which can be attributed to less shrinkage in the accelerated cure specimens.

Experimental Strain Relationships

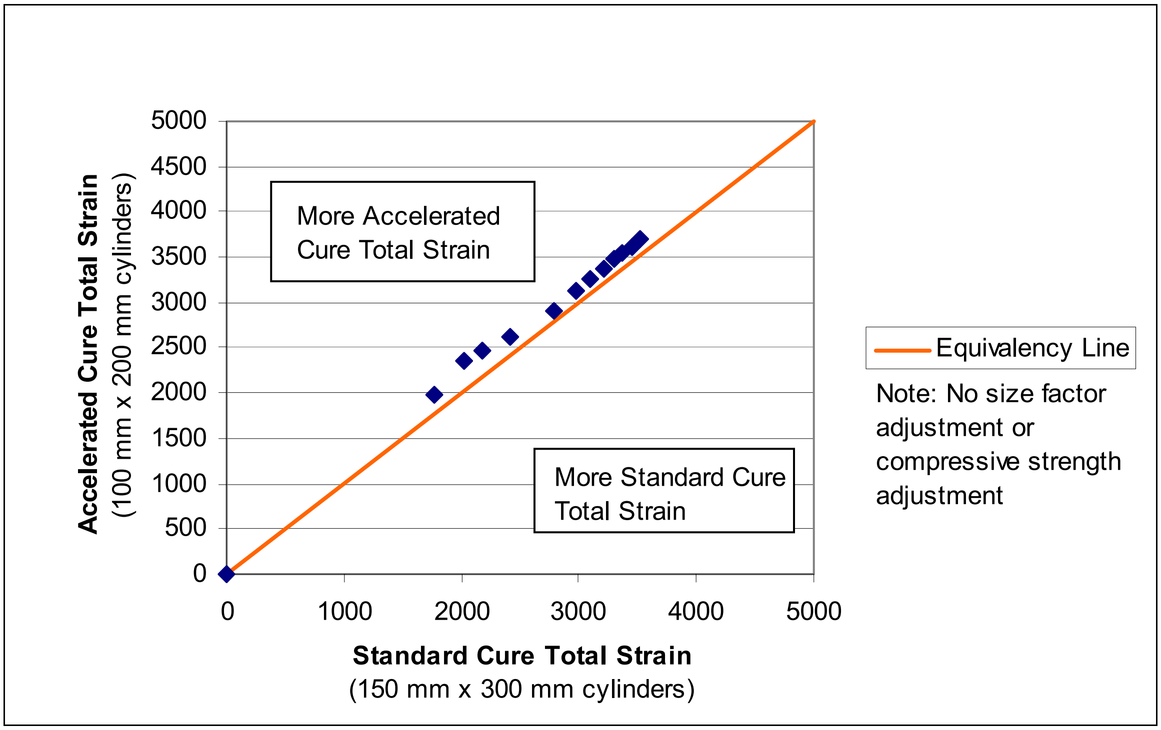

Figure 44 Average Total Strain: Size and Curing Relationship (microstrain).

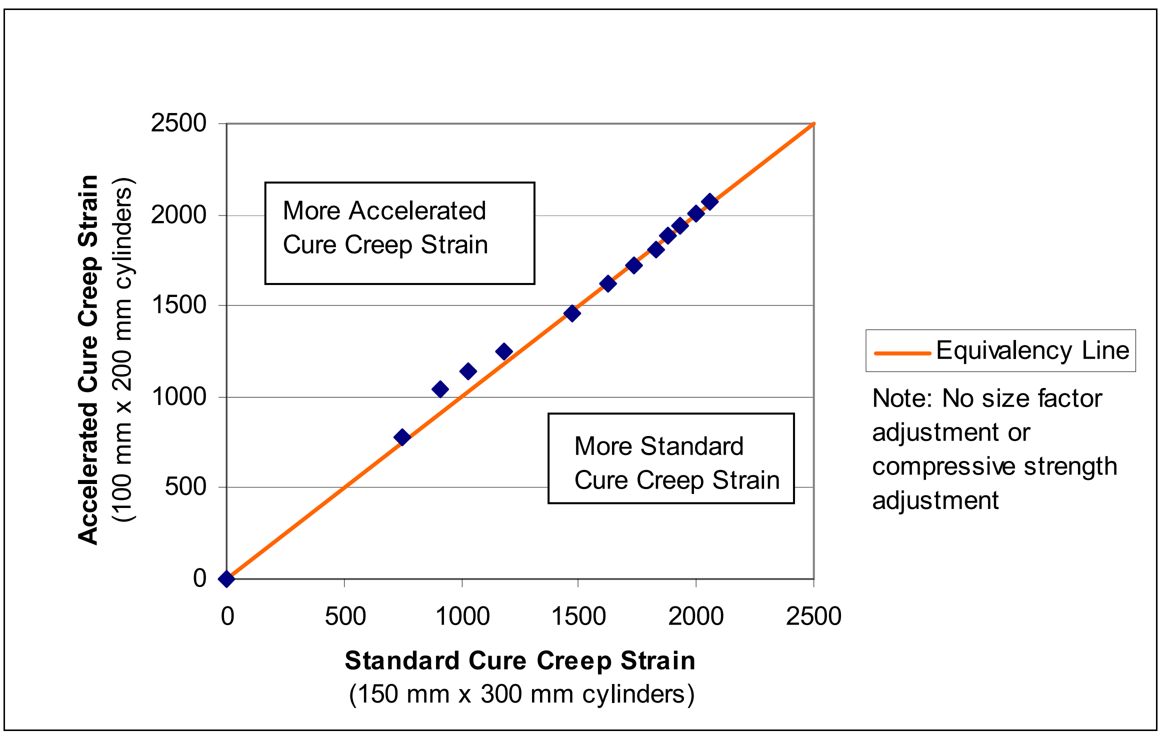

Figure 45 Average Creep Strain: Size and Curing Relationship (microstrain)

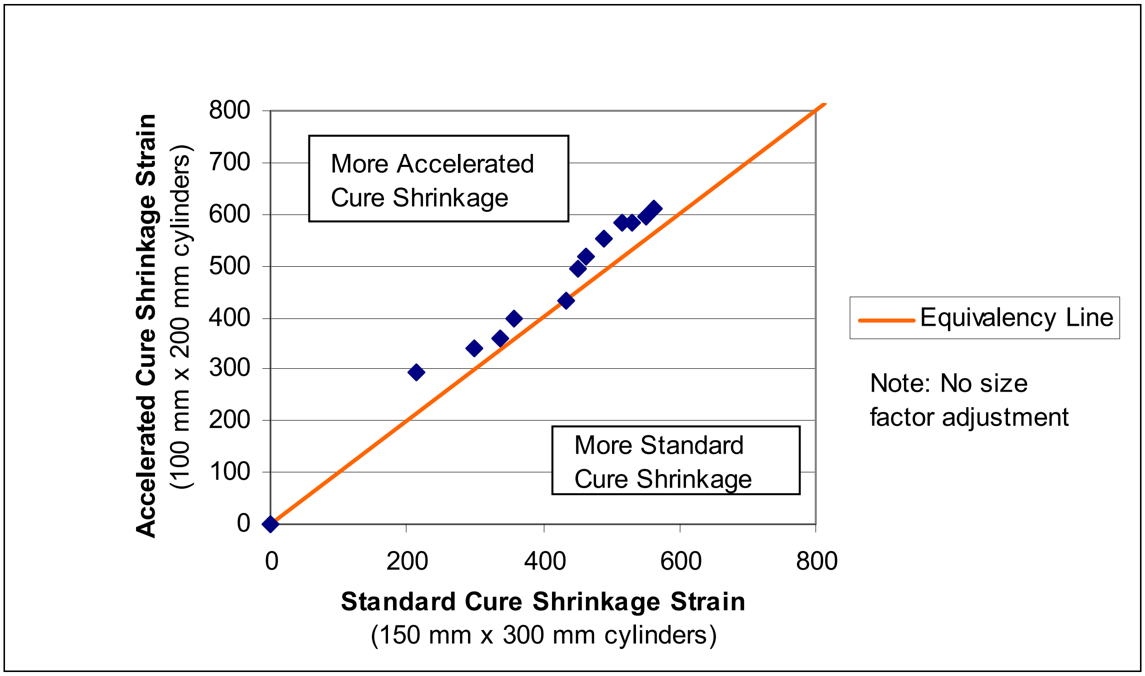

Figure 46 Average Shrinkage Strain: Size and Curing Relationship (microstrain).

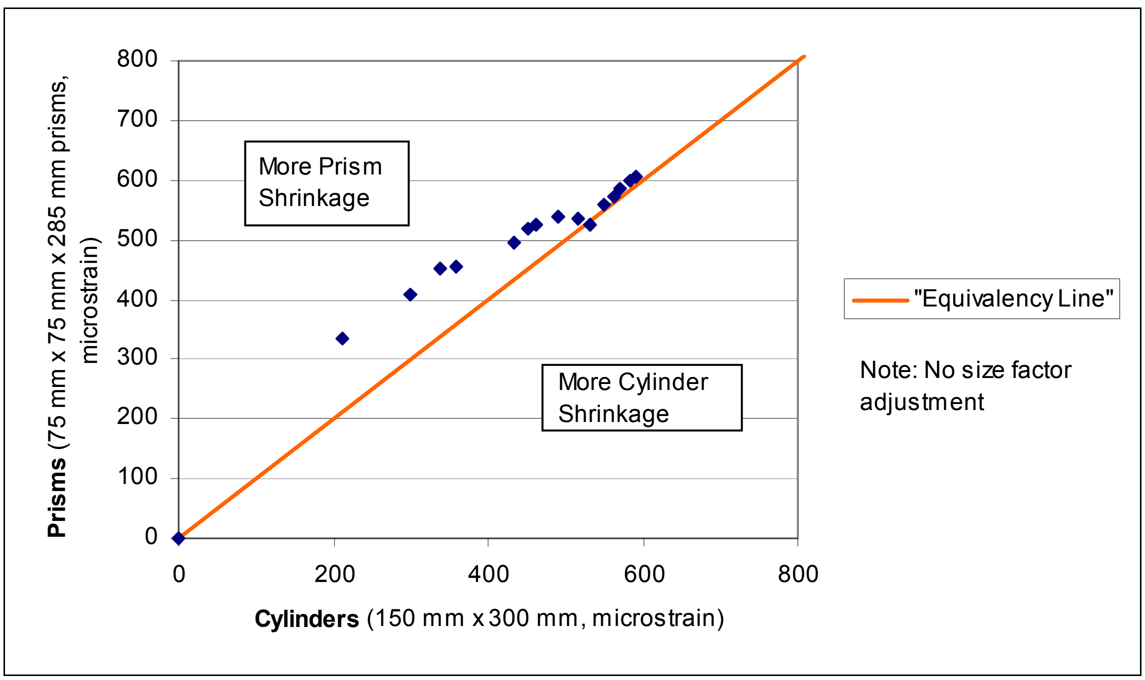

Figure 47 Standard Cure Shrinkage Specimens: Volume to Surface Area Relationship

5.8 Experimental Precision

5.8.1 Total and Creep Strains

ASTM C 512 defines the acceptable experimental creep strain precision limits as a within batch and between batch coefficient of variation (1s %) of 4.0 and 9.0 percent, respectively. The coefficient of variation is the population standard deviation divided by the mean. As per ASTM C 670, these population limits need to adjust for small sample sizes. For 2 or 3 tests, the adjustment factors are 2.8 or 3.3, respectively. These precision statements are applicable between 250 and 2000 microstrain. Due to this limitation, the precision values were tested at 63 days after loading, since batch 5 was approaching the upper bound limit of 2000 microstrain at 63 days after loading.

5.8.1.1 Standard Cure

Table 6 presents the standard cure within (WB) and between batch (BB) precision results. ASTM C 512 is greater than the within and between batch coefficients of variation of batches 2 and 3, thus the standard cure data may be combined.

Table 7 presents the within batch coefficient of variation for 7 to 63 days after loading. As shown, the within batch decreases over time. Whereas the between batch coefficient of variation is relatively constant between 7 and 63 days after loading.

Table 6 Standard Cure Experimental and Required Precision

	WB	BB	ASTM C 512	
Batch	3s%	2s%	3s%	2s%
2	5.7%		13.2%	
3	1.9%		13.2%	
2/3		17.5%		25.5%

Table 7 Standard Cure Statistical Analysis of the Creep Microstrain.

Time after Loading (days)	7	28	56	63
B2-1	669	900	1294	1333
B2-2	687	1048	1303	1320
B2-3	583	945	1164	1200
B3-1	841	1381	1662	1737
B3-2	856	1372	1677	1748
B3-3	881	1388	1725	1800

	Time after Loading (days)	7	28	56	63	ASTM Limit
	x_{bar} =	646	964	1254	1284	
	Standard Deviation =	55.6	75.9	77.8	73.3	
	CV (3s%) =	8.6%	7.9%	6.2%	5.7%	13.2%
	x_{bar} =	859	1380	1688	1762	
	Standard Deviation =	20.2	8.0	32.9	33.7	
	CV (3s%) =	2.4%	0.6%	1.9%	1.9%	13.2%
Between Batch	$x2_{bar}$ =	753	1172	1471	1523	
	Standard Deviation =	123	233	244	266	
	CV (2s%) =	16.3%	19.9%	16.6%	17.5%	25.2%

5.8.1.1Accelerated Cure

Table 8 presents the accelerated cure creep strain within and between batch precision results. The within batch coefficient of variations meet the ASTM C 512 precision requirements. The between batch coefficient of variation of 32.9 percent exceeds the upper requirement of 25.5 percent. Therefore, the accelerated cure batches should not be combined and will be examined separately.

Table 9 demonstrates that the coefficient of variation within batch tends to decrease over time. Whereas the between batch coefficients are more variable and appear to be somewhat uniform after 6 days.

Table 8 Accelerated Cure Experimental and Required Precision

Batch	WB 3s%	BB 2s%	ASTM C 512 3s%	ASTM C 512 2s%
4	3.8%		13.2%	
5	0.4%		13.2%	
4/5		32.9%		25.5%

Table 9 Accelerated Cure Statistical Analysis of the Creep Microstrain.

Time after Loading (days)	6	27	55	62	**Time after Loading** (days)	6	27	55	62	ASTM Limit
B4-1	658	825	1002	1036	x_{bar} =	604	817	1017	1040	
B4-2	551	784	997	1003	Standard Deviation =	53.5	29.8	30.4	39.2	
B4-3	604	842	1052	1081	CV (3s%) =	8.9%	3.6%	3.0%	3.8%	13.2%
B5-1	1020	1677	1902	1924	x_{bar} =	961	1672	1901	1931	
B5-2	954	1683	1919	1939	Standard Deviation =	55.8	13.6	18.5	7.5	
B5-3	909	1657	1882	1930	CV (3s%) =	5.8%	0.8%	1.0%	0.4%	13.2%
				Between Batch	x_{2bar} =	783	1245	1459	1486	
					Standard Deviation =	201	469	485	489	
					CV (2s%) =	25.7%	37.7%	33.2%	32.9%	25.2%

5.8.2 Shrinkage Strain and Percent Length Change Precision

The standard and accelerated cure shrinkage strains may be combined respectively since the 95% confidence limits overlap at various times. The standard cure shrinkage prisms data has also been combined.

5.9 Prediction Model Residuals

When predicting prestress losses, the most critical information to a designer is to know if a given model over or under predicts total strain and thus the accompanying prestress losses. The residuals, the difference between the model and the experimental value, identifies if a model over predicts, a positive value, and under predicting, a negative value. This identifies if a model is conservative or unconservative at a given time, but does not identify the best predictor. The residuals are calculated as the predicted model mean for a batch minus the experimental value for a test specimen at a given time. The residuals are plotted as the mean and the 95 percent confidence limits at the given test time. The standard cure residuals are for batches 2 and 3 combined for a total of six test values. Whereas the accelerated cure residuals are for batches 4 and 5 separately. The residuals have been presented in Figures 18 through 39.

Table 6 and 8 summarize the standard and accelerated cure residuals, respectively. The summary is based on the mean residual being positive or negative. Models that have a residual of zero or fall within the 95 percent confidence limits are not significant different from the experimental data and are identified with parentheses (). If a residual could not be distinguished as positive or negative, then the model is described as good in the chart. A negative residual means a model under predicted the strain. The accelerated cure values can be positive and negative since those two batches could not be combined. For the accelerated cure batches, parentheses () indicate that at least one accelerated cure batch is not significantly different from a model.

5.9.1 Standard Cure Residuals

The ACI 209, CEB 90, and GL2000 models predict total strain within the experimental 95 percent confidence limits for the standard cure data set. The CEB 90 model appears to be the best total strain predictor for the standard cure method.

The ACI 209 predicts all three measurements within the experimental confidence limits. Total strain and creep are under predicted. Whereas shrinkage is over predicted.

CEB 90 is a good predictor of total strain as a result of over predicting creep and under predicting shrinkage. The shrinkage strain is the only parameter that did not fall within the experimental confidence limits.

The B3 model under predicts total strain as a result of under predicting creep and shrinkage. B3 does predict creep within the experimental confidence limits.

GL2000 predicts total strain and creep within the experimental confidence limits. Whereas all three are under predicted.

Table 10 Standard Cure Mean Residual Summary

	ACI 209	CEB 90	B3	GL2000
Total Strain	(Under predicting)	(Good)	Under predicting	(Under predicting)
Shrinkage Strain	(Over predicting)	Under predicting	Under predicting	Under predicting
Creep Strain	(Under predicting)	(Over predicting)	(Under predicting)	(Under predicting)

Note: Parentheses () indicate that the standard cure data is not significantly different from the model.

5.9.2 Accelerated Cure Residuals

The best model cannot be identified with residuals when the experimental total strain and creep data cannot be combined. The residuals do show that the trends to over or under predict strains.

ACI 209 is a good predictor of shrinkage. Whereas the CEB 90, B3, and GL2000 models under predict shrinkage.

Table 11 Accelerated Cure Residual Summary

	ACI 209	**CEB 90**	**B3**	**GL2000**
Total Strain	Both over and under	Both over and under predicting	Both over and under	(Both over and under predicting)
Shrinkage Strain	(Good)	Under predicting	Under predicting	Under predicting
Creep Strain	Both over and under	Over predicting	Over predicting	Over predicting

Note: Parentheses () indicate that at least one accelerated cure batch is not significantly different from the model.

5.10 Residuals Squared Analysis

There are numerous methods of analyzing experimental data to determine the best prediction model. The residuals squared and error percentage methods are considered here, as these have been shown to be relatively consistent with the other methods (Meyerson). The residuals squared method puts more weight on larger residuals while preventing residuals of opposite signs from negating each other. The error percentage is best optimized when using the residuals from two means. For example, the error percentage can be found between the mean of a prediction model and a set of data. The error percentage method is not used in this analysis since the accelerated cure batches cannot be combined according to ASTM C 512. The residuals squared method identifies the model with the lowest value at a given time as the best predictor.

$$\text{Residuals Squared} = \sum_{i=1}^{6}\left[(\text{Re}_i)^2\right] \text{ at a given time}$$

Tables 12 through 18 present the average residuals so the reader can easily determine if the model is conservative with a positive residual or unconservative with a negative residual at a given time.

5.10.1 Standard Cure Residuals Squared

Figures 48 through 50 presents the residuals squared for the standard cure specimens. The rankings will be presented in order with the best first.

The total strain order of best prediction at 56 days is CEB90, GL2000, ACI209, and B3, respectively. The total strain order of best prediction at 250 days has not changed.

The shrinkage strain order of best prediction at 56 days is ACI 209, GL2000, CEB 90, and B3, respectively. The shrinkage strain order of best prediction at 250 days remains the same.

The creep strain order of best prediction at 56 days is GL2000, CEB 90, and both the ACI 209 and B3, respectively. The creep strain order of best prediction at 250 days is GL 2000, CEB 90, B3, and ACI209, respectively.

Standard Cure Total Strain Squared

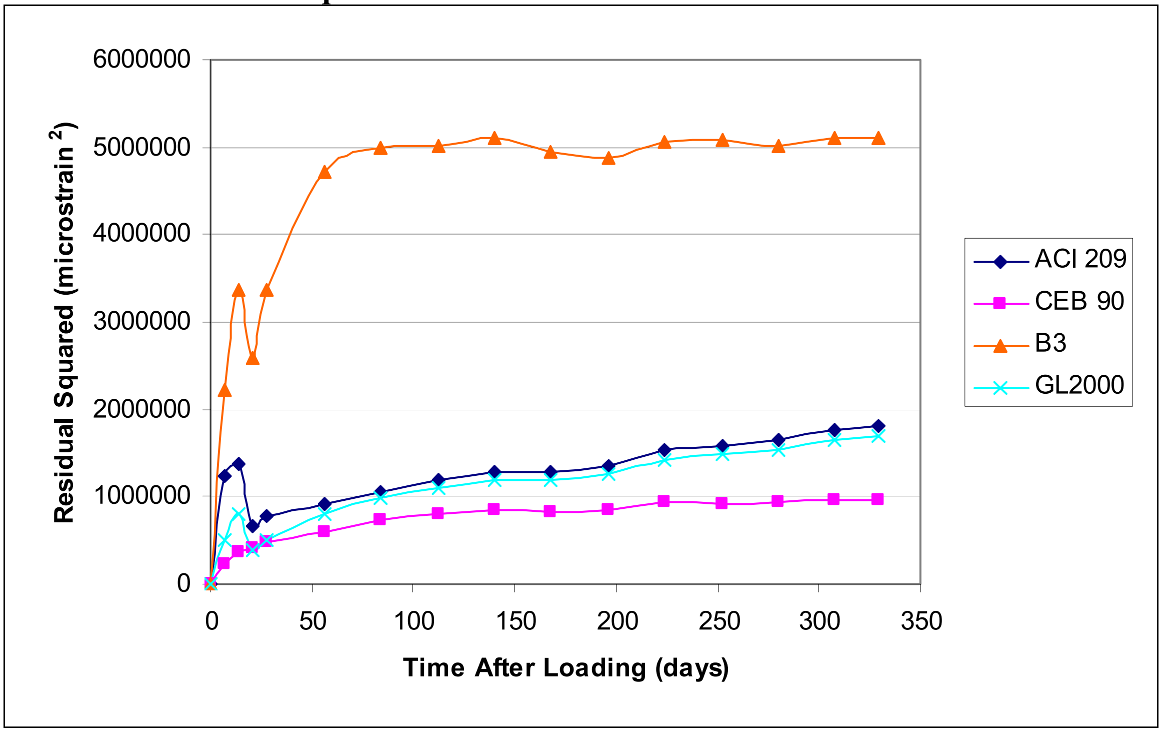

Figure 48 Standard Cure Total Strain Residuals Squared

Table 12 Standard Cure Average Total Strain Residuals (microstrain)

Time After Loading (days)	ACI 209	CEB 90	B3	GL2000
0	0	0	0	0
7	-425	-148	-591	-252
14	-429	-188	-723	-315
21	-167	-33	-599	-70
28	-197	-86	-697	-143
56	-201	-124	-834	-239
84	-168	-86	-842	-242
112	-153	-55	-832	-241
140	-169	-52	-838	-261
168	-171	-35	-822	-263
196	-181	-27	-811	-271
224	-214	-44	-822	-301
252	-240	-54	-826	-323
280	-250	-51	-815	-329
308	-276	-64	-821	-351
329	-293	-73	-824	-366

Standard Cure Shrinkage Strain Residuals Squared

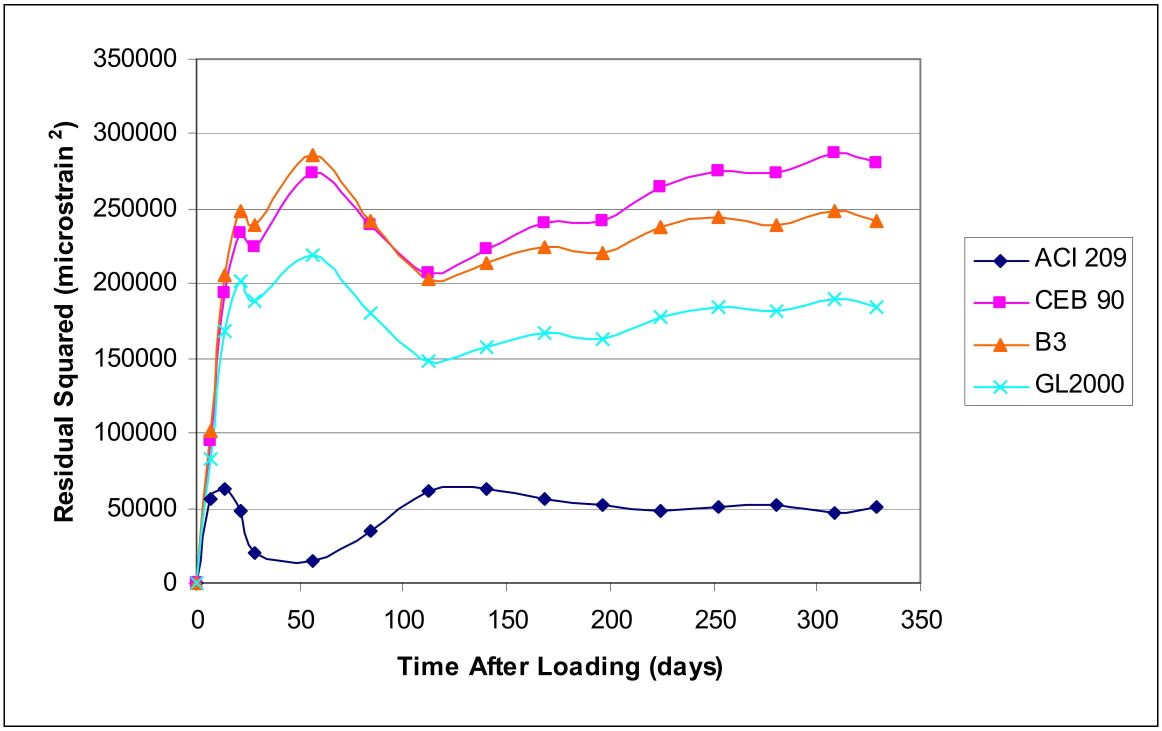

Figure 49 Standard Cure Shrinkage Residuals Squared

Table 13 Standard Cure Average Shrinkage Residuals (microstrain)

Time After Loading (days)	ACI 209	CEB 90	B3	GL2000
0	0	0	0	0
7	-94	-123	-128	-115
14	-96	-175	-181	-162
21	-72	-188	-195	-174
28	-42	-188	-194	-171
56	4	-206	-210	-182
84	50	-187	-189	-159
112	80	-170	-169	-139
140	79	-177	-173	-142
168	73	-186	-179	-149
196	72	-188	-179	-149
224	64	-196	-185	-155
252	62	-198	-185	-156
280	62	-198	-183	-154
308	55	-203	-187	-158
329	58	-200	-183	-154

Standard Cure Creep Strain Residuals Squared

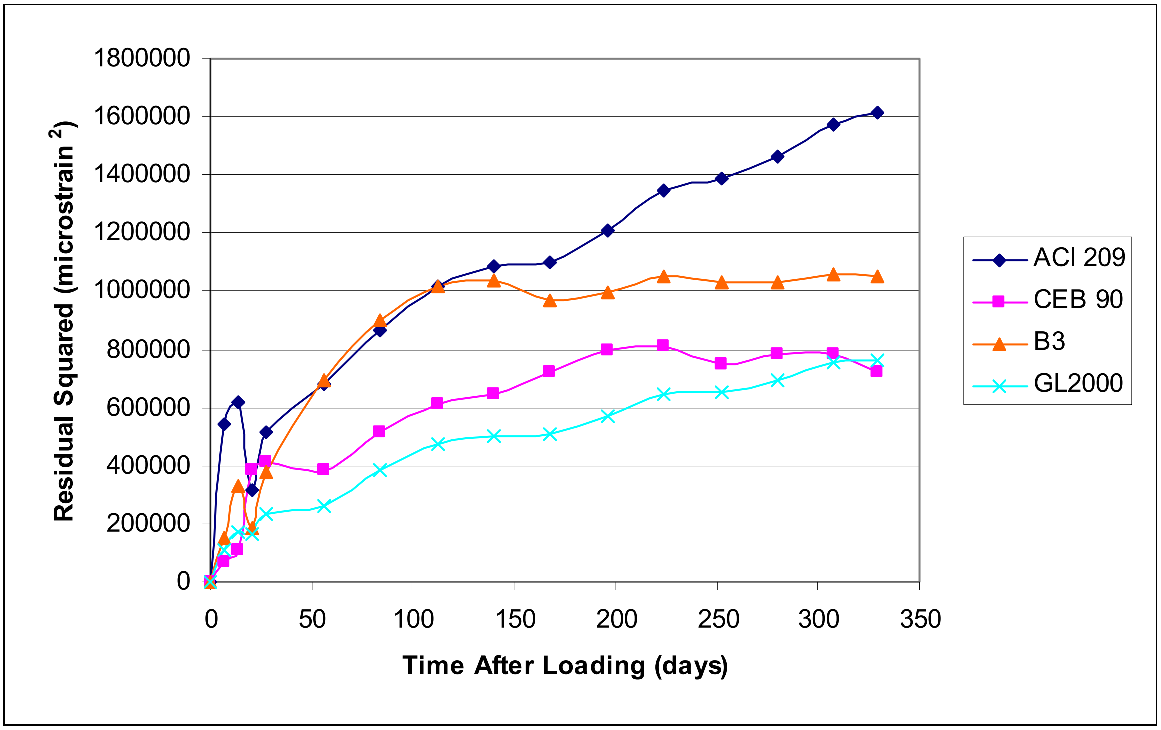

Figure 50 Standard Cure Creep Strain Residuals Squared

Table 14 Standard Cure Creep Strain Residuals Squared

Time After Loading (days)	ACI 209	CEB 90	B3	GL2000
0	0	0	0	0
7	-268	55	-101	-73
14	-269	65	-180	-89
21	-119	209	-68	80
28	-151	183	-138	32
56	-201	164	-259	-53
84	-213	183	-288	-78
112	-228	197	-299	-98
140	-244	207	-300	-115
168	-240	233	-278	-110
196	-249	242	-268	-118
224	-274	234	-273	-141
252	-297	226	-276	-163
280	-307	228	-268	-171
308	-326	221	-269	-188
329	-347	208	-277	-208

5.10.2 Accelerated Cure Residuals Squared

Figures 51 through 53 presents the residuals squared for the accelerated cure specimens. The rankings will be presented in order with the best first.

The total strain order of best prediction at 56 days is ACI 209, B3, GL2000, and CEB90, respectively. The total strain order of best prediction at 250 days has not changed.

The shrinkage strain order of best prediction at 56 days is ACI 209, GL2000, CEB 90, and B3, respectively. The shrinkage strain order of best prediction at 250 days is unchanged.

The creep strain order of best prediction at 56 days is ACI 209, B3, GL2000, and CEB90. The creep strain order of best prediction at 250 days is unchanged.

5.10.3 Shrinkage Prism Residuals Squared

Figure 54 shows the residuals squared for the shrinkage prisms. The CEB 90 model is initially the best predictor. At times over 100 days, the B3 model is the best predictor.

Accelerated Cure Total Strain Residuals Squared

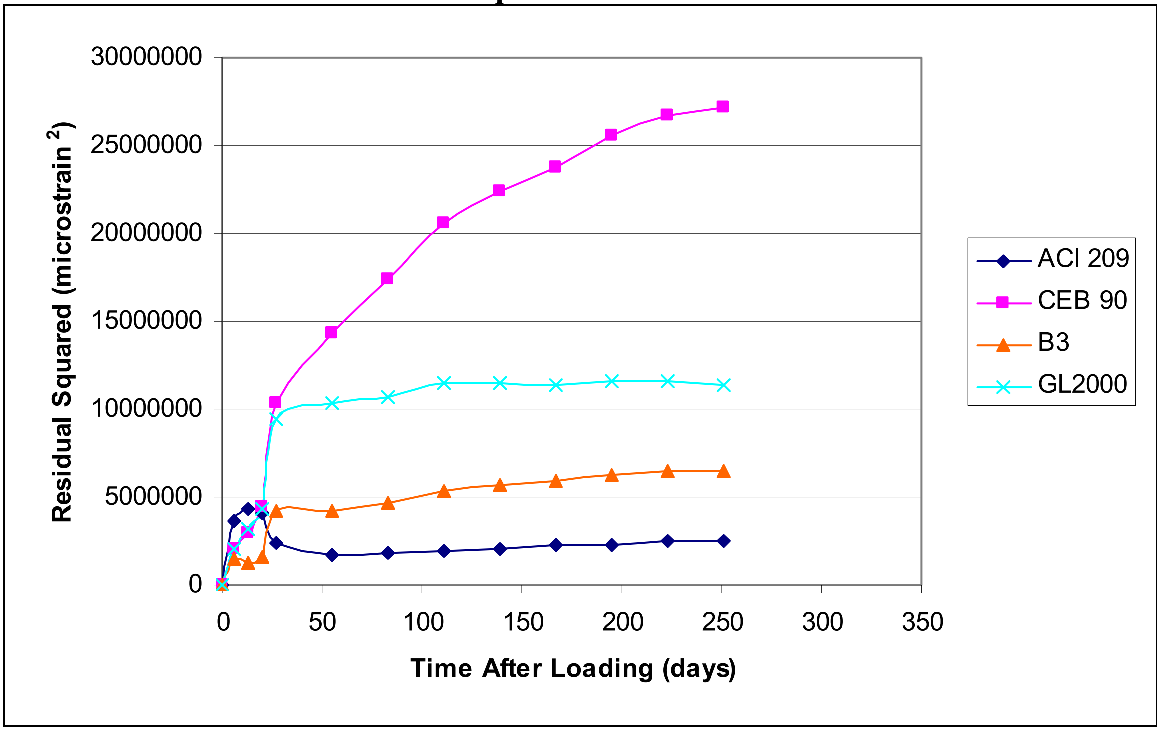

Figure 51 Accelerated Cure Total Strain Residuals Squared

Table 15 Accelerated Cure Average Total Strain Residuals (microstrain)

Time After Loading (days)	ACI 209	CEB 90	B3	GL2000
0	0	0	0	0
6	-686	152	50	234
13	-695	463	141	553
20	-622	612	152	659
27	-282	937	336	927
55	-147	1218	355	1011
83	-117	1352	349	993
111	-67	1485	393	1006
139	-64	1556	400	979
167	-77	1600	394	942
195	-61	1665	419	937
223	-68	1699	419	912
251	-91	1713	402	875

Accelerated Cure Shrinkage Strain Residuals Squared

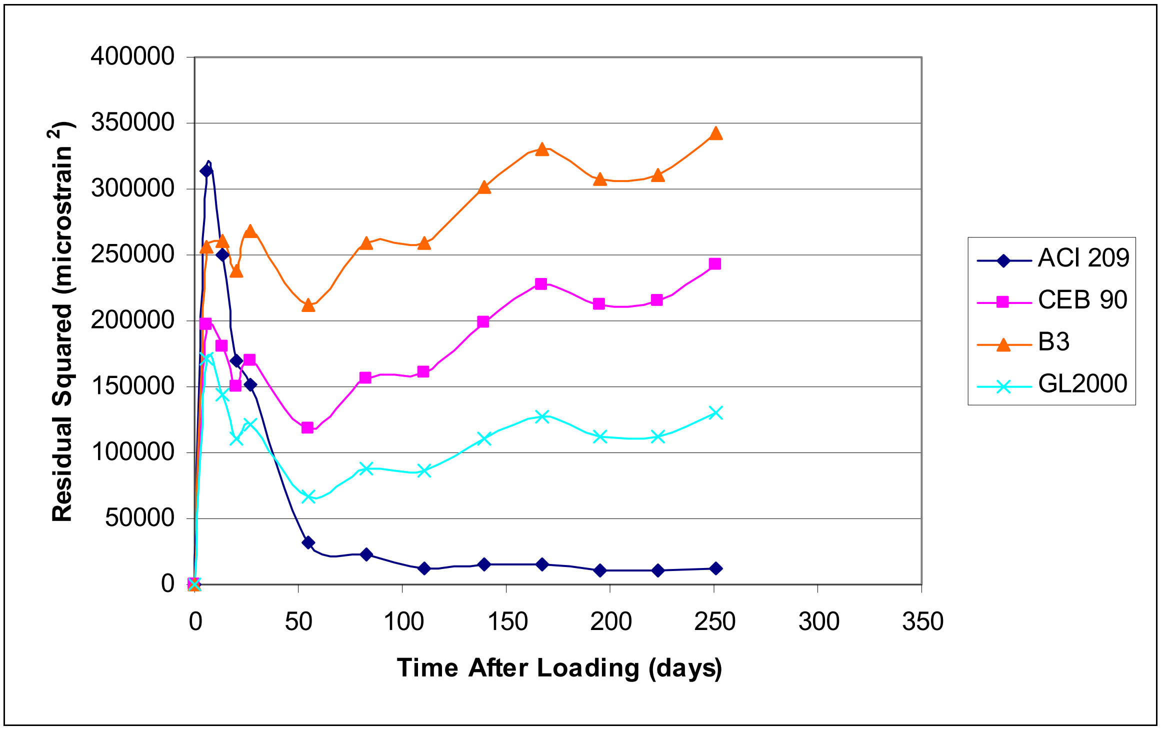

Figure 52 Accelerated Cure Shrinkage Residuals Squared

Table 16 Accelerated Cure Average Shrinkage Residuals (microstrain)

Time After Loading (days)	ACI 209	CEB 90	B3	GL2000
0	0	0	0	0
6	-223	-174	-200	-161
13	-201	-170	-205	-151
20	-165	-155	-194	-132
27	-156	-165	-208	-139
55	-68	-136	-182	-101
83	-52	-158	-202	-117
111	-29	-160	-202	-115
139	-29	-177	-218	-129
167	-30	-192	-231	-141
195	-13	-184	-222	-132
223	-7	-187	-224	-133
251	-11	-197	-234	-142

Accelerated Cure Creep Strain Residuals Squared

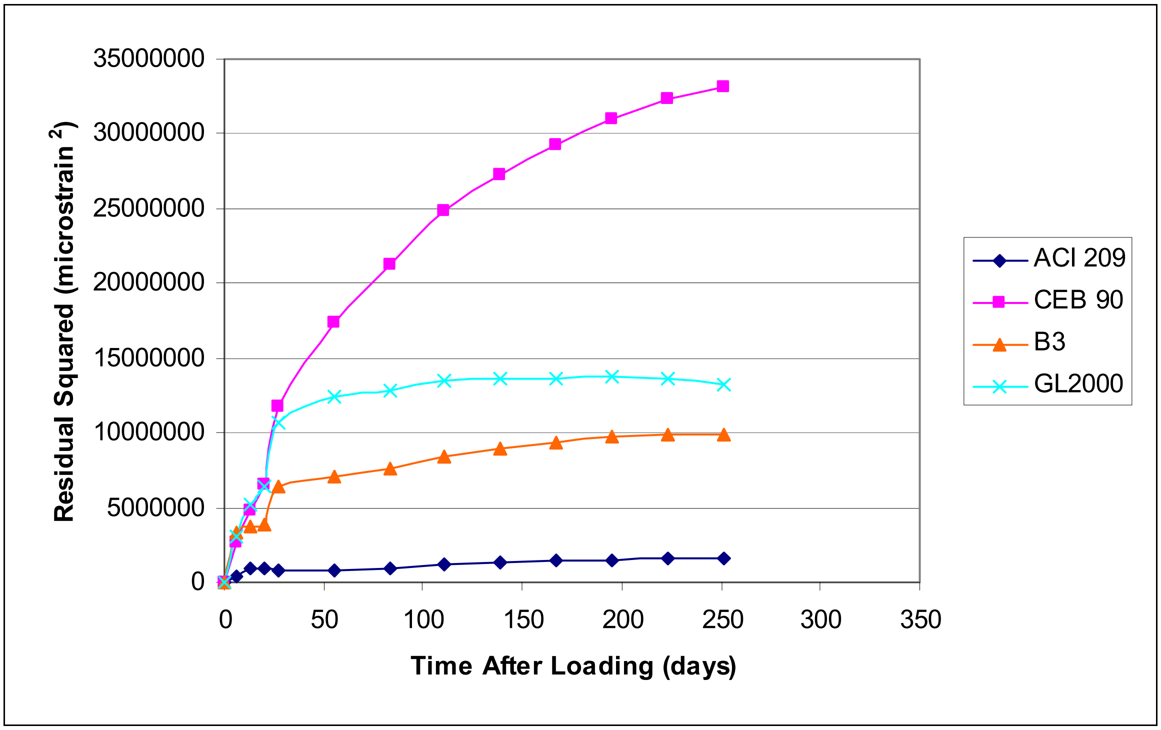

Figure 53 Accelerated Cure Creep Strain Residuals Squared

Table 17 Accelerated Cure Average Creep Strain Residuals (microstrain)

Time After Loading (days)	ACI 209	CEB 90	B3	GL2000
0	0	0	0	0
6	-224	565	704	634
13	-255	801	757	873
20	-218	935	758	959
27	-20	1208	904	1171
55	75	1508	946	1266
83	89	1664	960	1264
111	117	1799	1004	1275
139	119	1887	1027	1262
167	107	1946	1034	1237
195	106	2003	1050	1223
223	93	2040	1052	1199
251	74	2064	1045	1171

Standard Cure Shrinkage Prism Residuals Squared

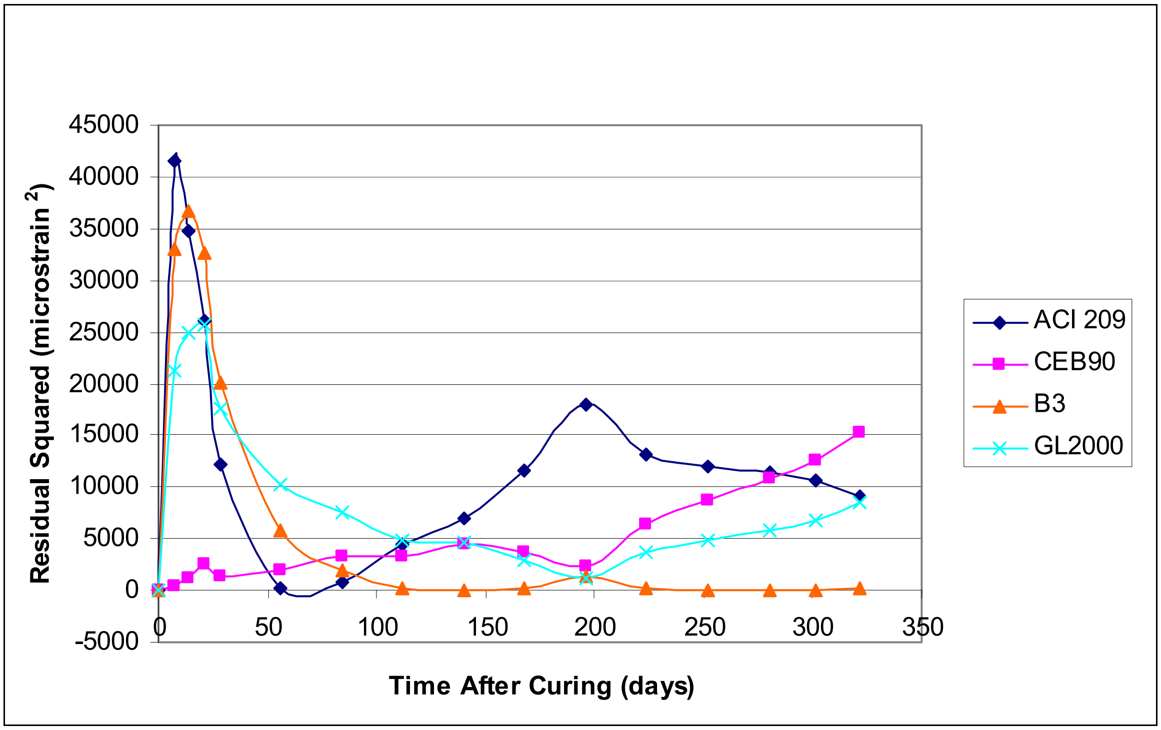

Figure 54 Residuals Squared for Shrinkage Prisms and the Prediction Models

Table 18 Average Shrinkage Strain of Prisms (microstrain)

Time After Curing (days)	ACI 209	CEB 90	B3	GL2000
0	0	0	0	0
7	-204	-19	-182	-146
14	-187	-35	-191	-158
21	-162	-50	-181	-160
28	-111	-36	-141	-133
56	-18	-45	-77	-101
84	29	-57	-44	-87
112	67	-57	-16	-70
140	83	-66	-6	-68
168	108	-61	14	-53
196	134	-48	37	-34
224	114	-79	14	-60
252	110	-93	6	-69
280	106	-104	0	-77
301	103	-112	-5	-83
322	96	-124	-13	-92

5.11 Prediction Model Rankings

This section presents the rankings of the four prediction models. If two or more models were not significantly different then multiple rankings were assigned. The rankings are summed and the model with the lowest value is the best overall predictor. If multiple rankings are assigned, the best ranking is summed.

5.11.1 Standard Cure Rankings

Tables 19 and 20 summarize the standard cure prediction rankings. The GL2000 model is the best predictor of standard cure time dependent strains. The CEB 90 model is the best predictor of total strain over time.

Table 19 Standard Cure Prediction Model Rankings at 56 Days

At 56 Days	**ACI 209**	**CEB MC 90**	**B3**	**GL2000**
Total Strain	1/2/3	1/2/3	4	1/2/3
Shrinkage Strain	1	3/4	3/4	2
Creep Strain	3/4	2	3/4	1
Sum of Ranks	5	6	10	4

Table 20 Standard Cure Prediction Model Rankings at 250 Days

At 250 Days	**ACI 209**	**CEB MC 90**	**B3**	**GL2000**
Total Strain	2/3	1	4	2/3
Shrinkage Strain	1	4	3	2
Creep Strain	4	2	3	1
Sum of Ranks	7	7	10	5

5.11.2 Accelerated Cure Summary

Tables 21 and 22 summarize the accelerated cure predicting model rankings. The ACI 209 model is the best predictor for total strain, creep, and shrinkage. This is reasonable conclusion since it is the only model developed with lightweight concretes.

Table 21 Accelerated Cure Prediction Model Rankings at 56 Days

At 56 Days	**ACI 209**	**CEB 90**	**B3**	**GL2000**
Total Strain	1	4	2	3
Shrinkage Strain	1	3	4	2
Creep Strain	1	4	2	3
Sum of Rank	3	10	8	8

Table 22 Accelerated Cure Prediction Model Rankings at 250 Days

At 250 Days	**ACI 209**	**CEB 90**	**B3**	**GL2000**
Total Strain	1	4	2	3
Shrinkage Strain	1	3	4	2
Creep Strain	1	4	2	3
Sum of Rank	3	10	8	8

5.11.3 Shrinkage Prisms Model Rankings

Table 19 summarizes the model rankings for the standard cure shrinkage specimens. The rankings are inconclusive. Although the CEB 90 is best early age predictor and the B3 is the best predictor at later ages. The B3 model is the best predictor of shrinkage during drying.

Table 23 Standard Cure Shrinkage Prism Model Ranking

	ACI 209	**CEB 90**	**B3**	**GL2000**
At 56 Days	1/2	1/2	3	4
At 250 Days	4	3	1	2
Sum of Ranks	5	4	4	6

5.12 GL2000 Standard Cure Sensitivity

A sensitivity analysis was preformed to adjust the model's cement type factor to the LTHSC Type II with a GGBFS. The GL2000 model allows the model's cement type, K, to be modified to calibrate the model with experimental data. Table 24 presents the GL2000 recommended cement type factors.

Table 24 GL2000 Recommended Cement Type factor.

Cement Type	K
I	1.0
II	0.7
III	1.15

Figure 55 presents the shrinkage strain residuals with K equal to 0.9 to 1.15. A K factor of 1.0 would minimize the residual. This would correspond with a 60 microstrain increase of predicted shrinkage and total strain. This also reduces the total strain residual, but not enough to predict better than the CEB 90 model (Figure 56).

Figure 57 presents a K factor sensitivity analysis for the accelerated cure specimens. This results in an optimal K factor of 0.9. This results in a 140 microstrain increase in the predicted shrinkage strain. This will not help the total strain ranking since the model is over predicting total strain.

Figure 58 presents a K factor sensitivity analysis for the shrinkage prisms. The resulting optimal K factor is 0.8. This corresponds with the recommended K factor for Type II A5-diabase/slag cement mixtures (Mokarem, 2002). Mokarem's measurements were also taken on 75 mm x 75 mm x 285 mm (3 in. x 3 in. x 11.25 in.) shrinkage prisms.

Table 25 presents the optimal K for the three specimen sizes tested. The optimized K value increases with specimen size. This indicates that theGL2000 shrinkage $\beta(t)$, the factor for time effects on shrinkage, should be examined in the future.

Table 25 Experimental K factors and V/S ratios.

Specimen Size	Volume to Surface Area (V/S)	Best K value	Curing Method
150 mm diameter cylinders	1.5	1.0	Standard
100 mm diameter cylinders	1.0	0.9	Accelerated
75 mm square prisms	0.75	0.8	Standard

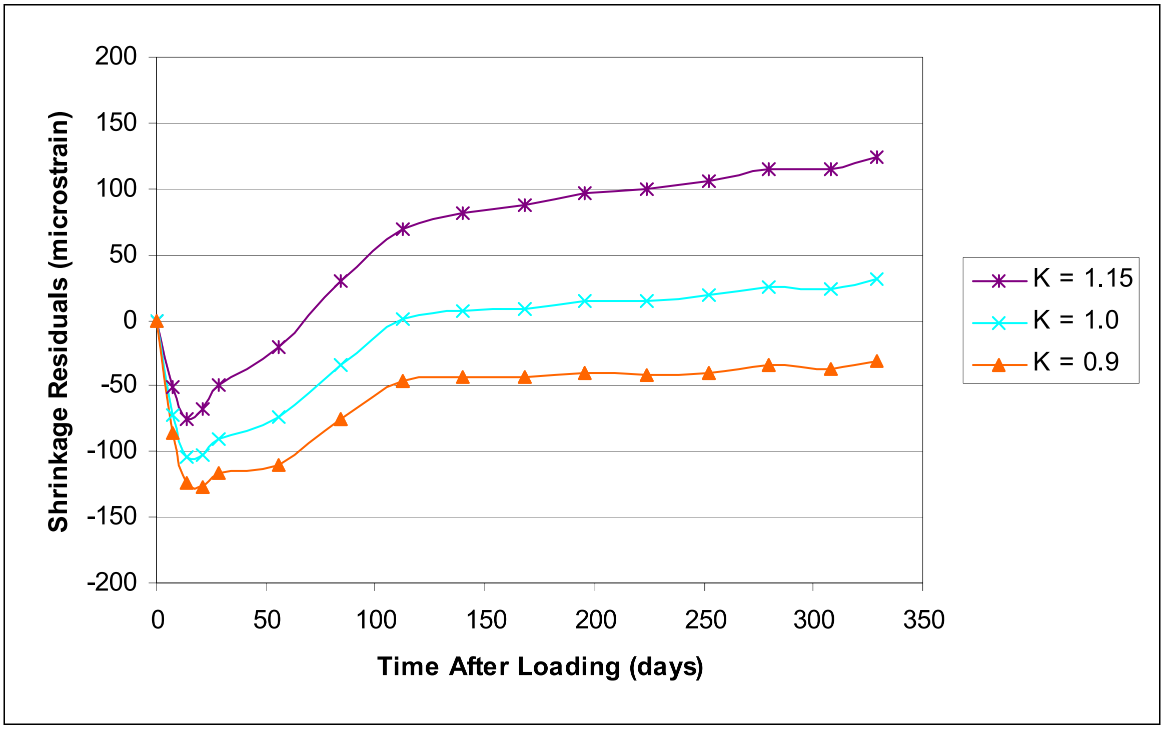

Figure 55 Standard Cure Shrinkage Strain Sensitivity Analysis of the GL2000 K factor.

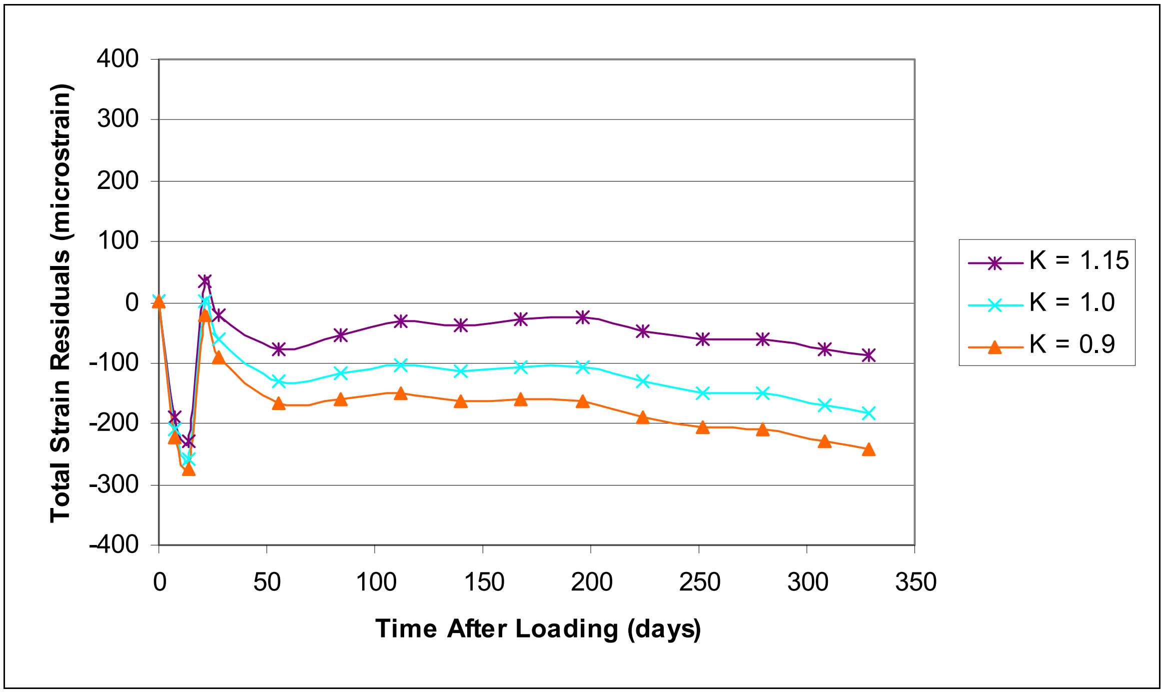

Figure 56 Total Strain Sensitivity Analysis of the GL2000 K factor, Standard Cure.

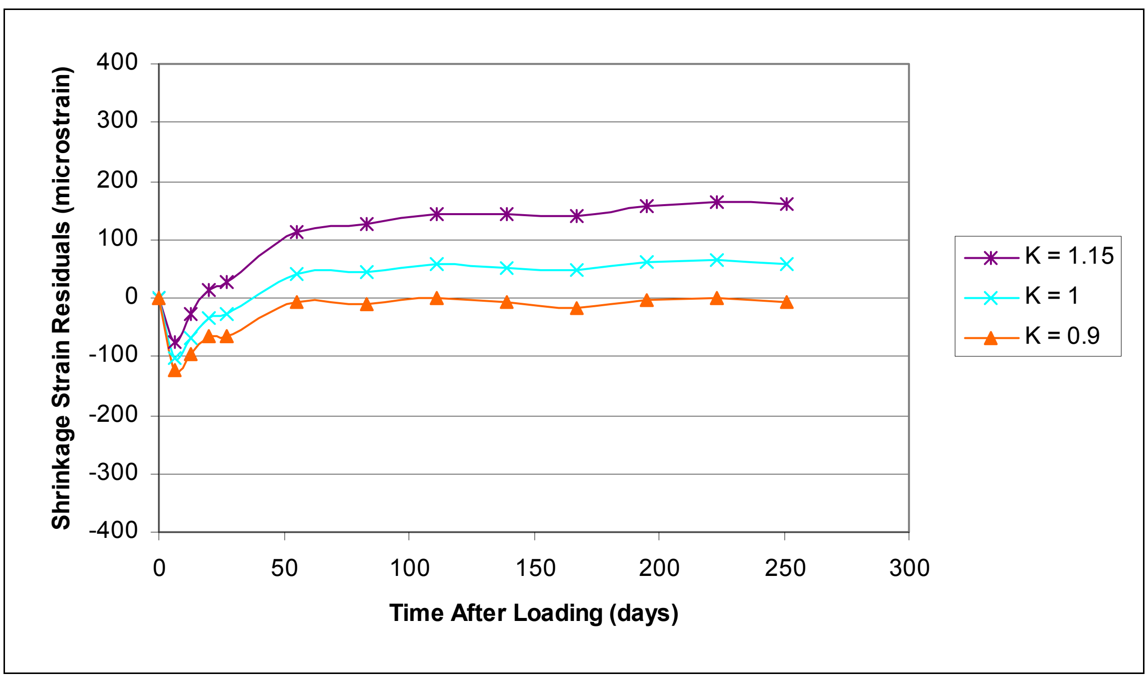

Figure 57 Accelerated Cure Shrinkage Strain Sensitivity Analysis of the GL2000 K factor.

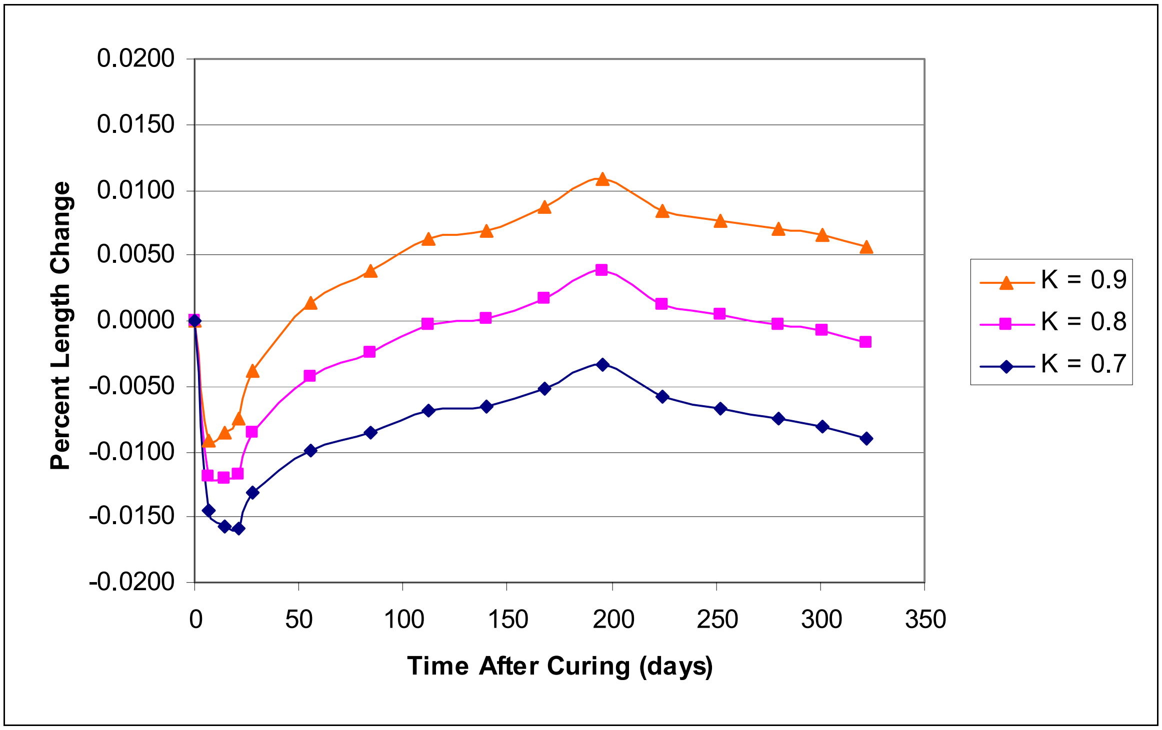

Figure 58 GL2000 K factor sensitivity with shrinkage prisms

CHAPTER 6: CONCLUSIONS AND RECOMMENDATIONS

Conclusions

For Accelerated Cure Applications

1. The total strain of the accelerated cure LTHSC batches 4 and 5 were 2510 ± 20 and 3800 ± 160 microstrain at 90 days and 2930 ± 40 and 4470 ± 180 microstrain at 250 days, respectively, at a five percent significant level.

2. ACI 209 is the best predictor of total strain for the Bayshore LTHSC mixture when loaded to 40 percent of the ultimate compressive strength and an accelerated curing method is used.

3. ACI 209 is the best predictor of time dependent deformations.

4. The use of the accelerated cure method significantly increased the variability of the strength and creep strains. Maturities and unit weights should be kept as similar as possible.

For Standard Cure Applications

6. The total strain of the standard cure LTHSC mixture was 2970 ± 330 microstrain at 90 days and 3510 ± 370 microstrain at 250 days at a five percent significant level.

7. The CEB Mode Code 90 is the best predictor of total strain for the Bayshore LTHSC mixture when loaded to 40 percent of the ultimate compressive strength and a standard cure is used.

8. The GL2000 model is the best predictor of time dependent deformations.

9. The total strain of Meyerson's VDOT A5 Limestone GGBFS mixture was reported as constant at 1470 ± 110 microstrain at 90 days, at a five percent significant level. This mixture has a shrinkage strain of 350 ± 30 microstrain at 90 days at a five percent significant level. The LTHSC mixture is increasing in magnitude of both total strain at 2970 ± 330 microstrain and shrinkage strain of 450 ± 60 microstrain at 90 days.

Both mixtures had Grade 120 GGBFS as 40 percent of the cementitious materials. The water to cementitious materials ratios were 0.33 and 0.37 and the cement contents were 249 kg/m^3 (420 lb/yd^3) and 268 kg/m^3 (451 lb/yd^3) for the A5 mixture and the LTHSC mixture, respectively.

The LTHSC mixture has a significantly larger magnitude of instantaneous and time dependent deformations. At 90 days after loading, the total strain is twice that of the VDOT A5 limestone GGBFS mixture and the shrinkage strain is 30 percent greater. Time dependent deformations also continue over a larger period. Part of this may be attributed to the higher water to cementitious materials ratio and higher cement paste content of the LTHSC mixture.

Recommendations

1. The relationship between laboratory specimens under a constant applied stress and prestressed beams that have a decreasing applied stress due to prestress losses needs to be developed or the laboratory testing procedure needs to be modified with a time step approach.

2. The relationship between the laboratory specimen and bridge beam volume to surface area ratios should be developed. The study of basic creep and drying creep separately could be of significance. Laboratory specimens experience a great deal more drying creep and drying shrinkage than a bridge beam placed over a river.

3. Further examination of the GL2000 model should be conducted with specimens of various volume to surface area ratios. The equation for shrinkage over time may need adjusted.

References

ACI 213R-87, Guide to Structural Lightweight Aggregate Concrete, ACI Manual of Concrete Practice, Part 1, 2002.

Mehta, P. K., and Monteiro, P. J. M., Concrete Structure, Properties, and Materials, Second Edition, Prentice Hall, 1993.

Mokarem, D. W., Development of Concrete Shrinkage Performance Specifications, Doctor of Philosophy in Civil Engineering, Virginia Tech, May 2002.

Meyerson, R., Compressive Creep of Prestressed Concrete Mixtures with and without Mineral Admixtures, Master of Science Thesis in Civil Engineering, Virginia Tech, February 2001.

Standard Specifications for Highway Bridges, Adopted and Published by the American Association of State Highway and Transportation Officials, Inc., sixteenth edition, 1996.

APPENDIX A

Literature Review and Prediction Models

TABLE OF CONTENTS

INTRODUCTION

Concrete undergoes volumetric changes throughout its service life. These changes are a result of applied loads and shrinkage. Applied loads result in an instantaneous recoverable elastic deformation and a slow, time dependent, inelastic deformation called creep. Creep without moisture loss is referred to as basic creep and with moisture loss is referred to as drying creep. The summation of instantaneous and time dependent deformations is called total deformation.

Shrinkage is a combination of autogeneous, drying, and carbonation shrinkage of the hardened concrete. Plastic shrinkage is not included since it occurs due to moisture loss before the concrete has set. Autogeneous shrinkage is a result of the hydration process. The hydrated cement paste has a smaller volume than the cement and water reactants. Drying shrinkage occurs as surface water evaporates and internal water moves outward in an attempt for hygral equilibrium. The opposite reaction is called swelling. Carbonation shrinkage occurs with the carbonation of the hydrated cement products with carbon dioxide in the atmosphere.

Creep testing is conducted on sealed or unsealed specimens. Sealed specimens with an applied stress have volumetric changes due to elastic deformation, basic creep, and autogeneous shrinkage. Sealed specimens without an applied stress deform due to autogeneous shrinkage. Basic creep is the total deformation of a loaded, sealed specimen minus the elastic deformation and autogeneous shrinkage.

Unsealed specimens are the most commonly used test method. Unsealed specimens without an applied stress have volumetric changes due to autogeneous and drying shrinkage. The total deformation of unsealed specimens is the result of an applied stress producing an elastic deformation, creep, and shrinkage. Creep includes both basic and drying creep. Shrinkage includes autogeneous and drying shrinkage. Drying creep of a loaded specimen is the total deformation minus the elastic deformation, basic creep, and autogeneous shrinkage and requires the testing of both sealed and unsealed specimens. Therefore, creep is typically examined as the total of basic and drying creep.

EFFECT OF LTHSC PROPERTIES ON CREEP

Properties of Lightweight Concrete

Lightweight aggregates are weaker than normal weight aggregates so higher cement contents are needed to get a required strength for a mixture. This increases the amount of cement paste, which will lead to increased creep (Clarke). This decrease in stiffness can be seen in modulus of elasticity measurements of lightweight concretes (Nawy).

Lightweight aggregates have relatively large pore volumes, which makes water absorption more important than with denser normal weight aggregates (Clarke). The water to cement ratio and slump can be impacted more significantly with changes in aggregate moisture conditions if water content is not adjusted. Workability can decrease between mixing and placing as moisture is absorbed by lightweight aggregates (Clarke). Possible segregation of the mix should be considered since lightweight aggregates can begin to float when larger slumps are used.

Volumetric Changes: Influences and Mechanisms

The two types of volumetric changes examined are drying shrinkage and creep. Drying shrinkage is the decrease in volume of hardened concrete with time due to the loss of moisture, while excluding thermal effects. Creep is the time dependent deformations due to a sustained stress. The term "creep" refers to both drying and basic creep, which occur with and without moisture loss respectively. Neville and Gilbert prefer to identify creep as the time-dependent deformation in excess of shrinkage.

The following are other types of volumetric changes. Plastic shrinkage occurs before the concrete sets. Carbonation shrinkage is a result to the hardened cement paste reacting with carbon dioxide in the atmosphere. Autogeneous shrinkage is due to drying as the cement paste hardens during hydration.

Creep Mechanisms

The literature considers many mechanisms as the theoretical basis of creep. Gilbert states no single theory accounts for all of the phenomena and that all of the following four mechanisms contribute. Viscous flow occurs from sliding of the colloidal sheets in the cement gel between absorbed water. Seepage or the expulsion and decomposition of the interlayer water within the cement gel. Delayed elasticity or the time dependent elastic deformation between the aggregate and gel crystals as viscous flow and seepage occur within the cement gel. Gilbert also notes the at high stress levels, the additional deformation can occur and the transition zone breaks down.

Mehta describes creep and drying shrinkage as the removal of adsorbed water from the hydrated cement paste. Drying shrinkage is caused by the loss of physically adsorbed water from the C-S-H that causes a shrinkage strain. The differential relative humidity or an applied load act as the driving force to create a hydrostatic tension in the small capillaries (< 50nm) of the hydrated cement paste. Mehta states that loads above 30 to 40 percent of the compressive strength lead to microcracking in the transition zone. Delayed elastic deformation also occurs as loads are transferred back and form between the aggregate and the cement paste as they each deform elastically over time.

Influences on Volumetric Changes

Lightweight, high strength concrete has many influences on its volumetric changes. These involve aggregate properties, cement type and fineness, cement and water content, cement replacements, admixtures, curing, environmental conditions, and specimen size.

Aggregate Properties

Aggregate strength is generally overlooked since normal weight aggregate is typically several times stronger than the cement paste and transition zone. Lightweight aggregate is an exception (Metha). Aggregates properties are critical to the amount of creep, since the aggregates have a restraining affect on the magnitude of creep (Neville). Mokarem noted that diabase aggregate mixtures experienced greater drying shrinkage than limestone and gravel mixtures.

The ACI 213 Guide for Structural Lightweight Aggregate Concrete discusses how the high magnitude and variation in lightweight aggregate absorption and absorption rates can significantly differ mixture proportions with that of normal weight mixtures. This results in significantly different water and cement contents. Lightweight aggregates typically absorb 5 to twenty percent by weight of the drying aggregate. If the lightweight aggregates are not presoaked then the aggregate can pull moisture out of the fresh mix resulting in a loss in workability. Additional strength can be gained by presoaking the aggregate for 24 hours before mixing. The excess moisture in the lightweight aggregate will internally prolong the curing process.

Aggregates have a large role in determining the modulus of elasticity of a concrete mix. Influential aggregate properties are porosity, maximum size, shape, surface texture, grading, and mineralogical composition. Mehta states with lightweight concrete, the modulus of elasticity of the aggregate is the most important.

As the load is transferred to the aggregate, the creep and drying shrinkage of the cement paste is partially restrained. Therefore, concretes with high aggregate contents are less vulnerable to high creep or shrinkage strains (Nawy). Nawy also notes research has shown that smaller aggregates, 9.5 mm (3/8 in.) maximum can increase the compressive strength from 44.8 MPa (6,500 psi) to over 55 MPa (8,000 psi). Smaller aggregate sizes are also known to increase creep and shrinkage.

The "ceiling" strength of a concrete depends on the aggregate type (Clarke). The "ceiling" is reached when the capacity of the cement paste and transition zone is reached and the concrete can no longer transfer load to the aggregate.

Effect of Cement Type and Fineness

The cement is the most important factor since creep occurs in the hydrated cement paste. It affects creep in two ways: the physical and chemical properties (Neville). The physical and chemical properties have a direct affect on the strength of the cement paste. The physical properties relate to fineness, which has a direct relationship with the rate of hydration. The smaller the cement particles, the faster they are going to hydrate and gain strength. There is not a direct relationship between chemical composition and creep, but there is relationship between chemical composition of the cement and strength. The finer the cement the more C_3A that is available at early ages, which results higher rate of strength gain (Neville). Higher strength normal weight concretes typically creep and shrinkage less.

Effect of Cement and Water Content

The quantity of cement paste is important due to aggregate having a restraining affect on the magnitude of creep (Neville). As cement content increases, the influence of the aggregates decrease as the mixture is being diluted with cement paste. For lightweight concrete, cement content is a good indication of strength for mix design purposes (Clarke). The compressive strength of a LTHSC mixture is usually rated to the cement content at a given slump than the water to cement ratio (ACI 213)

Lower water contents result in lower creep and shrinkage strains. A more dense cement paste will strain less. The variability of the absorption properties of lightweight aggregates have a direct relationship on the between batch consistency of water to cement ratios (ACI 213).

Effect of Cement Replacement

Cement replacements include ground granulated blast furnace slag(GGBFS), fly ash, and silica fume. An increase in creep will occur when GGBFS or other pozzolan material is used as a partial cement replacement for Type I cement (Mehta). Silica fume will increase the hydration rate with its particle size of one-hundreth that of a cement particle. Silica fume will increase shrinkage. Mehta states that pozzolans tend to increase the volume of fine pores (3 to 20 nm) which increases creep and shrinkage. Although, Nawy says pozzolans help fill the matrix voids which creates a denser matrix and stronger mix.

Effect of Admixtures

Cabrera et al found that superplasticizers that reduce the surface tension of water also increase creep and shrinkage strains in cement paste. This is being attributed to a larger volume of total pores and a courser size distribution, a larger negative pore pressure at constant humidity, and a lower degree of saturation at a constant humidity.

Concrete with entrained air would creeps more, but entrainment agents reduce the required water. This reduction in water compensates for the increased air voids (Neville).

Using calcium chloride or triethanolamine as an accelerator also increases creep and shrinkage (Mehta, Neville).

Effect of Curing

Moist curing allows concrete to continue hydration without being limited by the availability for water. Dry cured concrete specimens are dependent on the internal moisture for hydration. A dry cured specimen will have less creep potential due to less moisture being present in the paste (Neville). Lightweight aggregate concretes are more tolerant of poor curing conditions since the aggregate has a larger water reserve in the poor system (Nawy).

Effect of Environmental Conditions

Muller compared specimens of various thicknesses to both constant and cyclic humidity conditions. They found that cyclic humidity increases creep, but does not increase shrinkage (Mehta, Muller, Neville). If the concrete dries, then hydration will slow along with any strength increase (Neville, Clarke).

Muller also notes that Bazant's models are the only ones that take cyclic ambient conditions into consideration. The ACI 209, CEB90 and B3 consider the environmentally temperature in the prediction models.

Effect of Specimen Size

The specimen size factor is significant to drying creep and drying shrinkage since they are a function of water removal (Mehta). It is typically a function of the volume to surface area since it relates the distance water must travel to leave a specimen. The ratio of volume to surface area is also called the theoretical thickness (Mehta). An increase in the thickness of a member will result in a decrease in the members creep strain (Nawy).

PRESTRESSED CONCRETE APPLICATIONS OF LIGHTWEIGHT CONCRETE

Understanding of volumetric changes in lightweight concrete is critical in the prestressed concrete industry. Creep and shrinkage losses must be accounted for when prestressing members. They are generally lumped together with the elastic strain as total strain. If total strain is not accurately predicted, then a member could be over designed and increase costs. On the other hand, if total strain is under predicted, a prestressed member could lose a portion of its design capacity and possibly have a shortened service life, which is not cost effective either.

The Federal Highway Administration has performance grades for high-performance structural concrete. A mixture may be specified as a different grade for different characteristics. The following chart shows performance characteristics related to properties examined in this study (Myers). The applicable ASTM test number is listed.

Table 26 FHWA High-Performance Structural Concrete Grades (Myers)

	ASTM	1	2	3	4
Compressive strength	C 39	41 ≥ x > 55 MPa (6 ≥ x > 8 ksi)	55 ≥ x > 69 MPa (8 ≥ x > 10 ksi)	69 ≥ x > 97 MPa (10 ≥ x > 14 ksi)	x > 97 MPa (x > 148 ksi)
Elastic Modulus	C 469	28 ≥ x > 40 GPa (4 ≥ x ≥ 6 x 10^6 psi)	40 ≥ x > 50 GPa (6 ≥ x ≥ 7.5x 10^6 psi)	x > 50 GPa (x ≥ 7.5 x 10^6 psi)	----
Shrinkage (microstrain)	C 157	800 ≥ x > 600	600 ≥ x > 400	x < 400	----
Creep (specific creep)	C 512	75 ≥ x > 60/MPa (0.52 ≥ x > 0.41/psi)	60 ≥ x > 45/MPa (0.41 ≥ x > 0.31/psi)	45 ≥ x > 30/MPa (0.31 ≥ x > 0.21/psi)	x ≤ 30/MPa (x ≤ 0.21/psi)

Lightweight concrete has advantages by reducing the volume of construction materials and decreasing construction time. Lightweight concrete can allow for reduced dead load of a structure and smaller foundations. It can also allow for segmental construction of larger pieces since they have lower densities (Clarke).

Lightweight concrete also has disadvantages. Due to the lower modulus of elasticity, member deflections will be larger (Clarke). If the creep is also increased by a lower modulus, then the member will camber upward more than predicted. Lightweight aggregates, like expanded slate, are manmade so they are more expensive than natural aggregates.

PREDICTION MODELS

Five prediction models for creep and shrinkage are examined. The ACI 209 model is recommended by the American Concrete Institute. The CEB-FIP Mode Code 90 is used in Europe. Other models include the B3, which was developed by Bazant, the GL model, which was developed by Gardner, and the SAK model, which was developed by Sakata.

The models look at free shrinkage, creep strain, and elastic deformation. Free shrinkage is the combination of all shrinkage strains without an applied load. The creep strain is the combination of the basic and drying creep. The elastic deformation is the instantaneous recoverable deformation of a concrete specimen during the loading process.

The various creep models relate the creep strain to the loading conditions by using creep coefficient, specific creep, or creep compliance. The creep coefficient is the ratio of creep strain at given time to the initial elastic strain. Specific creep is the creep strain per unit stress. The creep compliance is the ratio of creep strain plus elastic strain per unit stress.

ACI 209R-92

The ACI 209 model was developed by the American Concrete Institute and is used in the AASHTO LRFD method. The ACI 209 Model was created from data that included normal weight, sand lightweight, and lightweight concrete while also incorporating Type I and III cement and moist and steam curing. It was found that there was no significant difference between different weight concretes for creep and shrinkage. The code notes that more consistent results were found by using the creep coefficient or the ratio of creep strain to initial strain. This was due to the initial stiffness of the concrete being accounted for.

The code allows for the following variation to the standard conditions: concrete composition, age at loading, ambient relative humidity, size factor, and ambient temperature. The concrete composition correction factors apply to slump, fine aggregate percentage, cement content, and air content. Either the average thickness method or the volume to surface ratio method can adjust the size factor. The volume to surface area ratio was used since it is more applicable to prestressed concrete beams.

CEB 90 Model Code

The CEB Model Code 90 is the European design code recommended by the Euro-International Concrete Committee and International Federation for Prestressing). This model was preceded by the CEB-FIP 1970 model and the CEB-FIP 1978 model. The CEB-FIP 1970 model was a product model that adjusted for mix properties and environmental conditions with multiplication factors from graphs. The CEB-FIP 1978 model was a summation model that had corrections factors that needed to be summed from graphs.

The CEB MC 90 is a product prediction model, which is designed to predict the mean time dependent deformation for normal weight, plane structural concrete. It only takes into account parameters that are generally known to the designer in the design stage. The CEB model has a coefficient of variation of 20.4% and 32.9% for creep compliance and shrinkage respectively.

The following parameters are required to predict the creep coefficient: mean or design strength of the concrete, member dimensions, mean relative humidity of the ambient atmosphere, age at loading, and duration of loading. In addition to these parameters, the cement type is needed to predict shrinkage strain.

B3 Model

The B3 model is the creation of Z. P. Bazant and S. Baweja. Earlier versions of the model were the BP model in 1978 and the BP-KX model in 1991. The BP-KX has an expanded and a short form. The expanded form is for structures highly sensitive to creep and shrinkage. The short form predicted creep compliance in a design code method. The B3 model is design to meet the requirements of the RILEM TC 107 for a simpler model.

The B3 model can be applied to concretes outside of the limitations if the parameters are calibrated with tests.

GL2000

N. J. Gardner and M. J. Lockman developed the GL2000 Model as a design office procedure to predict creep and shrinkage. Gardner and J. W. Zhao's GZ Model from 1993 preceded this product model.

The predicted values can be improved by measuring the compressive strength and modulus of elasticity. This model uses the modulus of elasticity and compressive strength measurements to adjust for aggregate stiffness. Aggregate stiffness is a factor in elastic deformation, creep, and shrinkage. The GL2000 model uses the experimental modulus to have a compressive strength back calculated from it. This value is averaged with the compressive strength and an adjusted modulus is calculated. The creep coefficient prediction uses the time at loading, time at the beginning of shrinkage, volume to surface area ratio, and the ambient relative humidity. The model has a factor, $\Phi(t_c)$, to adjust for moisture loss before loading. If the time of loading is equal to the time at the beginning of shrinkage, then $\Phi(t_c)$ equals one. The specific creep is found by dividing the creep coefficient by the adjusted modulus of elasticity. The instantaneous elastic strain can be found by dividing the applied load by the modulus of elasticity at the time of loading. Shrinkage strain is predicted with correction factors for the effect of cement type on shrinkage, the effect of time on shrinkage using the volume to surface ratio, and humidity. The ultimate shrinkage strain is a function of the mean 28-day compressive strength.

SAK

The SAK was developed by K. Sakata and is the recommended method of Japan Society of Civil Engineers. The model separately predicts ultimate values of drying creep, basic creep, and shrinkage. Water and cement content are used in predicting both drying and basic creep. The ambient relative humidity is used with the volume to surface area of the member to predict both drying creep and shrinkage. The specific creep prediction is a function of time with the ultimate drying and basic creep. The shrinkage prediction is a function of time based on the ultimate predicted value. The following chart shows the multiple correlation coefficients from the creation of the SAK model.

Table 27 Multiple correlation coefficient for each part of the SAK model

Basic Creep	r = 0.819
Drying Creep	r = 0.80
Shrinkage	r = 0.90

The range of experimental data used to create the SAK model defines its limitations. Ordinary Portland cement was used, which is assumed to be type I. The w/c ratios varied from 0.38 to 0.68. The cement content varied from 260 kg/m^3 to 500 kg/m^3 (16 pcf to 31 pcf). The specimen ages at the beginning of shrinkage or at loading varied between 3 and 56 days. Ambient humidity was 60 and 80%. The shrinkage tests included 160 different beam specimens with dimensions of 10 x 10 x 40 cm, 15 x 15 x 53 cm, and 30 x 30 x 120 cm. The creep tests included 104 different beam specimens with dimensions of 10 x 10 x 38 cm and 15 x 15 x 51 cm. The specimens had strengths that ranged from 150 kg/cm^2 to 550 kg/cm^2 (2000 psi to 7,800 psi)

Sakata reported that the SAK model agreed with data in the CEB-FIP experimental data bank. Therefore, this model is able to predict creep and shrinkage for the other normal concretes.

MODEL LIMITATIONS AND REQUIRED PARAMETERS

Table 28 Model limitations

Parameter	ACI 209R-92	CEB MC 90	B3	GL2000	SAK
f_{cm} (psi)	-	2,900-13,000	2,500-10,000	2,900-10,000	-
a/c	-	-	2.5-13.5	-	-
c (lbs/ft^3)	-	-	10-45	-	16-31
w/c	-	-	0.30-0.85		0.38 - 0.68
H (%)	40-100	40-100	40-100	40-100	60-80
Cement Type	I or III	R, SL, or RS	I, II, or III	I, II, or III	I or III
t_o or t_s (moist cured)	$\geq$ 7 days	$t_s \leq$ 14 days	$t_s \leq t_o$	$\geq$2 days	$\geq$ 3 days
t_o or t_s (steam cured)	$\geq$ 1-3 days	$t_s \leq$ 14 days	$t_s \leq t_o$	$\geq$ 2 days	$\geq$ 3 days
Model includes lightweight concretes?	Yes, normal, lightweight sand, & lightweight	No	No	No, but considers aggregate stiffness	No

Table 29 Model parameters

Parameter	ACI 209R-92	CEB MC 90	B3	GL2000	SAK
a/c	NR	NR	R	NR	NR
f_{cm} or $f'_{c(28)}$	R	R	R	R	NR
C	NR	NR	R	NR	R
H	R	R	R	R	R
W	NR	NR	R	NR	R
w/c	NR	NR	R	NR	R
t_o	R	R	R	R	R
t_s	R	R	R	R	R
Type of cement	R	R	R	R	R
V/S or A/u	R	R	R	R	R
σ	R	R	R	R	R

Nomenclature:

R	= Required parameter
NR	= Parameter not required
f_{cm} or f'_{c28}	= Mean 28 day compressive strength
a/c	= Aggregate to cement ratio by weight
c	= Cement content
w/c	= Water to cement ratio by weight
H	= Relative humidity
t_o	= Age of concrete at loading
t_s	= Age of concrete at the beginning of shrinkage
σ	= Applied stress
V/S	= Volume to surface area ratio
A/u	= Ratio of area to perimeter of member

Cement Types

ASTM Type I	= Normal Portland cement
ASTM Type II	= Moderate sulfate resistance cement
ASTM Type III	= High early strength cement
N, R	= European normal and rapid hardening cement (assumed equivalent to ASTM Type I)
SL	= European slow hardening cement (equivalent to ASTM Type II)
RS	= European rapid hardening high strength cement (equivalent to ASTM Type III)

SUMMARY OF PREDICTION MODEL NOMENCLATURE AND EQUATIONS

ACI 209 Code Model

Nomenclature

$C_c(t)$	= Creep coefficient at time t
t	= Time after loading (days)
E_{cmto}	= Modulus of elasticity at age of loading
$\varepsilon(t)$	= Total Strain; instantaneous plus creep and shrinkage
$\varepsilon_s(t)$	= Shrinkage strain (in./in.)
$f'_c(t_o)$	= Mean concrete compressive strength at age of loading (psi)
f'_{c28}	= Mean 28 day compressive strength (psi)
t_o	= Age of concrete loading (days)
γ	= Unit weight of concrete (lbs/ft^3)
t_s	= Time after the beginning of shrinkage (days)
K_{SS}	= Shape and size correction factor for shrinkage
K_{SH}	= Relative humidity correction factor for shrinkage
ε_{shu}	= Ultimate shrinkage strain (in./in.)
C_{cu}	= Ultimate creep coefficient
K_{CH}	= Relative humidity correction factor for creep
K_{CA}	= Age at loading correction factor
K_{CS}	= Shape and size correction factor for creep
H	= Relative humidity (%)
V/S	= Volume to surface area ratio (in.)
σ	= Applied stress (psi)
γ_{sc}	= Creep correction factor for slump
γ_{sc}	= Shrinkage correction factor for slump
s	= Slump (in.)
γ_{ac}	= Creep correction factor for fine aggregate percentage

γ_{as} = Shrinkage correction factor for fine aggregate percentage

ψ = Fine aggregate percentage (%)

$\gamma_{\alpha c}$ = Creep correction factor for air content

$\gamma_{\alpha s}$ = Shrinkage correction factor for air content

α = Air content (%)

ACI 209 Equations

Creep Compliance Function

$$\text{Compliance function } (\mu\varepsilon / \text{psi}) = \frac{1 + C_c(t)}{E_{cmto}}$$

Total Strain

$$\varepsilon(t) = \varepsilon_s(t) + \frac{\sigma}{E_{cmto}} * (1 + C_c(t))$$

Compressive Strength

$$f'_c(t_o) = f'_{c(28)} * \left[\frac{t_o}{b + c * t_o} \right]$$

Type of Cement	Moist Cured Concrete	Steam Cured Concrete
I	b = 4.0 c = 0.85	b = 1.0 c = 0.95
III	b = 2.3 c = 0.92	b = 0.7 c = 0.98

Note: Estimate not needed. The experimental $f'_c(t_o)$ was used.

Modulus of Elasticity

$$E_{cmto} = 33(\gamma)^{3/2} * \sqrt{f'_c(t_o)}$$

Note: Estimate not needed. The experimental E_{cmto} was used.

Creep Strain

$$\text{Creep Strain} = \frac{\sigma}{E_{cmto}} * C_c(t)$$

$$C_c(t) = \frac{t^{0.6}}{10 + t^{0.6}} * C_{cu} * K_{CH} * K_{CA} * K_{CS} * \gamma_{sc} * \gamma_{ac} * \gamma_{\alpha c}$$

$C_{cu} = 2.35$

$K_{CH} = 1.27 - 0.0067*H$

$K_{CS} = ⅔ * [1 + 1.13 * e^{(-0.54 * V/S)}]$

Moist Cured Concrete	**Steam Cured Concrete**
$t, t_o \geq 7$ days, $H \geq 40$ %	$t, t_o \geq 1$ to 3 days, $H \geq 40$ %
$K_{CA} = 1.25 (t_o)^{-0.118}$	$K_{CA} = 1.13 (t_o)^{-0.095}$

$\gamma_{sc} = 0.82 + 0.067s$

$\gamma_{ac} = 0.88 + 0.0024\psi$

$\gamma_{\alpha c} = 0.46 + 0.09\alpha$

Shrinkage Strain

$$\varepsilon_s(t) = \frac{t_s}{b + t_s} * K_{SS} * K_{SH} * \gamma_{ss} * \gamma_{as} * \gamma_{\alpha s} * \varepsilon_{shu}$$

$K_{SS} = 1.2e^{(-0.12 * V/S)}$

$\gamma_{ss} = 0.89+0.041s$

For fine aggregate percentage $\leq 50\%$

$\gamma_{as} = 0.30 + 0.014\psi$

For fine aggregate percentage $> 50\%$

$\gamma_{as} = 0.90 + 0.002\psi$

$\gamma_{\alpha s} = 0.95+0.008\alpha$

$\varepsilon_{shu} = 780 \times 10^{-6}$ in/in

Humidity	Moist Cured Concrete	Steam Cured Concrete
40 % ≤ H ≤ 80 %	b = 35 t ≥ 7 days	b = 55 t ≥ 1 to 3 days
	$K_{SH} = 1.4 - 0.01H$	$K_{SH} = 1.4 - 0.01H$
80 % ≤ H ≤ 100 %	b = 35 t ≥ 7 days	b = 55 t ≥ 1 to 3 days
	$K_{SH} = 3 - 0.03H$	$K_{SH} = 3 - 0.03H$

CEB 90 Code Model

Nomenclature

$\phi(t,t_o)$	= Creep coefficient defining creep between time t and t_o
E_c	= Modulus of elasticity at 28 days (N/mm^2)
$E_c(t_o)$	= Modulus of elasticity at age of loading (N/mm^2)
$\varepsilon(t)$	= Total strain; instantaneous plus creep and shrinkage (mm/mm)
$\varepsilon_{cs}(t-t_s)$	= Shrinkage strain between time t and t_s (mm/mm)
t	= Age of concrete after casting (days)
t_s	= Age of concrete at the beginning of shrinkage (days)
f_{cm}	= Mean 28 day concrete compressive strength (N/mm^2)
f_{ck}	= Characteristic compressive strength with 95% confidence (N/mm^2)
t_o	= Age of concrete at loading (days)
ϕ_o	= Notional creep coefficient
$\beta_c(t-t_o)$	= Coefficient describing creep development with time after loading
ϕ_{RH}	= Factor to allow for relative humidity on the notional creep coefficient (ϕ_o)
$\beta(f_{cm})$	= Factor to allow for effect of concrete strength on the notional creep coefficient (ϕ_o)
$\beta(t_o)$	= Factor to allow for the effect of age of concrete at loading on the notional creep coefficient (ϕ_o)
RH	= Relative humidity (%)
A_c	= Cross-section area of member (mm^2)
u	= Perimeter of member in contact with the atmosphere (mm)
h_o	= $2A_c/u$ = Notional size of member (mm)
β_H	= Coefficient to allow for the effect of relative humidity and the notional member size (h_o) on creep
ε_{cso}	= Notional shrinkage coefficient
$\beta_s(t-t_s)$	= Equation describing development of shrinkage with time
$\varepsilon_s(f_{cm})$	= Factor to allow for the effect of concrete strength on shrinkage

β_{RH}	= Coefficient to allow for the effect of relative humidity on the notional shrinkage coefficient (ε_{cso})
β_{sc}	= Coefficient depending on type of cement
β_s	= Coefficient to describe the development of shrinkage with time
σ	= Applied stress (N/mm^2)
α	= Coefficient for cement type
$t_{o,T}$	= temperature adjusted age of concrete at loading (days)
Δt_i	= number of days at temperature T
$T(\Delta t_i)$	= temperature during time period Δt_i (^oC)
n	= number of time intervals considered

CEB 90 Model Code Equations

Total Strain

$$\varepsilon(t) = \varepsilon_{cs}(t\text{-}t_s) + \left[\frac{\phi(t,t_o)}{E_c} + \frac{1}{E_c(t_o)}\right]\sigma$$

Mean Concrete Strength

$$f_{cm} = f_{ck} + 8\ \text{N/mm}^2$$

Note: Estimate not needed. The experimental f'_{c28} was used.

Modulus of Elasticity at Age t

$$E_c = 10000\ \sqrt[3]{f_{cm}}$$

$$E_c(t_o) = (E_c)\ e^{\left[\frac{S}{2}\left(1-\sqrt{\frac{28}{t}}\right)\right]}$$

S = 0.38, slow hardening cement
0.25, normal and rapid hardening cement
0.20, rapid hardening high strength

Note: Estimate not needed. The experimental E_c and $E_c(t_o)$ was used.

Creep Compliance Function

$$\text{Compliance function } [\mu\varepsilon/\text{ psi}] = \frac{\phi(t,t_o)}{E_c} + \frac{1}{E_c(t_o)}$$

$$\phi(t,t_o) = (\phi_o) * \beta_c(t\text{-}t_o)$$

$$\phi_o = \phi_{RH} * \beta(f_{cm}) * \beta(t_o)$$

$$\phi_{RH} = 1 + \frac{\left(1 - \frac{RH}{100}\right)}{0.1 * \sqrt[3]{h_o}}$$

$$\beta(f_{cm}) = \frac{16.8}{\sqrt{f_{cm}}}$$

$$\beta(t_o) = \frac{1}{(0.1 + t_0^{0.2})}$$

$$\beta_c(t\text{-}t_o) = \frac{(t - t_o)^{0.3}}{[\beta_H + (t - t_o)]^{0.3}}$$

$$\beta_H = 1.5 * [1 + (0.012 * RH)^{18}] (h_o) + 250 \leq 1500 \text{ days}$$

The effect of cement type can be modified for the creep coefficient by modifying the age at loading:

$$t_o = t_{o,T} * \left[\frac{9}{2 + (t_{o,T})^{1.2}} + 1 \right]^{\alpha} \geq 0.5 \text{ days}$$

$$t_{o,T} = \sum_{i=1}^{n} \Delta t_i * e^{-\left[\frac{4000}{273 + T(\Delta_i)} - 13.65\right]}$$

Cement Type	α
SL	-1
N, R	0
RS	1

Shrinkage Strain

$$\varepsilon_{cs}(t - t_s) = (\varepsilon_{cso}) * \beta_s (t - t_s)$$

$$\varepsilon_{cso} = \varepsilon_s (f_{cm}) * (\beta_{RH})$$

$$\varepsilon_s (f_{cm}) = [160 + \beta_{sc} (90 - f_{cm})] * 10^{-6}$$

Type of Cement	β_{sc}
Slow hardening (SL)	4
Normal and rapid hardening (N, R)	5
Rapid hardening high strength (RS)	8

Humidity	β_{RH}
40 % ≤ RH ≤ 99 %, stored in air	-1.55 x β_{sRH}
RH ≥ 99 %, immersed in water	0.25

$$\beta_{RH} = 1 - \left(\frac{RH}{100}\right)^3$$

$$\beta_s(t-t_s) = \sqrt{\frac{(t - t_s)}{[0.035 * h_0^2 + (t - t_s)]}}$$

The B3 Model

Nomenclature

$J(t,t')$	= Creep compliance function; creep plus elastic (always $x10^{-6}$/psi)
α	= Thermal expansion coefficient
$\Delta T(t)$	= Temperature change from reference at time t
$C_o(t,t')$	= Compliance function for basic creep
$C_d(t,t',t_o)$	= Compliance function for additional creep due to drying
$\varepsilon(t)$	= Total Strain; instantaneous plus creep and drying (in/in)
$\varepsilon_{sh}(t)$	= Shrinkage Strain (in./in.)
f'_c	= Mean 28 day concrete compressive strength (psi)
f_{ck}	= Specified concrete compressive strength at 28 days (psi)
E_{28}	= Modulus of elasticity at 28 days (psi)
q1	= Instantaneous strain due to unit stress
q2	= Aging visco-elastic compliance
q3	= Non-aging visco-elastic compliance
q4	= Flow compliance
q5	= Creep at drying
t	= Age of concrete after casting (days)
t'	= Age of concrete at loading (days)
t_o	= Age of concrete at the beginning of shrinkage (days)
c	= Cement content of concrete (lbs/ft^3)
w/c	= Water to cement ratio by weight
a/c	= Aggregate to cement ratio by weight
H(t)	= Spatial average of pore relative humidity within cross section
S(t)	= Time function for shrinkage
$\varepsilon_{sh\infty}$	= Ultimate shrinkage strain (negative, always x 10^{-6} in./in.)
w	= Water content of concrete (lbs/ft^3)
h	= Relative humidity (decimal)
τ_{sh}	= Shrinkage half-time (days)
k_s	= Cross section shape factor

V/S = Volume to surface are ratio (in.)

D = 2(V/S) = Effective cross-section thickness (in.)

k_h = Humidity function for shrinkage

B3 Model Equations

Creep Compliance Function

$J(t,t')\ [\mu\varepsilon/\ psi] = q_1 + C_o(t,t') + C_d(t,t',t_o)$

Total Strain

$\varepsilon(t) = J(t,t')\sigma + \varepsilon_{sh}(t) + \alpha\Delta T$

Note: Assume specimens are in thermal equilibrium with room at time of loading.

Mean Compressive Strength

$f'_c = f_{ck} + 1200$

Note: Estimate not needed. The experimental f'_c was used.

Elastic Strain and Modulus of Elasticity

$$q_1 = \frac{0.6 * 10^6}{E_{28}}$$

$E_{28} = 57000\ (f_c')^{1/2}$

Note: Estimate not needed. The experimental E_{28} was used.

Basic Creep Compliance

$C_o(t,t') = q_2 * Q(t,t') + q_3 * \ln(1 + (t - t')^n) + q_4 * \ln(t / t')$

$$Q(t,t') = Q_f(t') * \left[1 + \frac{[Q_f(t')]^{r(t')}}{[Z(t,t')]^{r(t')}}\right]^{\frac{-1}{r(t')}}$$

$Q_f(t') = [\ 0.086 * (t')^{2/9} + 1.21 * (t')^{4/9}\ ]^{-1}$

$Z(t,t') = (t')^{-m} * \ln(1 + (t - t')^{n})$

$m = 0.5$

$n = 0.1$

$r(t') = 1.7 * (t')^{0.12} + 8$

$q_2 = 451.1 * (c)^{0.5} * (f_c')^{-0.9}$

$q_3 = 0.29 * (w/c)^4 * q_2$

$q_4 = 0.14 * (a/c)^{-0.7}$

Drying Creep Compliance

$C_d(t,t',t_o) = q_5\ [\exp\{-8*H(t)\} - \exp\{-8*H(t')\}]^{1/2}$

$H(t) = 1 - (1-h) * S(t)$

$H(t') = 1 - (1-h) * S(t')$

$q_5 = 7.57 \times 10^5 * (f'_c)^{-1} * (\varepsilon_{sh\infty})^{-0.6}$

$$S(t) = \tanh \sqrt{\frac{t - t_o}{\tau_{sh}}}$$

$$S(t') = \tanh \sqrt{\frac{t' - t_o}{\tau_{sh}}}$$

$\tau_{sh} = k_t\ (k_s * D)^2$

$k_t = 190.8\ (t_o)^{-0.08}\ (f_c')^{-0.25}$

Type of Member or Structure	k_s
Infinite slab	1.00
Infinite cylinder	1.15
Infinite square prism	1.25
Sphere	1.30
Cube	1.55
Undefined member	1.00

Shrinkage Strain

$$\varepsilon_{sh}(t,t_o) = -\varepsilon_{sh\infty} * k_h * S(t)$$

$$\varepsilon_{sh\infty} = \alpha_1\, \alpha_2\, (26\,(w)^{2.1}\,(f_c')^{-0.28} + 270) \times 10^{-6}$$

$$S(t) = \tanh \sqrt{\frac{t - t_o}{\tau_{sh}}}$$

Type of Cement	α_1
I	1.0
II	0.85
III	1.1

Type of Curing	α_2
Steamed cured	0.75
Water cured or h = 100 %	1.0
Sealed during curing	1.2

Relative Humidity	k_h
for $h \le 0.98$	$1 - h^3$
for $h = 1$	-0.2
for $0.98 \le h \le 1$	Use linear interpolation

The GL2000 Model

Nomenclature

f_{cm28}	= Mean 28 day concrete compressive strength (psi)
f_{ck28}	= Specified 28 day concrete compressive strength (psi)
t_o	= Age of concrete at loading (days)
K	= Correction term for effect of cement type on shrinkage
E_{cmt}	= Mean modulus of elasticity at age t (psi)
E_{cmto}	= Modulus of Elasticity at Loading (psi)
f_{cmt}	= Mean concrete compressive strength at age t (psi)
f_{cmto}	= Mean concrete compressive strength at loading (psi)
$f_{cm28(calc)}$	= Compressive strength back calculated from the 28 day modulus of elasticity (psi)
$f_{cm28(average)}$	= Compressive strength from the average of f_{cm28} and $f_{cm28(calc)}$
E_{cm28}	= Mean modulus of elasticity at 28 days (psi)
$E_{cm28(average)}$	= Calculated modulus of elasticity from $f_{cm28(average)}$
$\Phi(t_c)$	= Correction term for effect of drying before loading
ϕ_{28}	= Creep Coefficient
J(t,to)	= Creep Compliance; creep plus elastic (psi^{-1})
h	= Relative humidity (decimal)
t	= Age of concrete after casting (days)
t_c	= Age of concrete at the beginning of shrinkage (days)
V/S	= Volume to surface area ratio
ε_{sh}	= Shrinkage strain (in./in.)
ε_{shu}	= Ultimate shrinkage strain (in./in.)
$\beta(h)$	= Correction term for the effect of humidity on shrinkage
$\beta(t)$	= Correction term for the effect of time on shrinkage
f_{cmtc}	= Mean concrete compressive strength at the beginning of shrinkage
$\varepsilon(t)$	= Total strain; instantaneous plus creep and shrinkage (in./in.)

GL2000 Model Equations

Mean Compressive Strength

$f_{cm28} = 1.1 * f_{ck28} + 700$ (in psi)

Note: Only use if the experimental mean compressive strength is not available.

Mean Compressive Strength Based on Time

$$f_{cmt} = f_{cm28} \frac{t^{3/4}}{(a + b(t)^{3/4})} \quad \text{(in MPa)}$$

Note: Only use if the experimental mean compressive strength at loading is not available.

Cement Type	a	b	K
I	2.8	0.77	1.0
II	3.4	0.72	0.7
III	1.0	0.92	1.15

Modulus of Elasticity

$E_{cmt} = 500{,}000 + 52{,}000 * \sqrt{f_{cmt}}$ (in psi)

Note: Only use if the experimental modulus is not available.

Mean Compressive Strength from Modulus of Elasticity and Experimental Data

To adjust for aggregate stiffness, adjust the mean compressive strength with the back calculated modulus of elasticity.

Use the experimental E_{cm28}, back calculate for f_{cm28} to get $f_{cm28(calc)}$. Then average it with the experimental f_{cm28} and get the $f_{cm28(average)}$. The $E_{cm28(average)}$ can also be calculated.

$$E_{cm28} = 500{,}000 + 52{,}000 * \sqrt{f_{cm28}}$$

$$f_{cm28(average)} = \frac{f_{cm28} + f_{cm28(calc)}}{2}$$

$$E_{cm28(average)} = 500{,}000 + 52{,}000 * \sqrt{f_{cm28(average)}}$$

Creep Strain

ϕ_{28} =

$$\Phi(t_c)\left[2\left(\frac{(t-t_c)^{0.3}}{(t-t_c)^{0.3}+14}\right)+\left(\frac{7}{t_o}\right)^{0.5}\left(\frac{t-t_c}{t-t_c+7}\right)^{0.5}+2.5(1-1.086h^2)\left(\frac{t-t_o}{t-t_o+97(V/S)^2}\right)^{0.5}\right]$$

If $t_o = t_c$,

$\Phi(t_c) = 1$

when $t_o > t_c$

$$\Phi\ (t_c) = \left[1-\left(\frac{t_o-t_c}{t_o-t_c+97*(V/S)^2}\right)^{0.5}\right]^{0.5}$$

<u>Without experimental data</u>

$$\text{Specific Creep} = \frac{\phi_{28}}{E_{cmto}}$$

$$J(t,t_o) = \left[\frac{1+\phi_{28}}{E_{cmto}}\right]$$

$$\text{Creep Strain} = \sigma * \left[\frac{\phi_{28}}{E_{cmto}}\right]$$

<u>With experimental data</u>

$$\text{Specific Creep} = \frac{\phi_{28}}{E_{cm28(average)}}$$

$$J(t,t_o) = \frac{1}{E_{cmto}} + \frac{\phi_{28}}{E_{cm28(average)}}$$

$$\text{Creep Strain} = \sigma * \frac{\phi_{28}}{E_{cm28(average)}}$$

Shrinkage Strain

$$\varepsilon_{sh} = \varepsilon_{shu} * \beta(h) * \beta(t)$$

Ambient Conditions	B(h)
for h < 0.96	$1 - 1.18h^4$
for sealed specimens h = 0.96	0.0

$$\beta(t) = \sqrt{\left(\frac{t - t_c}{t - t_c + 97 * (V/S)^2}\right)}$$

$$\varepsilon_{shu} = 1000 * K * \sqrt{\left(\frac{4350}{f_{cm}}\right)} \text{ x } 10^{-6}$$

Total Strain

$$\varepsilon(t) = \varepsilon_{sh} + \sigma * \left[\frac{1 + \phi_{28}}{E_{cmto}}\right]$$

If the experimental $E_{c28(average)}$ and E_{cmto} is available then use:

$$\varepsilon(t) = \varepsilon_{sh} + \sigma * \left(\frac{1}{E_{cmto}} + \frac{\phi_{28}}{E_{cm28(average)}}\right)$$

The SAK Model

Nomenclature

$\varepsilon'_{sh}(t,t_o)$	= Predicted shrinkage strain (x 10^{-5})
ε'_{sh}	= Ultimate shrinkage strain (x 10^{-5})
t	= Age of concrete after casting (days)
t_o	= Age of concrete at the beginning of shrinkage (days)
RH	= Relative humidity (%)
w	= Water content of concrete (kg/m^3)
V/S	= Volume to surface area ratio (cm)
$C(t,t',t_o)$	= Predicted specific creep (x 10^{-5} kgf/cm^2)
BC	= Basic creep (x 10^{-5} kgf/cm^2)
DC	= Drying creep (x 10^{-5} kgf/cm^2)
t'	= Age of concrete at loading (days)
c	= Cement content of concrete (kg/m^3)
w/c	= Water to cement ratio by weight (%)
E_{cmto}	= Modulus of elasticity at age of loading (MPa)
$\varepsilon(t)$	= Total strain; instantaneous plus creep and shrinkage

kgf/cm^2	= 9.8 x 10^{-2} MPa
1 MPa	= 1 / 145psi

SAK Model Equations

Shrinkage Strain

$$\varepsilon'_{sh}(t, t_o) = \varepsilon'_{sh} [1\text{-}\exp\{-0.108(t\text{-}t_o)^{0.56}\}] \times 10^{-5}$$

$$\varepsilon'_{sh} = -60 + 78\{1\text{-}\exp(RH/100)\} + 38(\ln w) - 5\{\ln(V/S)\}^2 + 4(\ln t_o)$$

Creep Strain

$$C(t, t', t_o) = (BC + DC) * [1 - \exp\{-0.09(t - t')^{0.6}\}]$$

$$BC = 1.5\ (c + w)^2 (w/c)^{2.4}\ (\ln(t'))^{-0.67}$$

$$DC = 0.0045\ (w/c)^{4.2}(c + w)^{1.4}\ [\ln(V/S)]^{-2.2}\ \{1 - (RH/100)\}^{0.36}\ (t_o)^{-0.3}$$

$$J(t,t_o) = C(t, t', t_o) + (1 / E_c(t_o))$$

Note: The experimental E_{cmto} is used.

Total Strain

$$\varepsilon(t) = \varepsilon'_{sh}(t, t_o) + \sigma * [C(t, t', t_o) + (1 / E_c(t_o))]$$

REFERENCES

ACI 209R-92, Prediction of Creep, Shrinkage, and Temperature Effects in Concrete Structures, ACI Manual of Concrete Practice Part 1, 2002.

ACI 213R-87, Guide to Structural Lightweight Aggregate Concrete, ACI Manual of Concrete Practice, Part 1, 2002.

Bazant, Z. P. and Baweja, S., Creep and shrinkage prediction model for analysis and design of concrete structures – model B3, RILEM Recommendation, Materials and Structures, v. 28, 1995, pp. 357-365.

Bazant, Z. P. and Baweja, S., Justification and refinements of Model B3 for concrete creep and shrinkage 1. Statistics and Sensitivity, Materials and Structures, v. 28, 1995, pp. 415-430.

Bazant, Z. P. and Baweja, S., Justification and refinements of Model B3 for concrete creep and shrinkage 2. Updating and theoretical basis, Materials and Structures, v. 28, 1995, pp. 488-495.

CEB-FIP Model Code, Evaluation of the Time Dependent Behavior of Concrete, September 1990.

Gardner, N. J. and Lockman, M. J., Design Provisions for Drying Shrinkage and Creep of Normal-Strength Concrete, ACI Materials Journal, v. 98, March-April 2001, pp. 159-167.

Gilbert, R.I., Time Effects in Concrete Structures, Developments in Civil Engineering, v. 23, 1988.

Huo, X. S., Al-Omaishi, N., and Tadros, M.K., Creep , Shrinkage, Modulus of Elasticity of High Performance Concrete., ACI Materials Journal, v. 98, n.6, November-December 2001.

Lakshmikantan, S., Evaluation of Concrete Shrinkage and Creep Models, Masters of Science Thesis in Civil Engineering, San Jose State University, May 1999.

Mehta, P. K., and Monteiro, P. J. M., Concrete Structure, Properties, and Materials, Second Edition, Prentice Hall, 1993.

Meyerson, R., Compressive Creep of Prestressed Concrete Mixtures with and without Mineral Admixtures, Master of Science Thesis in Civil Engineering, Virginia Tech, February 2001.

Mokarem, D. W., Development of Concrete Shrinkage Performance Specifications, Doctor of Philosophy in Civil Engineering, Virginia Tech, May 2002.

Myers, J. J., and Yang, Y., Practical Issues for the Application of High-Performance Concrete to Highway Structures," Journal of Bridge Engineering, v. 6, n. 6, 2001.

Nawy, E. G., Fundamentals of High-Performance Concrete, John Wiley & Sons, Inc., New York, 2nd ed., 2001

Lakshmikantan, S., Evaluation of Concrete Shrinkage and Creep Models, Master of Science in Civil Engineering, San Jose State University, May 1999.

Neville, A. M., Dilger, W. H., and Brooks, J. J., Creep of Plain and Structural Concrete, Construction Press, New York, 1983.

Sakata, K., Prediction of Creep and Shrinkage, Creep and Shrinkage of Concrete, Proceedings of the Fifth International RILEM Symposium, Barcelona Spain, pp. 649-654, September 6-9, 1993.

Structural Lightweight Aggregate Concrete, edited by Clarke, J. L., Blackie Academic Professional, London, 1993.

APPENDIX B

Mixing and Curing Data

Introduction

This appendix presents the mixture properties, the accelerated curing data, and the mixture proportions for the individual batches.

Mixture Properties

Table 26 presents the absorption and specific gravity values measured according to ASTM C 127-01 and ASTM C128-01. The lightweight coarse aggregate values correspond with the values provided by the Carolina Salite Company on their website.

Table 27 presents the fresh concrete properties for the standard cure batches. Table 28 presents the fresh concrete properties the accelerated cure batches, the bridge beams, and the VDOT requirements for prestressed concrete.

Table 30 Aggregate Absorption and Specific Gravity

Aggregate Properties	Absorption (%)	Specific Gravity (pcf)
Lightweight Fine	10.5	1.45
Lightweight Coarse	6.0	1.45
Normal Weight Fine	1.8	2.48
Normal Weight Coarse	0.6	2.96

Table 31 Standard Cure Fresh Concrete Properties

Fresh Concrete Properties	LTHSC 2B	LTHSC 3B
Slump, mm (in.)	165 (6.5)	140 (5.5)
Air Content (%)	6.5	5.5
Temperature, ^oC (^oF)	26 (78)	26 (78)
Unit Weight, kg/m^3 (pcf)	1880 (117.3)	1910 (119.1)
Yield	1.02	1.01
w/cm ratio	0.369	0.369
Curing Method	Standard	Standard

Table 32 Accelerated Cure Fresh Concrete Properties

Fresh Concrete Properties	**LTHSC 4B**	**LTHSC 5B**	**Bayshore BB1**	**Bayshore BB2**	**VDOT specs.**
Slump, mm (in.)	100 (4.0)	150 (6.0)	180 (7)	215 (8.5)	0-100 (0-4)
Air Content (%)	6.0	7.1	5.5	6.0	3 – 6
Temperature, ^oC (^oF)	24 (75)	24 (76)	21(70)	20 (68)	----
Unit Weight, kg/m^3 (pcf)	1930 (120.3)	1875 (117.1)	1950 (122.0)	1900 (118.8)	----
Yield	1.00	1.02	0.98	1.01	----
w/cm ratio	0.369	0.369	0.369	0.369	< 0.4
Curing Method	Sure Cure	Sure Cure	Steam	Steam	N/A

Accelerated Cure Maturity Summary

The match cure system was used to replicate the curing cycle of the lightweight high strength girders used in the field assessment of this study. Temperature data was recorded for two girders. The temperature values are the average of three values that were recorded at the centroid of the prestressing strand at mid-span. The maturities have been calculated as the area under the temperature-time curve from 14^{o}F or -10^{o}C (Mehta, 1993).

Table 33 Average Maturity before De-tensioning of Girders

Reference	**Maturity** ^{o}F-hr (^{o}C-hr)
Bayshore Beam 1	1810 (1000)
Bayshore Beam 2	1500 (830)

Table 34 Average Maturity at Removal from Match Cure System

Accelerated Cure Batches	**Maturity** ^{o}F-hr (^{o}C-hr)
LTHSC-4B	1870 (1040)
LTHSC-5B	1700 (940)

The match cured creep specimens were loaded approximately three hours after the end of the curing cycle. This time was needed to sulfur cap the cylinders, install the gage points, measure the initial compressive strength, and take initial strain measurements. This time also allowed the specimen temperature to near the test temperature. Thus, small thermal impacts will be negated when it is subtracted out with the shrinkage strain.

Figure 59 and 60 present the internal curing temperatures for the LTHSC bridge beams and the upper and lower extremes for the laboratory specimens.

Experimental and Field Curing Plots

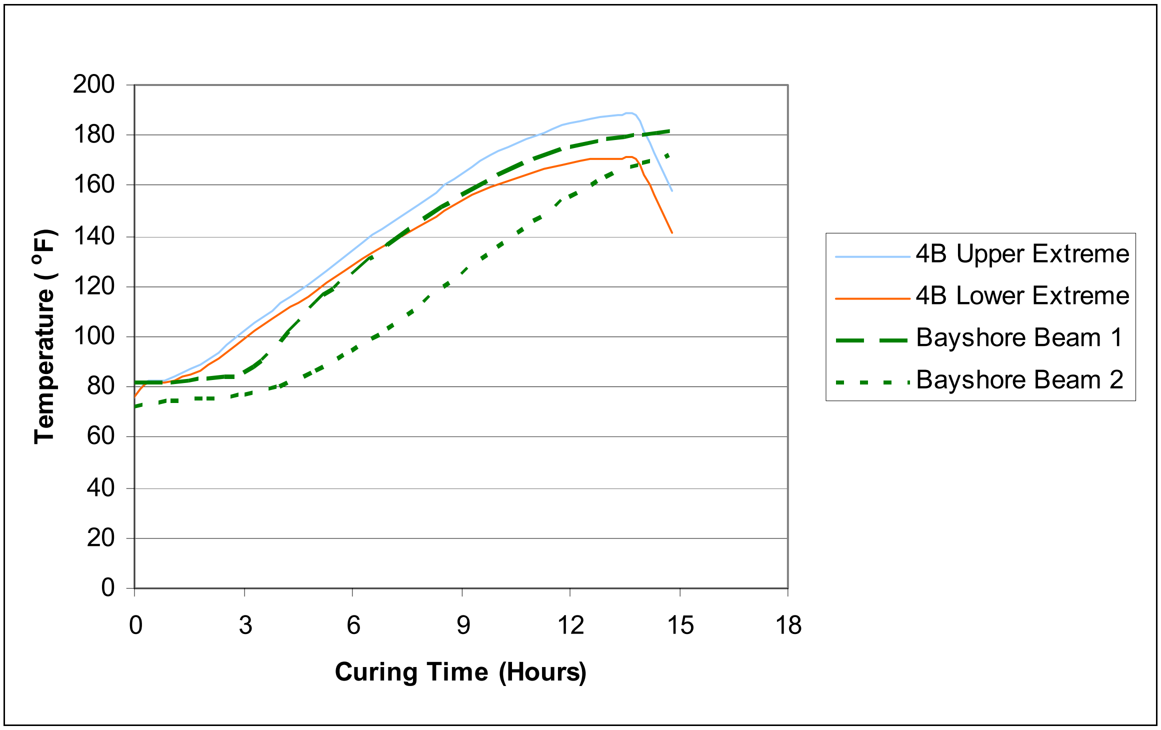

Figure 59 Batch 4 Maturity Curve Extremes and Bridge Beam Internal Curing Temperatures.

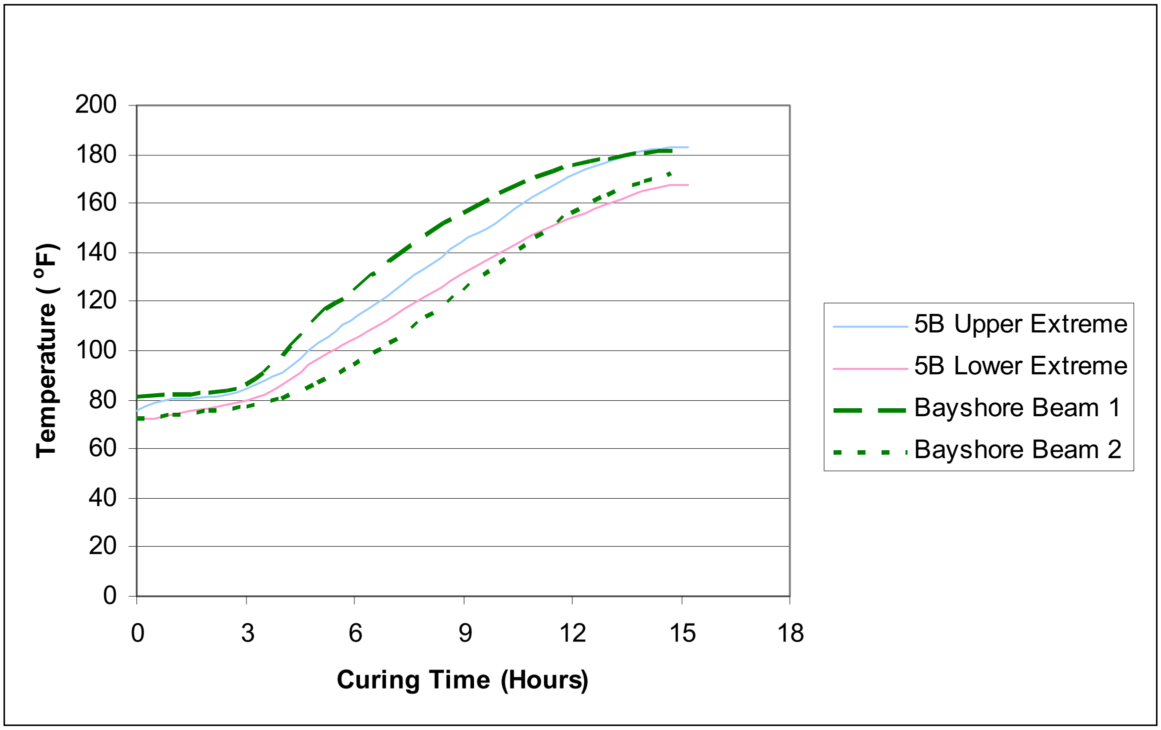

Figure 60 Batch 5 Maturity Curve Extremes and Bridge Beam Internal Curing Temperatures.

LTHSC-2B

Mixing Date: December 3, 2001

Standard Cure

Batch Volume = 2.4 cubic feet

Mixture Proportions (Dry Weights):

Portland Cement (Type II)	40.08 lbs.
Slag Cement (Grade 120)	26.76 lbs.
Coarse Aggregate (lightweight)	58.37 lbs.
Coarse Aggregate (normal weight)	53.49 lbs.
Fine Aggregate (lightweight)	31.38 lbs.
Fine Aggregate (normal weight)	47.24 lbs.
Water	22.76 lbs.
AEA (Daravair)	23 mL
WR (Hycol)	58 mL
HRWR (Adva)	75 mL
CI or Accel (DCI)	1010 mL

Water Calculations:

Mixing Water	22.76 lbs.
Absorption Water	7.93 lbs.
Total Water	30.69 lbs.

Fresh Concrete Properties:

Slump (in.)	6.5
Air Content (%)	6.5
Temperature (°F)	78
Unit Weight (pcf)	117.3

LTHSC-3B

Mixing Date: December 12, 2001

Standard Cure

Batch Volume = 2.4 cubic feet

Mixture Proportions (Dry Weights):

Portland Cement (Type II)	40.08 lbs.
Slag Cement (Grade 120)	26.76 lbs.
Coarse Aggregate (lightweight)	58.37 lbs.
Coarse Aggregate (normal weight)	53.49 lbs.
Fine Aggregate (lightweight)	31.38 lbs.
Fine Aggregate (normal weight)	47.24 lbs.
Water	22.76 lbs.
AEA (Daravair)	15 mL
WR (Hycol)	58 mL
HRWR (Adva)	75 mL
CI or Accel (DCI)	1010 mL

Water Calculations:

Mixing Water	22.76 lbs.
Absorption Water	7.93 lbs.
Total Water	30.69 lbs.

Fresh Concrete Properties:

Slump (in.)	5.5
Air Content (%)	5.5
Temperature (°F)	78
Unit Weight (pcf)	119.1

LTHSC-4B

Mixing Date: February 17, 2002

Accelerated Cure

Batch Volume = 1.3 cubic feet

Mixture Proportions (Dry Weights):

Portland Cement (Type II)	21.71 lbs.
Slag Cement (Grade 120)	14.50 lbs.
Coarse Aggregate (lightweight)	31.61 lbs.
Coarse Aggregate (normal weight)	28.97 lbs.
Fine Aggregate (lightweight)	18.50 lbs.
Fine Aggregate (normal weight)	25.59 lbs.
Water	12.28 lbs.
AEA (Daravair)	8 mL
WR (Hycol)	31 mL
HRWR (Adva)	41 mL
CI or Accel (DCI)	547 mL

Water Calculations:

Mixing Water	12.28 lbs.
Absorption Water	2.80 lbs.
Total Water	15.08 lbs.

Fresh Concrete Properties:

Slump (in.)	4.0
Air Content (%)	6.0
Temperature (°F)	75
Unit Weight (pcf)	120.3

LTHSC-5B

February 21, 2001

Accelerated Cure

Batch Volume = 1.6 cubic feet

Mixture Proportions (Dry Weights):

Portland Cement (Type II)	26.72 lbs.
Slag Cement (Grade 120)	17.84 lbs.
Coarse Aggregate (lightweight)	38.92 lbs.
Coarse Aggregate (normal weight)	35.65 lbs.
Fine Aggregate (lightweight)	22.77 lbs.
Fine Aggregate (normal weight)	31.49 lbs.
Water	15.11 lbs.
AEA (Daravair)	10 mL
WR (Hycol)	39 mL
HRWR (Adva)	25 mL
CI or Accel (DCI)	673 mL

Water Calculations:

Mixing Water	15.11 lbs.
Absorption Water	3.44 lbs.
Total Water	18.55 lbs.

Fresh Concrete Properties:

Slump (in.)	6.0
Air Content (%)	7.1
Temperature (°F)	76
Unit Weight (pcf)	117.1

APPENDIX C

Photographs

Figure 61 Creep Room Photograph

Figure 62 The Sure Cure Accelerated Curing System Photograph

Figure 63 Whittemore Gage Photograph

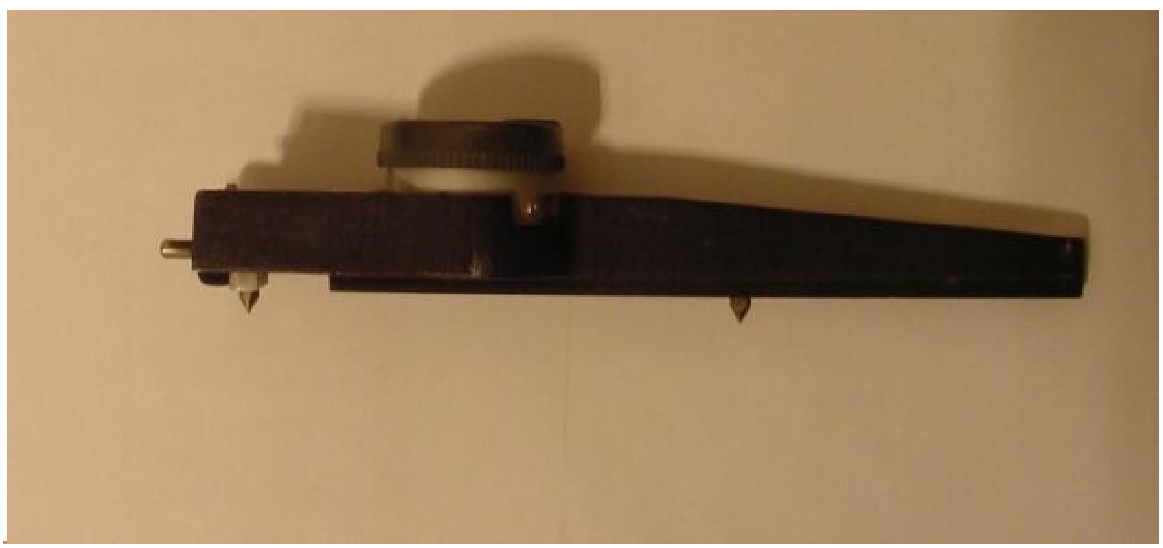

Figure 64 Side View Photograph of the Whittemore Gage

APPENDIX D

Creep Frame Calibration

Creep Frame Calibration

The four creep frames were built and calibrated by Richard Meyerson and David Mokarem. The hydraulic pressure gage for frame 3 was replaced so recalibration of frame three was required. Details of Meyerson's calibration can be found in his thesis, Compressive Creep of Prestressed Concrete Mixtures with and without Mineral Admixtures.

Figures 63, 64, and 66 are from Meyerson's thesis and represent the current calibration of frames 1, 2, and 4, respectively.

The calibration of frame three was conducted by measuring strains, applied loads and the hydraulic gage pressure. The frames have four vertical rods with 350 ohm strain gages attached. The gage factor is 2.090 ± 0.5% at 24^{o}C. The applied load was measure with a 60 kip load cell. The frame was loaded in 5 kip increments up to 55 kips. This repeated with two different load cells.

Figure 65 presents the applied load vs. the gage pressure for frame 3. The calibration chart is the average measurement of two load cells. The strain in the rods was also measured and the calculated load verse applied load was checked.

A photograph of the frames is in Appendix C.

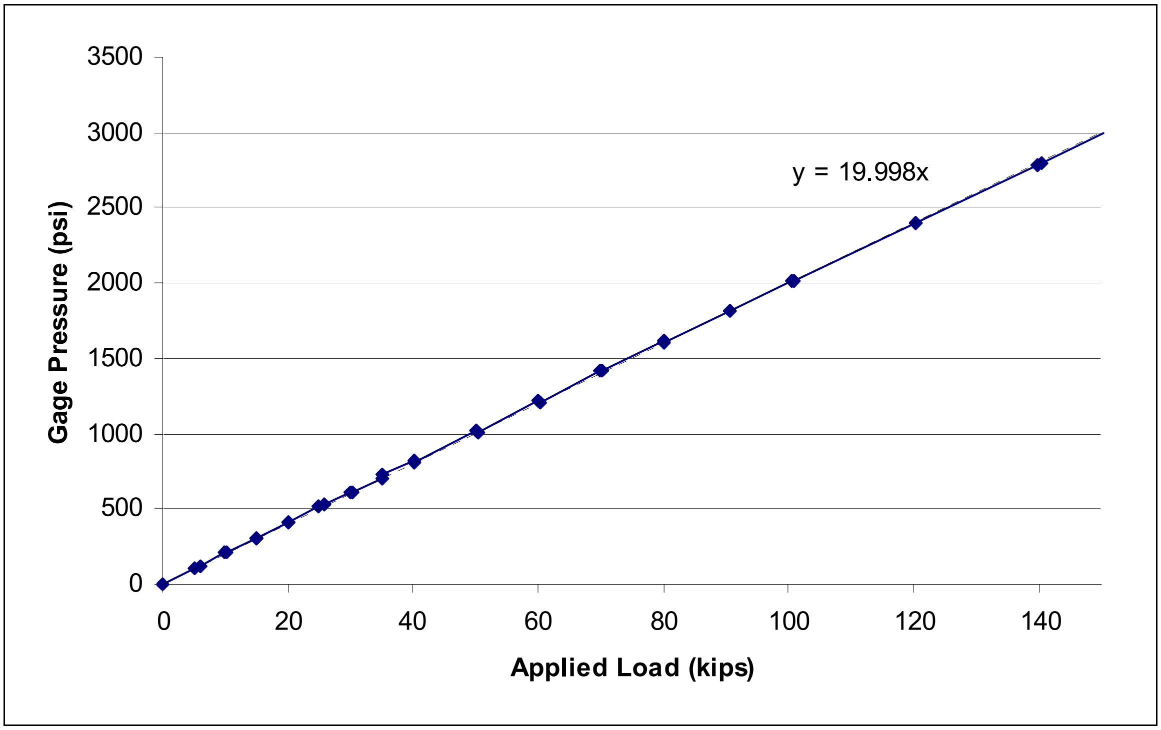

Figure 65 Frame 1: Gage Pressure versus Applied Load

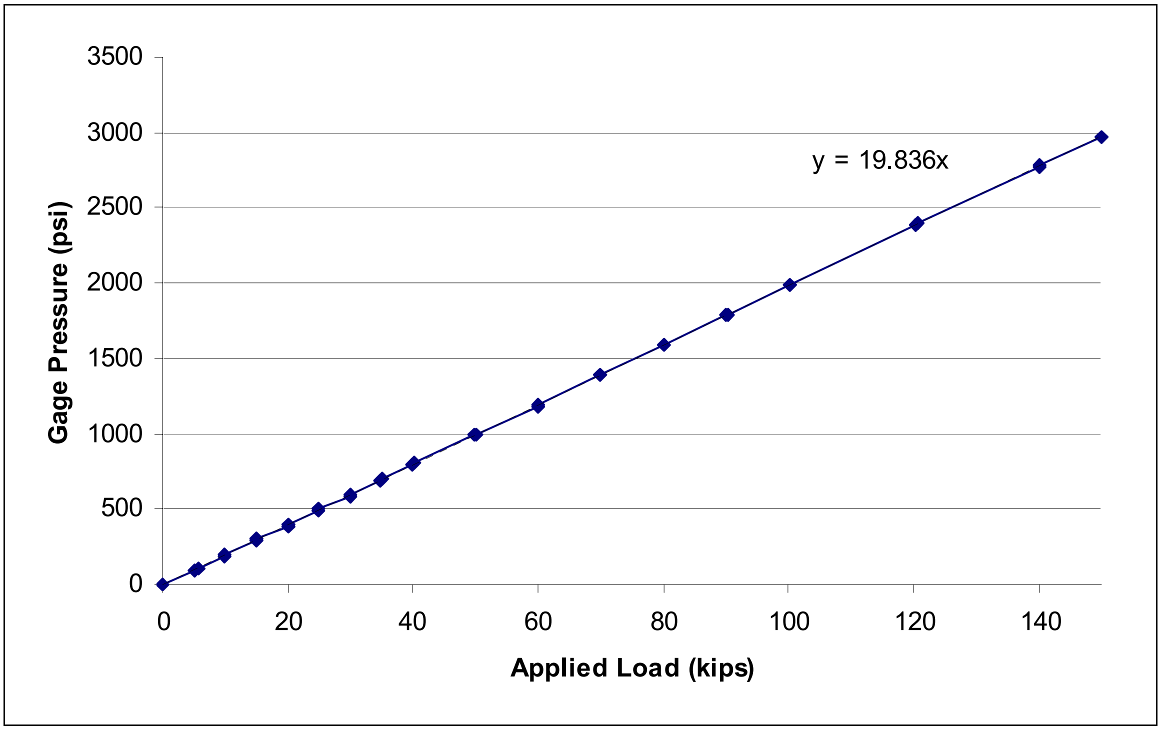

Figure 66 Frame 2: Gage Pressure versus Applied Load

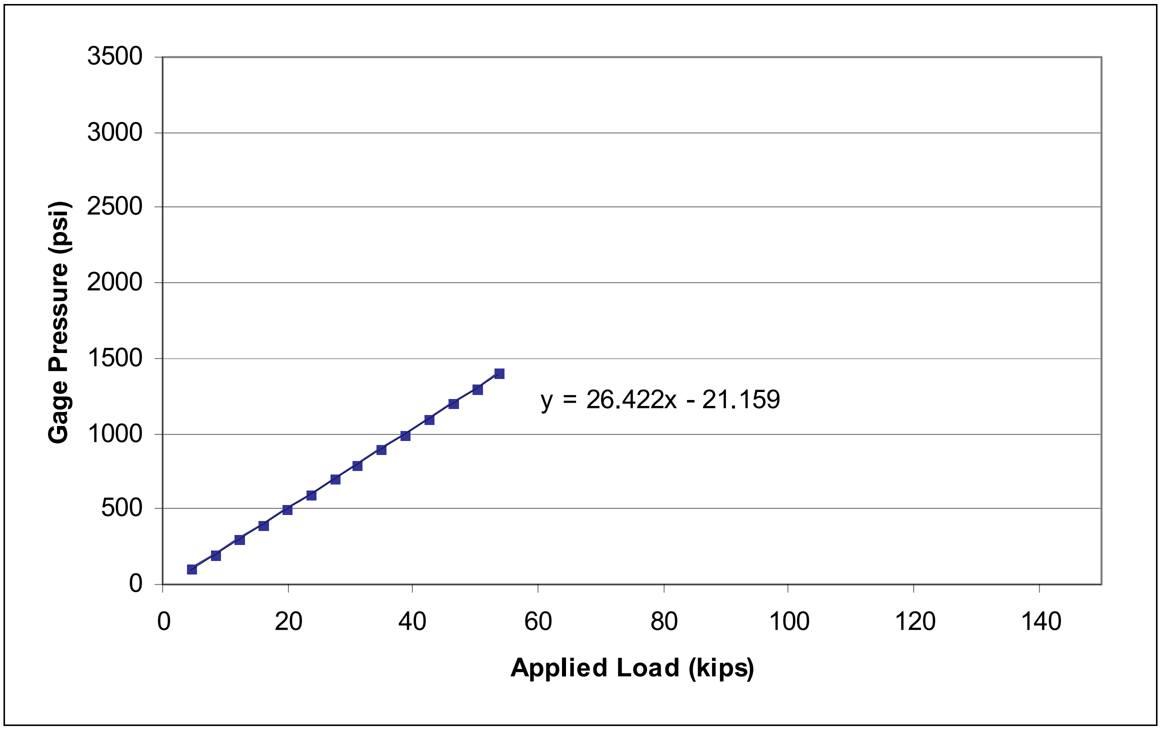

Figure 67 Frame 3: Gage Pressure versus Applied Load

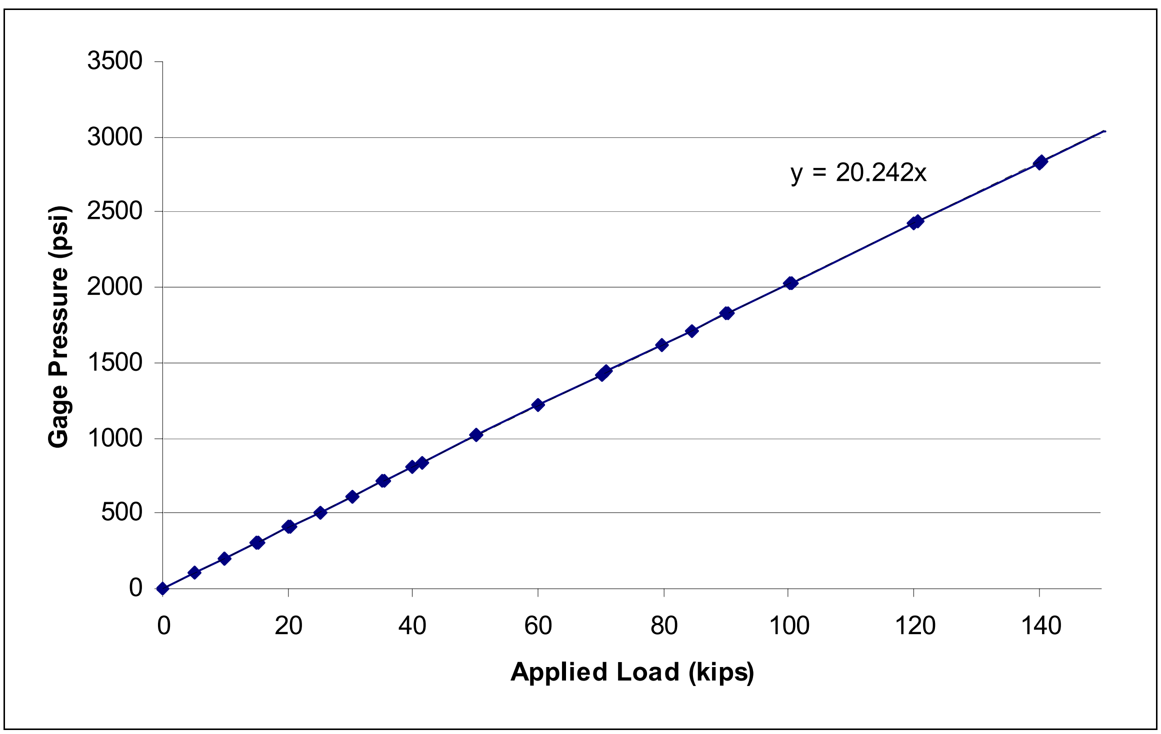

Figure 68 Frame 4: Gage Pressure versus Applied Load

APPENDIX E

Accelerated Curing

Sure Cure System Summary

In order to replicate the steam curing process at prestressing plants, the Sure Cure System was used. The system is controlled by a Windows based computer through the match cure microprocessor. This system is for 100 mm x 200mm (4 in. x 8 in.) cylinders only.

The microprocessor has the ability to match a curing cycle for 8 channels at once. A channel is a pair of a power cord and a controllable thermocouple connection that go to a single cylinder mold. The system also has six uncontrolled inputs to record data from other thermocouples.

This study required additional cylinders so "y" cords and a control box were used to expand the system. We were able to borrow 9 additional cylinders and a control box from VTRC. The "y" cords were used to split the power from one output channel to two molds. The molds were paired up so that two molds sharing a channel had similar resistances. One of the molds would control the power output for both. Some of these additional molds were monitored with thermocouples.

The maximum number of cylinders that can be made with "y" cords is 16. We have 17 molds so a control box was used to replicate one of the "y" cord molds. The control box has a separate power supply. It also has a reference thermocouple and a cylinder thermocouple. If the temperature of the cylinder is less than the reference then the control box heats the mold. The control box molds were monitored with thermocouples for quality control.

Notes about the Sure Cure system:

1) The system can start a curing cycle without the start button being pushed first. It is recommended that the computer be started when you want the curing cycle to begin.
2) The Virginia Tech Sure Cure Microprocessor has a wiring issue. Power output number 7 goes with thermocouple number 8 and the opposite inputs go together. This was discovered during initial system testing.

The following show the curing cycle and the resulting maturities. The maturities have been calculated as the area under the curve from 14^{o}F or -10^{o}C (Mehta, 1993).

APPENDIX F

Strain Measurements

Table 35 Data from Standard Cure Batch 2 Measurements

Time After Loading (days)	Total Strain (microstrain)	Std. Dev.	95% CI	Applied Stress (psi)	Elastic Deformation (microstrain)	Std. Dev.	95% CI	Shrinkage Strain (microstrain)	Std. Dev.	95% CI	Creep Strain (microstrain)	Std. Dev.	95% CI
1	1132	52	59	2052	786	18	21	48	19	22	298	15	17
2	1311	43	49	2052	786	18	21	94	6	7	432	22	25
3	1391	65	74	2052	786	18	21	131	11	12	473	50	56
4	1436	64	73	2052	786	18	21	133	16	18	517	41	46
5	1541	77	88	2052	786	18	21	154	16	18	600	48	54
6	1572	82	93	2052	786	18	21	175	12	14	611	56	63
7	1622	82	93	2052	786	18	21	190	16	18	646	56	63
14	1843	124	140	2052	786	18	21	265	30	34	792	78	88
21	1960	111	126	2052	786	18	21	288	29	32	886	84	95
28	2126	80	91	2324	842	19	22	319	34	39	964	76	86
56	2478	130	147	2324	842	19	22	382	35	40	1253	78	88
84	2606	137	155	2324	842	19	22	393	41	47	1370	77	88
91	2612	136	154	2324	842	19	22	389	47	54	1380	70	80
112	2704	163	184	2324	842	19	22	400	51	57	1461	101	114
140	2810	152	173	2324	842	19	22	423	54	62	1544	79	90
154	2871	171	193	2324	842	19	22	442	61	69	1586	93	106
168	2892	167	189	2324	842	19	22	454	60	68	1595	90	102
182	2928	178	202	2324	842	19	22	458	63	71	1628	97	110
196	2956	180	204	2324	842	19	22	477	60	67	1637	103	117
210	2979	184	208	2324	842	19	22	485	61	69	1652	105	119
224	3024	182	206	2324	842	19	22	493	65	74	1689	98	110
252	3099	184	208	2324	842	19	22	502	76	86	1755	90	102
280	3139	189	214	2324	842	19	22	509	76	86	1787	95	108
308	3194	203	230	2324	842	19	22	525	78	88	1826	111	126
329	3238	203	230	2324	842	19	22	521	78	89	1874	109	124

Table 36 Data from Standard Cure Batch 3 Measurements

Time After Loading (days)	Total Strain (microstrain)	Std. Dev.	95% CI	Applied Stress (psi)	Elastic Deformation (microstrain)	Std. Dev.	95% CI	Shrinkage Strain (microstrain)	Std. Dev.	95% CI	Creep Strain (microstrain)	Std. Dev.	95% CI
1	1284	3	3	2004	812	8	9	85	29	33	387	28	31
2	1463	16	19	2004	812	8	9	117	7	8	535	21	23
3	1586	37	41	2004	812	8	9	142	26	30	632	18	20
4	1680	30	34	2004	812	8	9	172	15	17	696	22	25
5	1776	52	59	2004	812	8	9	187	10	11	777	51	58
6	1821	7	8	2004	812	8	9	219	6	7	790	17	19
7	1906	17	19	2004	812	8	9	235	7	8	859	20	23
14	2198	23	26	2004	812	8	9	332	28	32	1054	8	9
21	2396	38	43	2004	812	8	9	389	43	48	1195	11	13
28	2718	29	33	2244	942	3	3	396	29	33	1380	8	9
56	3114	48	55	2244	942	3	3	485	31	35	1688	33	37
84	3337	55	63	2244	942	3	3	511	42	47	1885	29	33
91	3380	66	75	2246	942	3	3	521	49	55	1918	21	24
112	3486	59	66	2244	942	3	3	524	44	50	2021	21	23
140	3614	57	65	2244	942	3	3	556	33	38	2116	27	31
154	3664	60	67	2247	942	3	3	576	41	47	2147	28	32
168	3691	56	64	2244	942	3	3	576	40	45	2173	29	33
182	3732	59	67	2247	942	3	3	581	43	49	2209	35	39
196	3772	53	60	2244	942	3	3	586	44	50	2245	34	39
210	3820	60	67	2248	942	3	3	599	45	51	2280	31	35
224	3871	62	70	2244	942	3	3	608	45	51	2321	36	41
252	3934	61	69	2244	942	3	3	623	48	54	2369	46	52
280	3989	62	70	2244	942	3	3	631	47	53	2416	40	45
308	4049	64	72	2244	942	3	3	642	50	57	2466	43	48
329	4083	72	81	2244	942	3	3	648	48	54	2494	58	65

Table 37 Data from Accelerated Cure Batch 4 Measurements

Time After Loading (days)	Total Strain (microstrain)	Std. Dev.	95% CI	Applied Stress (psi)	Elastic Deformation (microstrain)	Std. Dev.	95% CI	Shrinkage Strain (microstrain)	Std. Dev.	95% CI	Creep Strain (microstrain)	Std. Dev.	95% CI
1	1228	27	31	2522	824	18	20	147	48	117	257	64	159
2	1372	25	29	2522	824	18	20	195	53	130	352	82	203
3	1507	29	33	2522	824	18	20	245	59	145	439	44	108
4	1581	59	67	2522	824	18	20	264	57	141	493	25	62
5	1649	127	144	2522	824	18	20	271	52	127	554	74	181
6	1714	98	111	2522	824	18	20	286	51	58	604	53	60
13	1871	87	98	2522	824	18	20	324	40	45	724	55	63
20	1932	72	82	2522	824	18	20	327	35	39	781	44	50
27	2008	46	52	2522	824	18	20	367	36	41	817	30	34
55	2331	13	14	2928	921	31	35	394	37	42	1017	31	35
83	2507	14	16	2928	921	31	35	455	23	26	1131	27	30
90	2513	20	23	2928	921	31	35	460	17	20	1132	39	44
111	2583	23	26	2928	921	31	35	483	18	20	1180	17	19
139	2680	25	28	2928	921	31	35	518	26	29	1241	30	34
153	2710	17	19	2928	921	31	35	544	23	26	1245	18	21
167	2766	12	13	2928	921	31	35	553	20	23	1293	27	31
181	2776	25	28	2928	921	31	35	551	21	24	1304	38	43
195	2810	43	49	2928	921	31	35	556	21	23	1334	46	52
209	2856	31	35	2928	921	31	35	568	21	24	1367	35	39
223	2861	27	31	2928	921	31	35	566	28	31	1374	24	27
251	2932	38	43	2928	921	31	35	579	38	43	1433	41	46

Table 38 Data from Accelerated Cure Batch 5 Measurements

1	1635	60	68	1848	965	70	79	125	47	115	544	92	227
2	1802	82	92	1848	965	70	79	171	75	184	665	131	322
3	1959	72	82	1848	965	70	79	230	92	227	763	114	281
4	2101	75	84	1848	965	70	79	251	115	283	885	133	327
5	2170	83	94	1848	965	70	79	301	65	161	904	82	202
6	2231	93	105	1848	965	70	79	304	71	80	961	56	63
13	2831	114	128	2228	1119	77	87	359	44	49	1352	23	26
20	3023	124	141	2228	1119	77	87	394	33	37	1510	22	25
27	3219	106	120	2228	1119	77	87	427	31	35	1672	13	15
55	3495	104	118	2228	1119	77	87	474	24	27	1901	19	21
83	3764	135	153	2228	1119	77	87	531	49	56	2114	11	12
90	3794	137	156	2228	1119	77	87	539	50	57	2136	10	12
111	3928	159	180	2228	1119	77	87	557	53	60	2252	32	36
139	4076	134	152	2228	1119	77	87	590	66	74	2367	29	32
153	4133	135	153	2228	1119	77	87	594	57	64	2419	9	10
167	4210	153	173	2228	1119	77	87	611	55	63	2480	24	27
181	4231	163	184	2228	1119	77	87	608	59	66	2504	37	42
195	4290	155	176	2228	1119	77	87	614	56	64	2558	24	27
209	4345	161	182	2228	1119	77	87	613	57	65	2613	31	35
223	4383	154	174	2228	1119	77	87	624	51	58	2640	28	32
251	4466	162	183	2228	1119	77	87	645	57	65	2702	28	32

APPENDIX G

Percent Shrinkage Measurements

Table 39 Percent Length Change Measurements

Days after Curing	% Shrinkage 2-1	2-2	2-3	% Shrinkage 3-1	3-2	3-3	2B AVERAGE	3B AVERAGE	2B 95%CI	3B 95%CI	2B/3B AVERAGE	95%CI
0	0.0000	0.0000	0.0000	0.0000	0.0000	0.0000	0.0000	0.0000	0.0000	0.0000	0.0000	0.0000
7	0.0302	0.0320	0.0276	0.0347	0.0391	0.0364	0.0299	0.0367	0.0025	0.0025	0.0333	0.0034
14	0.0356	0.0400	0.0329	0.0436	0.0480	0.0453	0.0361	0.0456	0.0041	0.0025	0.0409	0.0047
21	0.0409	0.0462	0.0400	0.0471	0.0498	0.0480	0.0424	0.0483	0.0038	0.0015	0.0453	0.0032
28	0.0409	0.0471	0.0400	0.0471	0.0498	0.0489	0.0427	0.0486	0.0044	0.0015	0.0456	0.0033
56	0.0444	0.0489	0.0436	0.0533	0.0533	0.0542	0.0456	0.0536	0.0032	0.0006	0.0496	0.0038
84	0.0462	0.0524	0.0453	0.0560	0.0569	0.0551	0.0480	0.0560	0.0044	0.0010	0.0520	0.0040
112	0.0471	0.0524	0.0453	0.0560	0.0587	0.0560	0.0483	0.0569	0.0042	0.0017	0.0526	0.0043
140	0.0480	0.0533	0.0480	0.0569	0.0596	0.0578	0.0498	0.0581	0.0035	0.0015	0.0539	0.0040
168	0.0480	0.0542	0.0471	0.0560	0.0587	0.0578	0.0498	0.0575	0.0044	0.0015	0.0536	0.0040
196	0.0462	0.0516	0.0462	0.0569	0.0578	0.0569	0.0480	0.0572	0.0035	0.0006	0.0526	0.0043
224	0.0498	0.0551	0.0498	0.0587	0.0613	0.0604	0.0516	0.0601	0.0035	0.0015	0.0559	0.0041
252	0.0507	0.0569	0.0498	0.0604	0.0631	0.0631	0.0524	0.0622	0.0044	0.0017	0.0573	0.0048
280	0.0516	0.0587	0.0507	0.0613	0.0640	0.0649	0.0536	0.0634	0.0050	0.0021	0.0585	0.0049
301	0.0516	0.0587	0.0516	0.0631	0.0658	0.0658	0.0539	0.0649	0.0046	0.0017	0.0594	0.0053
322	0.0533	0.0604	0.0524	0.0640	0.0667	0.0667	0.0554	0.0658	0.0050	0.0017	0.0606	0.0051

VITA

Edward Creed Vincent was born is Charleston, West Virginia on October 3, 1977 to Frank and Catherine Vincent. He grew up in Charleston and attended George Washington High School. He became an Eagle Scout and an All-State musician playing tuba. He graduated high school with honors in 1996. After high school, Ed attended Virginia Tech and completed a co-op position with the U.S. Geological Survey. He graduated with a Bachelors of Science in Civil Engineering in 2001. He then pursued a Master of Science degree in Civil Engineering at Virginia Tech. Upon completion of his graduate degree in January 2003, Ed will be a structural engineer with the US Army Corps of Engineers in Huntington, WV.